CRANFIELD UNIVERSITY

CHUN-WEI CHANG

HUMAN-LIKE MOTORWAY LANE CHANGE TRAJECTORY PLANNING FOR AUTONOMOUS VEHICLES

SCHOOL OF AEROSPACE, TRANSPORT AND MANUFACTURING
Advanced Vehicle Engineering Centre

DEGREE OF DOCTOR OF PHILOSOPHY (PhD – FULL TIME)
Academic Year: 2015 - 2019

Supervisors:
Dr. Efstathios Velenis
Dr. Abbas Fotouhi
Dr. Stefano Longo
Oct 2019

CRANFIELD UNIVERSITY

SCHOOL OF AEROSPACE, TRANSPORT AND MANUFACTURING
Advanced Vehicle Engineering Centre

DEGREE OF DOCTOR OF PHILOSOPHY (PhD – FULL TIME)

Academic Year 2015 - 2019

CHUN-WEI CHANG

HUMAN-LIKE MOTORWAY LANE CHANGE TRAJECTORY PLANNING FOR AUTONOMOUS VEHICLES

Supervisor: Dr. E. Velenis, Dr. A. Fotouhi, Dr. S. Longo
Oct 2019

This thesis is submitted in partial fulfilment of the requirements for the degree of Doctor of Philosophy
(NB. This section can be removed if the award of the degree is based solely on examination of the thesis)

ABSTRACT

The human lifestyle can be foreseen to have a tremendous change once the automation of transportation has been fully realised. The majority of current researches merely focus on improving the efficiency performance of autonomous vehicles (e.g. the energy management system, the handling, etc.) instead of putting the human acceptance and preference into consideration, leaving the knowledge gap of achieving the personalised automation. The primary objective of this research is to develop a novel human-like trajectory planning algorithm that is able to mimic the performance of human drivers and generate a feasible trajectory for an autonomous vehicle to complete a motorway lane change, which is the most representative and commonest manoeuvre on the motorway.

This thesis can be divided into four main sections. Starting with the part of literature review, which summarises the existing techniques and the associated knowledges that can be taken the advantage of; including the trajectory planning, the driving styles, the lane change manoeuvre and the Model Predictive Control (MPC). An appropriate-designed experiment is then introduced and implemented, with the purpose of constructing a precise and reliable human driving database. This database contains 551 lane changes on the motorway from 12 different male drivers. Through applying data statistics methods, the human characteristics can be mined from the experimental data, showing that the vehicle velocity $\boldsymbol{v}$, the hand steering wheel angle $\boldsymbol{\delta_{handreal}}$, the longitudinal acceleration $\boldsymbol{a_x}$, the rate of hand steering $\boldsymbol{\gamma_{handsteer}}$ and the rate of longitudinal accelerating $\boldsymbol{\gamma_{longAcc}}$ are the essential features for the motorway lane change manoeuvre. An off-line constraint table for the three nominated driving styles can be therefore constructed based on these features. Finally, the obtained human information is then fused with the traditional MPC planning technique so as to achieve the proposed human-like trajectory planning algorithm.

The main contribution of this study is proposing a novel approach of combining the real human driving data and the traditional planning technique (i.e. MPC) to

achieve human-like lane change trajectory planning for autonomous vehicles. An integrated human driving database which contains both the video footages and the vehicle-dynamic-based signals from 12 different participants is built. Moreover, the draft marginal values of the essential parameters for the driving styles while performing a right lane change on the motorway are also presented. Both the collected driving database and the driving styles' constraint table can be seen as distinctive achievements, providing resourceful materials for future researches.

Keywords:

Human-like; Trajectory Planning; Model Predictive Control; Autonomous Vehicle; Driving Style Recognition; Data Statistics

ACKNOWLEDGEMENTS

First of all, I would like to thank my primary supervisor Dr. Efstathios Velenis, who has encouraged me to keep the faith in my research and always willing to assist me, even when I faced the toughest period in my life. I also like to show my appreciation to the other primary supervisor Dr. Abbas Fotouhi for providing the professional comments and recommendations in the field of data statistics. I want to thank my previous supervisor Dr. Dongpu Cao who provided me the chance to start my PhD and always inspires me to improve my research skills.

I am grateful for my second supervisor Dr. Stefano Longo for the discussions and the suggestions of constructing a control algorithm, as well as the knowledge of sailing a boat. Furthermore, I also like to mention my colleagues in the research office, thank you for accompanying me within the past few years. Also, specially thanks all the participants who spent their spare time helping me to build a human driving database.

Finally, I would like to thank my parents and my family, who always being my backup and never give up on me. Love you forever.

TABLE OF CONTENTS

LIST OF FIGURES

LIST OF TABLES

LIST OF EQUATIONS

LIST OF ABBREVIATIONS

ACC	Adaptive Cruise Control
ADAS	Advanced Driver Assistance Systems
AI	Artificial Intelligence
ANSI	American National Standards Institute
AP	Automatic Parking
CAN	Controller Area Network
CAS	Collision Avoidance Systems
CoG	Centre of Gravity
CYRA	Constant Yaw Rate and Acceleration
DARPA	Defense Advanced Research Projects Agency
FIR	Finite Impulse Response
FOV	Field of View
GPS	Global Positioning System
HAV	Highly Automated Vehicle
IMU	Inertial Measurement Unit
LDA	Lane Departure Avoidance
LED	Light-Emitting Diode
LKA	Lane Keeping Assistance
LP	Lattice Planner
LTI	Linear-Time-Invariant
MDP	Markov Decision Processes
MIMO	Multi-Input Multi-Output
MPC	Model Predictive Control
NHTSA	National Highway Traffic Safety Administration
OBD	On-Board Diagnostics
PMP	Partial Motion Planning
RACE	Robust and Reliant Automotive Computing Environment for Future eCars
RRT	Rapidly-exploring Random Tree
RTK	Real-Time Kinematic
SAE	Society of Automotive Engineers
SISO	Single-Input Single-Output

ST	Swerving Trajectories
SUV	Sports Utility Vehicle
SVM	Support Vector Machine

1 INTRODUCTION

Nowadays, autonomous driving is foreseen one of the ultimate goals in the transportation engineering. In order to achieve this ambition, significant effort has been devoted in both the academia and the industry. In the meantime, numbers of official and civil competitions were held to accelerate the progress in this field [1]. This chapter introduces the background of study and the development of autonomous driving; as well as the motivation of this PhD research.

The pioneering autonomous vehicle can be dated back to 1987, which is generated from a vagarious project between Mercedes-Benz and Bundeswehr University Munich. In the following thirty years, a dramatic evolution of approaching autonomous driving has been achieved and contributes numerous matured Advanced Driver Assistance Systems (ADAS); such as Automatic Parking (AP), Lane Departure Avoidance (LDA), Collision Avoidance Systems (CAS), Lane Keeping Assistance (LKA), etc. These ADAS not only improve the performance of vehicles but also prevent accidents during the period of driving, and can be treated as the prototype functionalities of a fully autonomous vehicle.

Since transportation automation has been foreseen as the trend which is nearly irresistible, the precise classification of on-vehicle intelligence has become an urgent task and drawn an amount of attention. From the rough three levels of vehicle autonomy [2] to the 4+1 levels proposed by the NHTSA in the United States [3], the primary principle can be summarised as that the dependence to a human driver during driving is reduced with the number of level increase. In addition, a more elaborate taxonomy was issued by Society of Automotive Engineers (SAE) in 2014, comprising 5+1 levels from no automation at Level 0 to full automation at Level 5. As stated by the policy which is proposed by U.S. Department of Transportation and NHTSA in 2016 [4], a vehicle with Level 3 or Level 4 functionality is termed as “highly automated vehicle” (HAV) and an autonomous vehicle belongs to Level 5.

To better distinguish and standardise the degree of automation, 5+1 levels published by SAE are treated as the common indicators [5]. There is no doubt that the human lifestyle or even the government policy will have a tremendous shift once the automation of transportation has been fully realised. Though, the reliability and the safety of automation techniques still require great effort to increase public acceptance. With the purpose of establishing a consistent framework for both industries and governments and protecting the traveling public during the forthcoming development of autonomous vehicles, the U.S. Department of Transportation and the National Highway Traffic Safety Administration (NHTSA) declared “Federal Automated Vehicles Policy” in September 2016 based on SAE 5+1 level automation [4] and continues updating the policy every year (e.g. “Preparing for the Future of Transportation” in 2018 [6]).

Urban driving, as one of the indispensable scenarios for future autonomous navigation, is comprised of numerous complex manoeuvres (e.g. crossroad turning, roundabout driving, automatic parking, etc.). Hence, a reliable framework for autonomous vehicles under the urban environment is not only a challenging target but also a demanding task. To speed up the technical transition from conventional manual driving to fully autonomous driving, the United States Defense Advanced Research Projects Agency (DARPA) held an autonomous vehicle rivalry called “The Urban Challenge” in 2007, which comprise numerous urban navigation assignments [7]. On the other hand, numerous researchers started making every effort in investigating how the autonomous driving potentially affects human’s daily life and their mobility decision. According to these researches, the scenarios in the urban area might comprise fully automated vehicles, Vehicles on Demand that allow for different personal mobility and Valet Parking vehicles [8]. For instance, people who have no driving license, children or even elders are able to utilise Vehicles on Demand to reach their destinations [4]; Valet Parking vehicles not only help drivers to save the time and the parking cost but also retain the function that vehicles can be fully controlled by drivers. Theoretically, one of the most important welfares of transportation automation is that drivers are able to spend

the time on other activities instead of the driving tasks in vehicles, and might force drivers to reconsider the daily journeys or even influence their home selection. Nevertheless, some of the researches even deduce that the driving automation might alter governments' choices of selecting residential locations and the design of urban spaces development [4][8].

To popularise autonomous vehicles, several preconditions must be satisfied, including product reliability, consumer acceptability, etc. A correlative survey has been done in 2015, which investigates more than 3200 adults from six different countries. It tried to figure out what activities the human subjects prefer to do in an autonomous vehicle. The report reveals that 55.7% of the participants have insufficient trust in the self-driving technology and choose to supervise navigation tasks or even not to board an autonomous car; reading, social contacting and sleeping account for 8.53%, 11.07% and 8.2% respectively [9]. Hence, how to improve the public faith and acceptance of autonomous vehicles has become an urgent issue. Furthermore, U.S. Department of Transportation intends to accelerate the HAV revolution by taking safety elements into account and contains the sections with the ambitions of sharing safe testing data and deployment, suggesting unified standard state requirements, and seeking suitable regulatory tools for autonomous vehicles [4][6]. Specifically, providing numbers of automated driving system safety elements so as to analyse, identify and resolve safety considerations; establishing the standards and guidance for both the autonomous vehicles and the transportation infrastructures; ensuring the consistency of the national or interstate travel; refining the regulatory constraints to the autonomous vehicles' safe integration.

In general, the on-vehicle automation system is primarily designed to replace the role of human drivers in a driving task in order to enhance the performance and avoid the possible fatalities (e.g. correcting human mistakes and reducing the traffic crashes related to human behaviours and decisions). However, most published researches rarely considered that the human's performance and preference does not always lead to negative consequences. An explicit

example is the motion sickness. It has been confirmed as one of the serious after-effects while riding an autonomous vehicle but rarely happens when the vehicle is driven by the person himself.

This research targets on imitating the performance of human drivers so as to achieve human-like autonomous driving. In other words, developing a novel trajectory planning for the particular driving scenario, lane changes on the motorway, while taking the real human driving data into account. Figure 1-1 briefly illustrates the original idea of this PhD research.

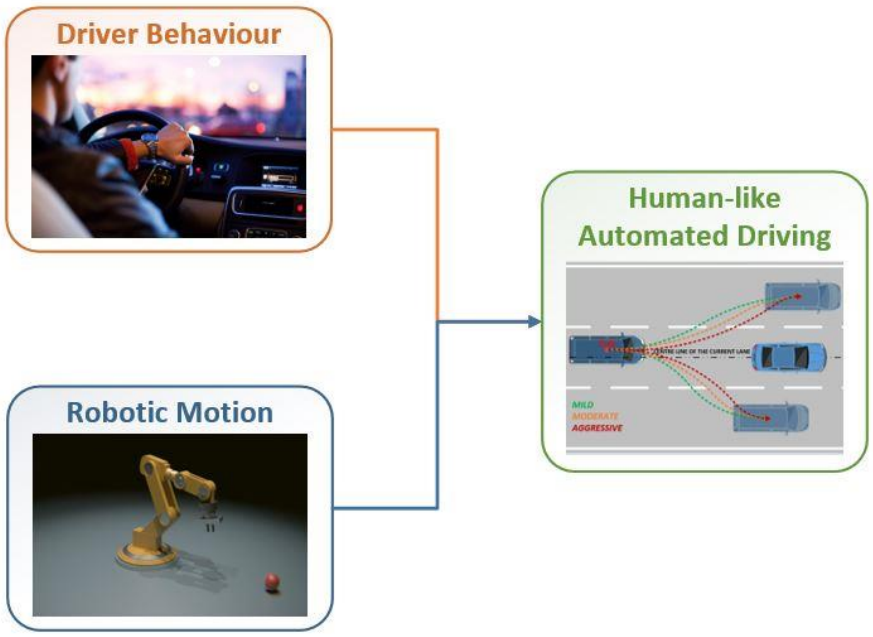

Figure 1-1 Combining human factors with a vehicle-dynamics-based trajectory so as to generate the human-like trajectory.

Before starting a rigorous research, a comprehensive understanding of the background of study is always indispensable. In the past 30 years, the autonomous driving draws significant attention and both the academia and the industry dedicate in maturing reliable autonomous driving systems. It is worthwhile mentioning that the SAE's 5+1 level of automation is accepted as the standard indicator in the transportation engineering. This research is therefore inspired by the desire of autonomous driving techniques and the demand of personalisation, which plans to combine human factors with the

robotic motion and generating a human-like trajectory for an autonomous vehicle.

2 LITERATURE REVIEW

To step into the main body of this research, the literatures that has been published in the relevant fields of autonomous vehicles should be studied and reviewed in advance. Through understanding the different stages of motion planning and the planning methodologies, the possible techniques for this study can be guided. Furthermore, the performance of human drivers used to be clustered into different driving styles. In order to adopt human characteristics from real drivers, a summary for the knowledge and the classification algorithms of driving styles is necessary. While the target manoeuvre of this work is lane changes on the motorway, its definition and the essential parameters are required to be understood. As the most suitable technique has been determined as Model Predictive Control (MPC) in Section 2.1, a discussion for the theory of a MPC and the general framework of the MPC-based trajectory planning algorithm should be carried out. After reviewing these researches, the project novelty can be highlighted in the meantime.

2.1 Motion Planning for Autonomous Vehicles

People believe that the matured technology of autonomous vehicles has the ability to improve the safety of driving, lessen traffic congestions, lower vehicle emissions and achieve greater mobility. And these ambitions can be fulfilled by a well-designed autonomy software, in other words, the motion planning methods. In the view of engineering, critical planning which is realised through complex mathematic algorithms is the key element to the autonomy. Similar to the fact that a good execution strategy often leads to a successful outcome, and therefore autonomous vehicles require reliable motion planning to guarantee the safe and collision-free navigation is performed. The motion planning methods normally include the functionalities of avoiding pedestrians or obstacles, searching possible paths and determining the best trajectory in order to transport passengers or stuffs safely, efficiently and comfortably between the origin and the destination [10][11]. Moreover, the environmental conditions (e.g. traffic regulations, vehicle dynamics, path boundaries, manoeuvre capabilities,

etc.) are essential factors and need to be considered in the meantime during the planning process.

The techniques of motion planning which are recently utilised in the autonomous driving are originated from the early robot motorisation research. The primary difference of the motion planning between mobile robots and autonomous vehicles is that the former mainly concentrates on increasing execution speed while maintaining the low risk of structure damages, for instance, preventing the excessive vibrations and accelerations [12]. On the other hand, the latter is requested to take additional constraints into account, such as driving safety, traffic rules, riding comfort, etc.

Some of the previous researches demonstrate the path planning and the local trajectory planning for the robot to navigate from a start point to a target one [12][13]; the kinematic and the dynamic properties of the robot were considered in the meantime [14]. In the robotic point of view, the goal of path planning is to provide a geometric pathway through a specific methodology without considering the time information, such as roadmap methods, cell decomposition algorithms, and artificial potential techniques. A particular time law and different optimality criterions such as minimum execution time, minimum energy, minimum jerk, etc., are then assigned to the acquired path from the path planner in the trajectory planning stage so as to specify the supposed state of the robot at every time step [12].

Base on the foundation of robotic motion research, the development progress of autonomous vehicles has been sped up in recent years. One of the well-known examples is the autonomous vehicle “BOSS”, which is awarded in “The Urban Challenge” in 2007, with a prominent auto-driving framework that was developed by Carnegie Mellon University. Specifically, this reasoning framework for “BOSS” was mainly composed of four different sections:

1) Perception
2) Mission Planning
3) Behavioural Executive
4) Motion Planning

The Mission Planning section takes the provided mission tasks and other driving restrictions into account and computes the optimal navigation route to reach the target place. In the Perception stage, a general picture of the surrounding environment is constructed via analysing and fusing the collected data from different sensors; the observed data includes current vehicle state, geometric world model, dynamic and static obstacle distribution, and road blockages. Then, the Behavioural Executive part utilises the obstacle information and the strategic route provided by the above two sections to generate a series of local pose objectives. Finally, the finest trajectory that conforms to the constraints from the Behavioural Executive is determined in the Motion Planning stage [15]. In other words, these four sections contain both global planning and local planning, and therefore enable “BOSS” to accomplish the competition missions successfully. Figure 2-1 shows the planning system of the autonomous vehicle “BOSS”. It is worthwhile mentioning that the Motion Planning section of “BOSS” is more like a combined functionality of the path planning and the trajectory planning, instead of indicating the entire planning process of the autonomous driving.

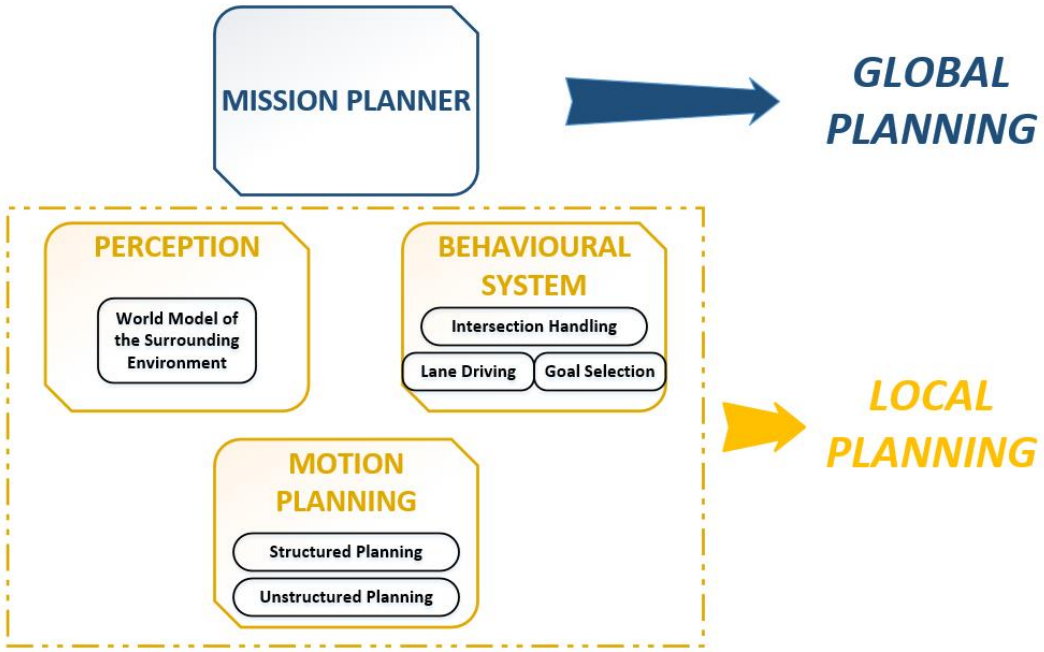

Figure 2-1 A depiction of the planning system of “BOSS”.

According to previous studies, the stage of motion planning for autonomous driving can be split into three different classes, from the highest level to the lowest one, which are:

1) Global Route Planning
2) Path Planning
3) Rigid Trajectory Planning

Global route planning is a macroscopic strategy of searching the optimal route between the start point and the terminal point, which might consider the integral conditions of traffic in a particular period. Apart from the global route planning, the latter two classes can be treated as local planning. The local planning process mainly focuses in evaluating the instantaneous factors and driving conditions, either dynamic or static (e.g. road boundaries, obstacles, pedestrians and vehicles interactions, vehicle dynamics, etc.) and generates the most appropriate local trajectory with ensuring the driving safety [10][11][16][17]. Specifically, the path planning section contains two sub-functionalities, which are the search space for planning and the manoeuvre selection. Briefly, the term path is composed of a set of waypoints, while a trajectory can be treated as the time or the velocity parameter is added to the path. The objective of path searching is to generate a possible connection method from the start point to the destination within the feasible region. On the other hand, the aim of trajectory fitting is to fit a smooth curve with time parameters between two waypoints of the path. A basic framework of the motion planning system for autonomous vehicles is illustrated in Figure 2-2 [10][11].

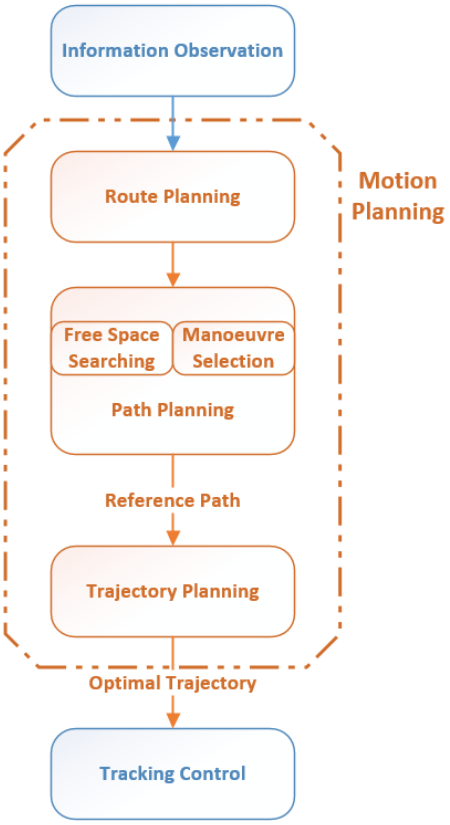

Figure 2-2 The motion planning framework for autonomous vehicles.

Generally, there are four essential achievements that a practical motion planning cycle of an autonomous vehicle has to be included: (1) generating the optimal global route, (2) generating the optimal decision or manoeuvre, (3) generating the optimal local path, and (4) generating the optimal detailed trajectory [16]. In other words, the motion planning process starts with selecting a global route between the current location and the destination by the route planner. In the following path planning stage, one or more chosen methodologies are then utilised to search space for path planning in prior so as to transfer the searching results to the manoeuvre determination module. A feasible path can be computed and acquired after one of the possible manoeuvres is selected according to the available space, while it has close relations with the manoeuvres or the decisions which are performed by the autonomous vehicle. This procedure might be operated recursively in order to finalise the most suitable path. Finally, the entire cycle ends up determining the optimal trajectory in the trajectory planning stage. Numerous reasonable

geometric curves which are related to the final decided path can be generated through interpolating a certain type of curve or optimising associated weight factors and cost functions. It should be noted that the shorter the time interval between two planning cycles is, the more reliable and precise the trajectory will be; nevertheless, the computational cost will increase in the meantime, which is a trade-off between the efficiency and the reliability.

2.1.1 Route Planning

Route planning can be seen as a high-level planning for moving objects, which often utilises one or several digital maps and Global Positioning System (GPS) as the geometric information and produces several possible routes from the current location to the destination [18]. Focusing on the vehicle navigation scenario, digital maps are primarily composed of country roads, motorways, urban streets, roundabouts, etc. Additional data which is related to the navigation might be included in particular maps, for instance, the speed limitations, the restrictions of the driving direction or even the traffic flow situations. As a result, the precision of the pre-record maps and the GPS will affect the performance of route planners. Unlike the local planning, the route planning process does not take the vehicle dynamics into account since the dimensions of reference maps are much larger than the size of the host vehicle.

Referring to the research of Artificial Intelligence (AI), the route planning can be fulfilled through three different approaches, which are (1) roadmap, (2) cell decomposition, and (3) potential field [10][11]. The roadmap category transfers the start point, the target point, and the obstacles into nodes so as to build the visibility graphs. The cell decomposition methods attempt to segment the reference maps into numerous cells, either with uniform shapes or different forms; each of these cells conveys the information of whether it is occupied by obstacles or free for navigation. This information is then analysed by a searching algorithm (e.g. A*, Dijkstra, etc.) and the remaining free cells can be connected to provide several cell-based routes between the origin and the destination. Finally, the approaches of the numerical potential field utilise Laplace functions or other mathematical functions to reconstruct the reference

maps; for instance, the obstacles and the end point are endowed with maximum values and a minimum value respectively. Therefore, the possible routes can be produced by following the minimum gradient from the start point to the end point [19].

The route planner might provide several possible routes to reach the destination during the route planning process. To determine the most suitable route, one or more cost functions can be employed (e.g. distance, travelling time, safety, etc.). Figure 2-3 shows an example of route planning from Cranfield to Laindon, which considers the distance, the traffic flow situation and other additional information. Since the navigation of autonomous vehicles requires on-line redirection functionalities and must satisfy the time constraints during driving tasks, the real-time route planning has been considered as an indispensable part of the motion planning.

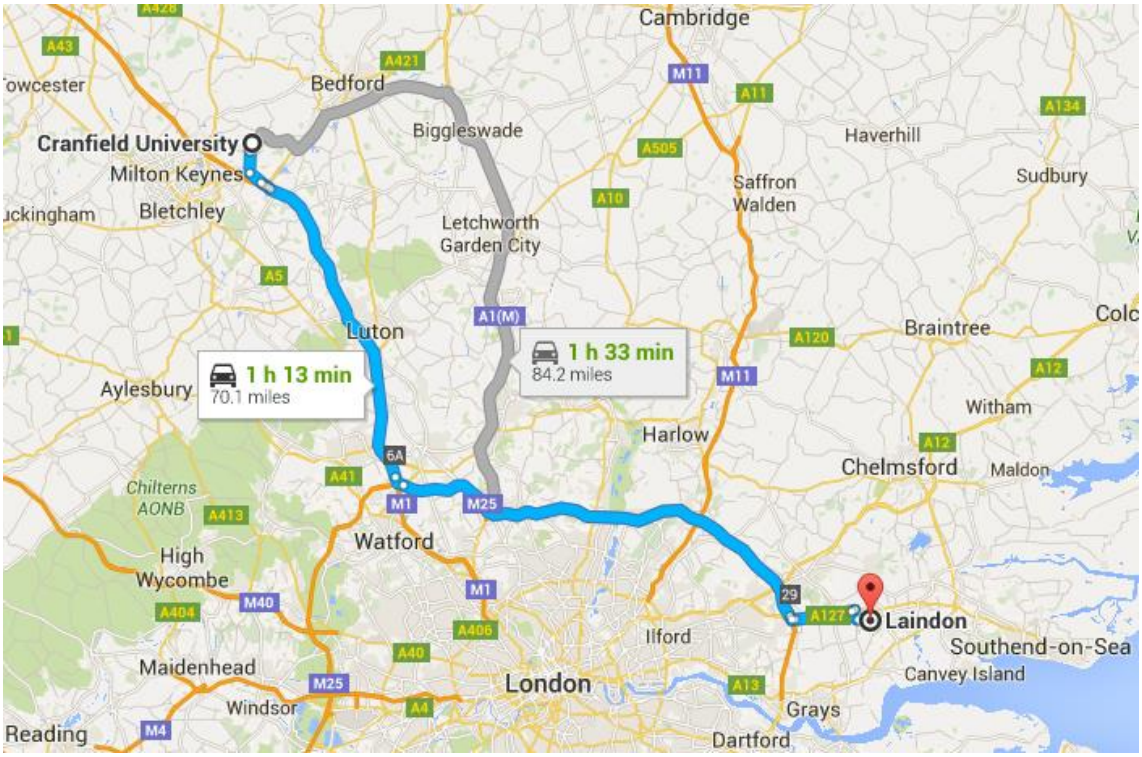

Figure 2-3 Global route planning from Cranfield to Laindon.

2.1.2 Path Planning

After the global route for reaching the destination is determined, the next procedure is to activate the local planning and input the obtained route and the local environmental information to the path planner. Generally, real-time path planning of autonomous vehicles is a recursive process and often focuses in determining the best local driving path since the global route of travelling can be attained by using GPS, digital maps or route planners. In order to generate a safe and reliable result with less deviation, numerous essential factors that include the dynamic traffic conditions, the surrounding environment, the vehicle motion constraints, the driving checkpoints and the status of obstacles have to be considered. As mentioned previously, selecting the ideal decision or manoeuvre, and generating the optimal local path are the two primary objectives which the vehicle autonomy needs to achieve in the path planning stage. The path planning starts with analysing the surrounding space of the vehicle and computing the available area for the forthcoming navigation task. The generated result is then sending to the paths searching and decision making block so as to output the optimal path based on the selected manoeuvre. The framework of the path planning can be found in Figure 2-4.

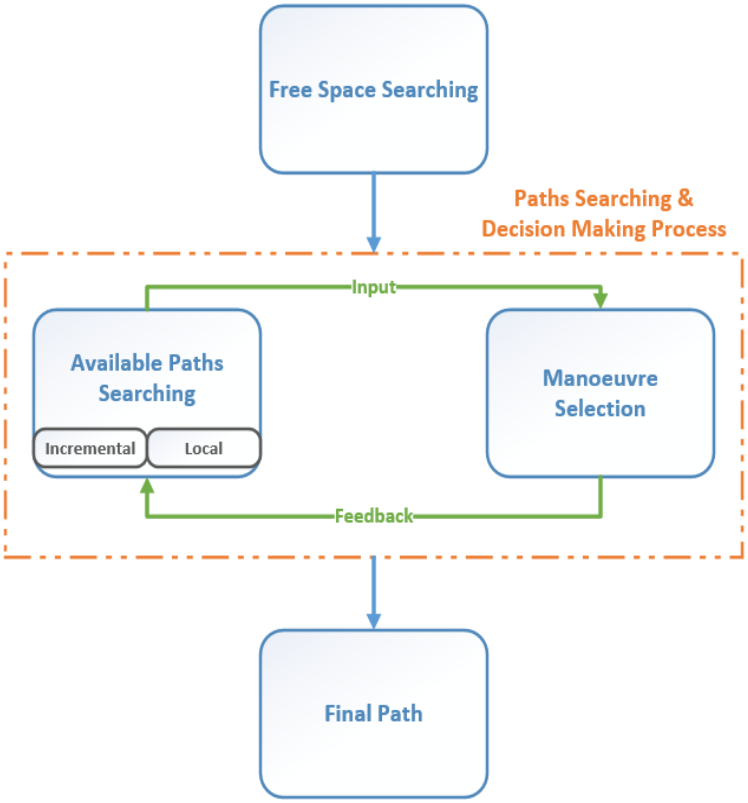

Figure 2-4 The structure of the path planning process.

A local geometric track that enables the vehicle to travel from an initial position to the intended terminal without any collision is defined as a ***Path***. Hence, ***Path planning*** is a computational procedure of figuring a feasible path that every configuration along the path is practicable. It is worthwhile mentioning that a reasonable configuration on the path not only achieves the collision-free performance but also refer to the constraints of motion (e.g. road boundaries, speed limitations, traffic regulations, etc.). On the other hand, a ***Manoeuvre*** can be treated as a description of potential motions that the vehicle is able to execute during driving. For instance, the general manoeuvres for vehicles on the motorway involve lane changing, overtaking, following, etc. Specifically, a manoeuvre that takes traffic regulations and other constraints into account and guarantees the safety of motion executions is called a nominal manoeuvre. Therefore, ***Manoeuvre planning*** is a process of considering the information which is provided from the available paths and on-board sensors (e.g. Radar,

Lidar, Camera etc.), and generating the best decision of potential manoeuvres for the vehicle [16].

Search Space for Planning

It should be noted that the entire planning process has to be operated under digital conditions, enabling the autonomy to compute and generate the optimal path. This means that the physical environment around the host vehicle at each time step has to be transformed into digital information before starting a planning cycle. Correspondingly, the location, the velocity, the orientation and other essential factors of the vehicle have to be digitalised and become the state variables of the vehicle. Both the digital map of the environment and the vehicle state space are indispensable to the autonomous vehicle. During the above discretisation, the level of the comprehensiveness will affect the performance and the accuracy of the planning. For instance, a good expressiveness map can provide precise results but might lead to heavy computation; an insufficient representation is able to increase the planning speed, however, has a high possibility to result in risk operations.

The existing algorithms of searching space for planning can be generally divided into the decomposition methodology and the boundary detecting technique [16]. The former includes Voronoi Diagrams [20][21], occupancy grids [22][23][24][25], cost maps [26][27][28] and state lattices [29][30]; these algorithms examine the available space with high resolution. The latter considers the location of obstacles, the boundary of lanes and roads, and other driving constraints, for instance, the driving corridors methodology [31][32].

Voronoi Diagrams

The possible driving space for an autonomous vehicle can be generated through Voronoi Diagrams or so-called Dirichlet tessellation techniques. This methodology figures the maximum distances which are also named Voronoi edges from the host vehicle to other adjacent obstacles on the road in order to avoid collisions. Briefly, the quality completeness and safety can be treated as its advantages. Nonetheless, Voronoi edges might potentially be discontinuous

during space searching and result in the fact that Voronoi Diagrams are lack of capability of dynamic path planning. Hence, Voronoi Diagrams are suggested to be utilised in static conditions and fixed environments [16]. An example of Voronoi Diagrams is illustrated in Figure 2-5.

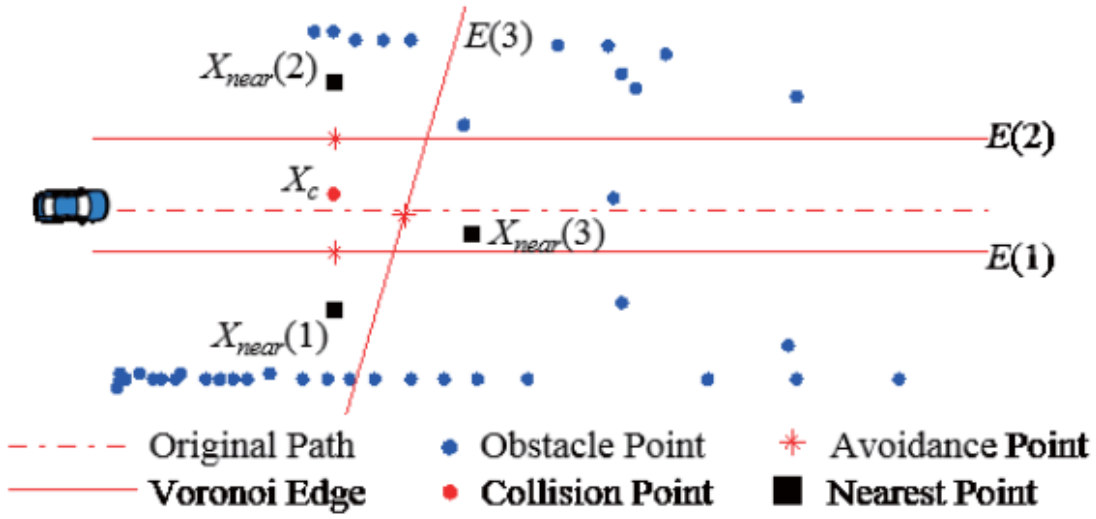

Figure 2-5 Voronoi Diagrams [20]**.**

Occupancy Grids

Apart from Voronoi Diagrams, the manoeuvre of Occupancy Grids is to segment the real world or state space into grids and each grid contains essential information. The information illustrates the probability of the grid being occupied by either surrounding vehicles or other obstacles, and enables the autonomy to calculate the available space for latish planning. Figure 2-6 (a) shows the conceptual diagram of Occupancy Grids.

Cost Maps

Cost Maps is similar to Occupancy Grids since both their primary principle is to discretise the state space. The main difference is that the grids in Cost Maps present cost proportions which are related to potential hazards or feasibilities of driving. Accordingly, the essential factors (e.g. the presence of driving boundaries, surrounding vehicles, obstacles, etc.) have to be considered during

computing the hazards or feasibilities. An instance of Cost Maps can be found in Figure 2-6 (b).

Both Occupancy Grids and Cost Maps are able to achieve fast discretisation without heavy computations and can be categorised as the grid-based methodology. However, these approaches have difficulties in managing the real-time vehicle dynamics and the presence deviations of obstacles [16].

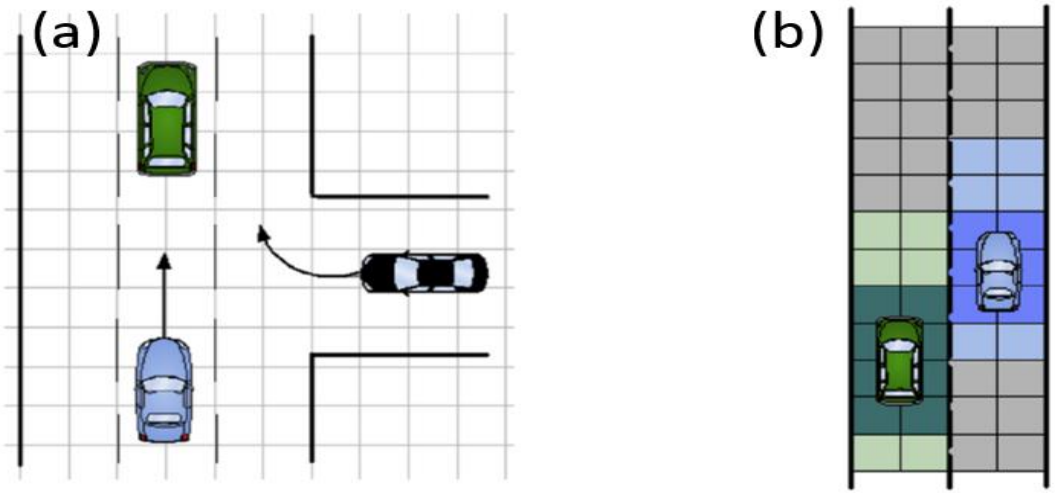

Figure 2-6 (a) Occupancy Grids and (b) Cost Maps [16]**.**

State Lattices

Another technique of searching space for planning is State Lattices which is depicted in Figure 2-7 (a). It is a generalisation of grid-based approaches and has the same procedure of discretising a continuous state space into numerous square or rectangular lattices. Vehicle positions, driving curvature and travelling time are taken into account so as to connect reasonable vehicle states and construct state lattices for space searching. Comparing to the normal grid-based methodologies, State Lattices consumes less time to achieve space searching and enhances the efficiency without increasing computational cost; the reason is that this approach is based upon the predefined curves and the pre-calculated edges. Hence, State Lattices can be treated as the improved version of Occupancy Grids and Cost Maps but has several limitations which

are the problems of curvatures, restricted motions and difficulties in solving emergency manoeuvres [16].

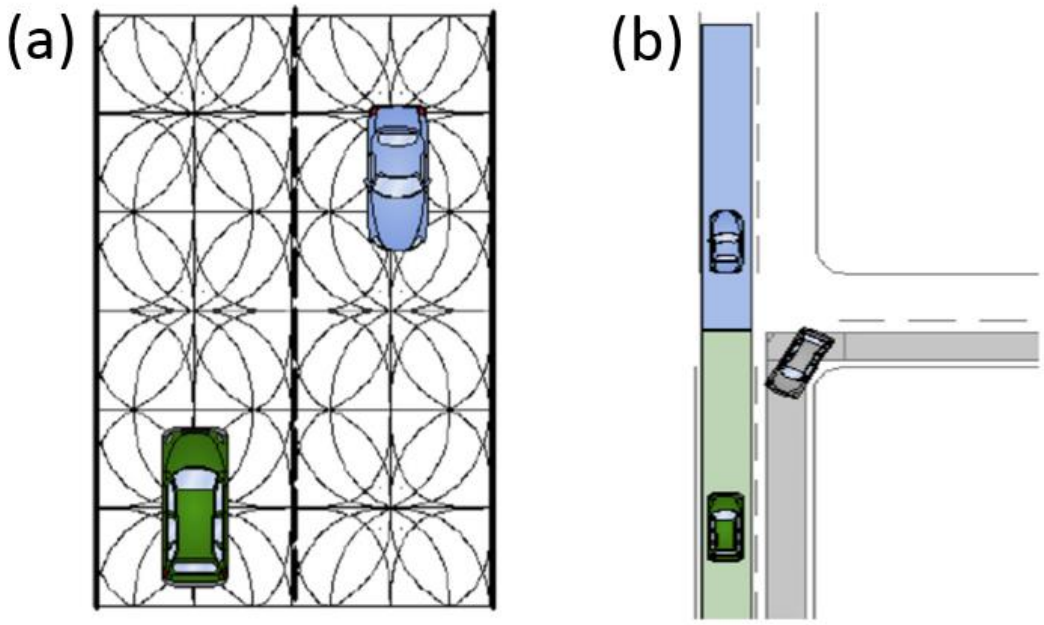

Figure 2-7 (a) State Lattices and (b) Driving Corridors [16]**.**

Driving Corridors

Driving Corridors is another approach of finding the available space for driving, which is established on the constraint information from precise digital maps and the chosen manoeuvre of the host vehicle. By using simultaneous mapping techniques, the essential information including road area, lane boundaries and surrounding obstacles can be acquired and utilised to compute continuous collision-free corridors. It should be noted that the occurrence of obstacles is constrained in the meantime since the lane boundaries restrict the area of the corridors. Although the vehicles and obstacles that are outer the driving corridors can be neglected, the continuous space which involves complex coordinates and road networks still force the Driving Corridors method to consume heavy computational power. Furthermore, the constraint on motion of the autonomous vehicle is another drawback of this methodology [16]. Figure 2-7 (b) presents a possible space searching result of using Driving Corridors.

The above methods of search space for planning have superior characteristics on different aspects and the corresponding expenses. By taking the restrictions and the demands of a specific application into account, the most suitable approach or even multiple methodologies of space searching are employed and cooperated in the computations, so as to provide good capabilities and ideal preparations for the following path, manoeuvre and trajectory planning. Briefly, the autonomy is able to activate the mathematical algorithms for planning in the next section and determine the best solution for autonomous driving once the available space is searched or established.

Paths Searching Techniques

The Available Paths Searching is one of the essential sections that the vehicle autonomy should operate after the surround free space of the vehicle is constructed. The searching or planning techniques can be distributed into Incremental Approach and Local Search according to the different manipulative purposes. The former reuses the historical data which is computed in the earlier searches to increase calculation speed and generate the optimal state conversion sequence of the vehicle. On the contrary, the latter concentrates on calculating the most appropriate single state transition for the current situation. As shown in Figure 2-4, this section collaborates with the Manoeuvre Selection block, and the combination of these two functionalities enables the autonomy to achieve and determine the final optimal path.

Paths Searching - Incremental Approach

The incremental approach represents the methodologies that are used for generating the optimal path when several vehicle states or relative configurations are undefined before the searching. Rapidly-exploring Random Tree (RRT) and Lattice Planner (LP) are the two common techniques of the incremental approach.

Rapidly-exploring Random Tree (RRT)

The primary concept of RRT is to build a search tree that uses stochastic samples from the configuration space and expands incrementally until the tree

reaches the objective configuration [33]. The entire process is operated recursively and can be mainly divided into two steps: (1) randomly adding new vertices or configurations near the terminals of the tree, and (2) connecting the new vertex to the nearest terminal point with an edge. It is worthwhile mentioning that RRT often requires an algorithm to detect potential collisions since the obstacle-free status of new vertices or configurations has to be approved. RRT is treated as one of the common methodologies that have been applied to solving autonomous driving, according to its strengths which are exploring the free space rapidly, guaranteeing the feasibility of real-time and kinematic implementations, ensuring the path safety through collision examinations and having the capability to manage general dynamical models. Nevertheless, the jagged paths, the necessity of impact examinations during expanding, the heavy computational cost under complex traffic scenarios and the strong dependence between the expansion and the nearest terminal points are the major disadvantages of RRT [16]. A demonstration of on-road driving using RRT is shown in Figure 2-8.

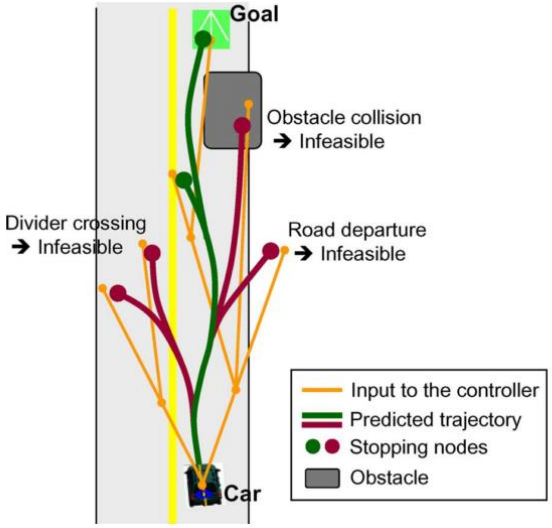

Figure 2-8 Rapidly-exploring Random Tree (RRT) for autonomous driving [33]**.**

Lattice Planner (LP)

Another incremental approach of path planning is Lattice Planner and its diagrammatic drawing can be found in Figure 2-9. This technique is based on the state lattice methodology of searching space for planning and therefore inherits its characteristics. As a result, Lattice Planner is often utilised to manage highly restricted or non-holonomic environments and has good performance in general [34]. Apart from RRT, the configuration space is discovered steadily within Lattice Planner. Moreover, Lattice Planner is able to promise the smoothness and the optimality of the generated paths and reduce the computational power within the precomputation lattice. Although the created path references of Lattice Planner mostly comply with the real motions and dynamic abilities of the vehicles, lack of performance in dealing with evasive manoeuvres is still one of the main disadvantages of Lattice Planner. Additional drawbacks of Lattice Planner can be summarised as the transferability and the possibility of exhaustive sampling and orientation oscillations [16].

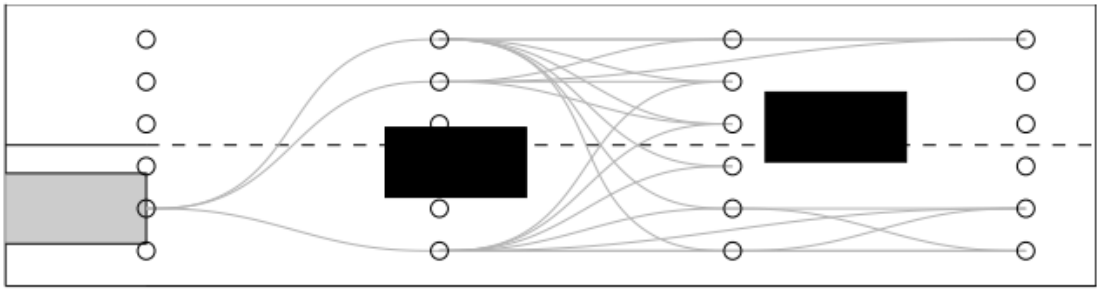

Figure 2-9 Path planning of using Lattice Planner [34]**.**

Paths Searching - Local Search

According to the fact that it is time-consuming for a path planner to search the complete graph within real-time applications, the Local Search, which is another category of path planning techniques, is then developed. Swerving Trajectories (ST) and Partial Motion Planning (PMP) are the two popular approaches in the local search category.

Swerving Trajectories (ST)

Swerving Trajectories, or can be called as rolling-out trajectories, firstly transforms the search space into a geometric curve and numerous duplications of this curve with different lateral shifts; the geometric curve can be a clothoid or a spline. Each generated curve represents a candidate path. Then, these candidates are assessed via one or more cost functions which contain several objective weight factors (e.g. safe margin, time constraint, etc.), so as to acquire the desired path. Based on the operating target of the lateral shifts, ST can be further classified as (1) lateral shifting in the vehicle state space and (2) lateral shifting in the vehicle action space, and is revealed in Figure 2-10. Although ST is able to produce feasible paths, it might fail or have poor performance within complex or dynamic environments [16].

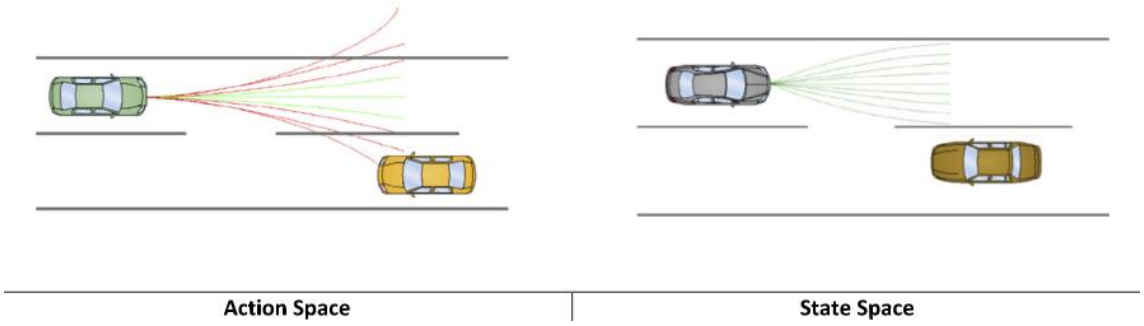

Figure 2-10 Two different classifications of Swerving Trajectories [16]**.**

Partial Motion Planning (PMP)

Another common approach is Partial Motion Planning. It is developed to solve the drawback of the high computational cost of other methodologies which analyse the entire vehicle state space with an infinite time horizon. PMP focuses in the next short time period and combines the technique of RRT with the functionality of safety checking to guarantee the obtained paths are collision-free. However, the surrounding environment information of the host vehicle must be fully observed in this approach and thus PMP might encounter difficulties while evaluating the path with a large number of obstacles [16]. Figure 2-11 shows the principle of PMP.

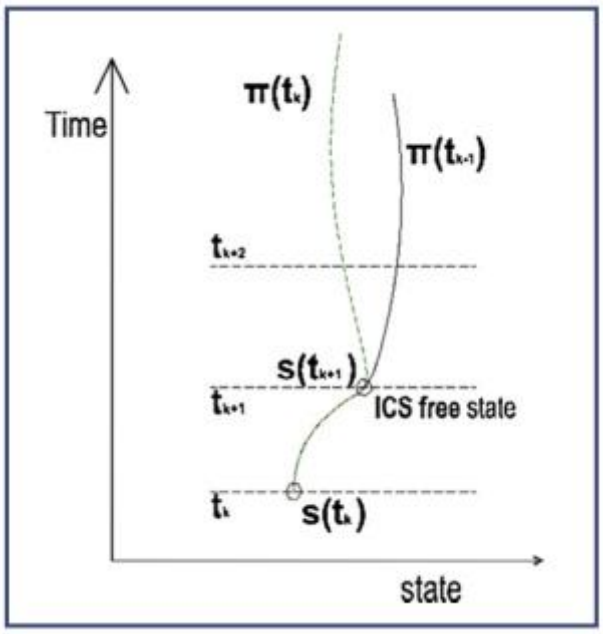

Figure 2-11 The Partial Motion Planning approach [16]**.**

Manoeuvre Selection and Decision Making

Since the available reference paths or the possible driving waypoints for the autonomous vehicle have been acquired from the path planner, the next essential task is to ensure that the most suitable and safest manoeuvre is always implemented at every self-driving moment. The entire decision process requests this step to take the interactions between the host vehicle and the surrounding traffic environment into account. Hence, the techniques of evaluating the adjacent traffic situation of the autonomous vehicle and predicting the behaviour of each surrounding transportation participants are incorporated in the manoeuvre planning (decision making) stage, enabling the autonomous vehicle to determine the optimal action and update the potential paths.

For instance, one of the common traffic accidents in daily life is the longitudinal collision, which is often caused by driver errors. Either steering, braking or warning the driver are the manoeuvres (decisions) that can be carried out by the vehicle autonomy so as to mitigate the fatality. Considering the situation that a vehicle has low velocity, braking seems to be the most efficient solution of avoiding longitudinal collisions, as well as the instinctive response of drivers

when encountering accidents [35]. This evaluation procedure which refers to the current situations of the host vehicle (e.g. low velocity, front obstacle) often happens within a short time period and is known as the manoeuvre selection or the decision making for an autonomous vehicle.

The manoeuvre selection process primarily depends on the autonomy or the intelligent system of autonomous vehicles. According to the reference architecture of American National Standards Institute (ANSI), an intelligent system comprises four processing units, which are World Model, Sensory Processing, Value Judgement and Behaviour Generation [36]. The basic structure of an intelligence system is illustrated in Figure 2-12. Each of the units is responsible for a specific functionality: the World Model is in charge of environments modelling and parameters estimation, the Sensory Processing relates to information filtering and data fusion, the Value Judgment evaluates control criterions, and the Behaviour Generation takes charge of control algorithms. Nonetheless, some practical systems might lack such fundamental functions considering computational and speed limitations.

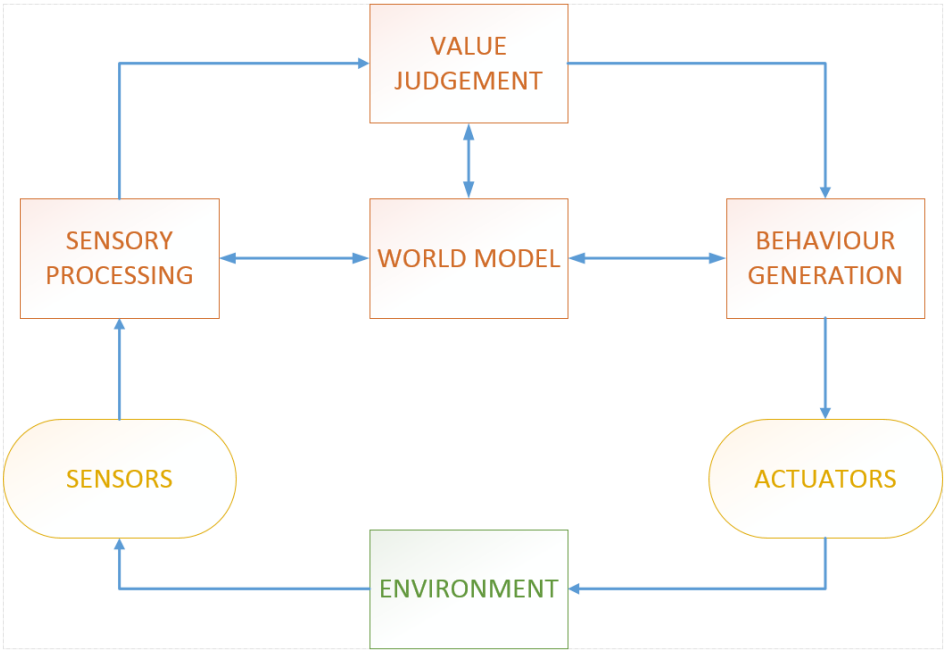

Figure 2-12 The reference structure of an intelligence system from ANSI.

From the various object-oriented programming methodologies in most previous research to the numerous techniques of agent-oriented programming recently,

all these efforts are made for enabling the autonomous software to handle essential factors (e.g. sensory objects, behavioural plans, memory, etc.) and make an appropriate decision. From the architectural point of view, six types of decision making mechanisms can be categorized: (1) reactive decision making, (2) behavioural decision making, (3) logic-based decision making, (4) situation calculus, (5) layered architectures, and (6) belief-desire-intention [36]. The logic-based architectures employ a set of deduction rule to model a decision making process since the 1980s. The behaviour-based and reactive architectures are then developed to solve the computational complexity problem in the logic-based methodologies via determining the decisions through environment situations. On the other hand, the situation calculus has the capability to infer actions and the related influences, and can be treated as a second-order logic. Apart from the above categories, the beliefs-desire-intention architectures attempt to imitate the human decision: (1) what goals a human want to achieve, and (2) how they are going to be achieved. Finally, the layered architectures which comprise several different layers, focus on solving the problem that internal states are required to remain minimum.

More generally, the methodologies of decision making can be split into two classifications, which are the techniques that emphasise obstacle predictions and risk assessments (e.g. Bayesian filter, hierarchical hidden Markov model, etc.), and the decision theoretic techniques (e.g. Partially Observable Markov Decision Process, Game Theory, etc.). The former often generates more precise solutions but the environmental situations might be neglected during the planning process; the high computational cost while anticipating the state of adjacent traffic participants can be treated as another drawback. On the contrary, the latter copes well with the surrounding environment and therefore might be able to solve the negotiation problems in urban areas or the manoeuvre compliances during the motorway driving (e.g. merging situations [37]) [16]. One of the well-known techniques of decision making is Markov Decision Processes (MDP). It can be utilised for either attentive perception determination or helping an autonomy to learn the actions which should be executed under given environmental states. The goal of using MDP is to obtain

the maximum reward during decision making so as to select the most appropriate action. Consequently, manoeuvre planning can be seen as a decision pivot which filters the possible outcomes from the path planner and approves the most feasible path inputting to the trajectory planning stage.

2.1.3 Trajectory Planning

Although numerous aerospace literatures have been published in the past decade and the trajectory planning of aircrafts is lucubrated much earlier than the intelligent vehicles, these outcomes and consequences are only able to provide limited assistance in the studies of on-road vehicles trajectory planning; the cause can be attributed to the fact that the operating environments between aircrafts and vehicles are quite different. Furthermore, it can be reasonably realised that the trajectories of aircrafts are generally treated with 6 degrees of freedom but the trajectories of vehicles are 3.

In the field of autonomous vehicles, once the optimal reference path and the best manoeuvre for the current driving situation have been determined, the next stage is to generate the local trajectory. A set of sequential states that are encountered by the vehicle during manoeuvre execution is signified as ***Trajectory***. The purpose of ***Trajectory Planning*** is to output the optimal trajectory, and the procedure can be illustrated as the on-line planning of vehicle transitions between two practicable states, which satisfies complex traffic limitations and driving requirements. In another word, trajectory planning can be seen as the stage of finalising the optimal connection between every two determined adjacent waypoints in the path [16].

The final trajectory which is obtained from the trajectory planning stage must fulfil specific requirements according to the original objective, for instance, the smoothness, the riding comfort, the driving constraint, the dynamical motion model, etc. Mostly, the trajectory planning process can be divided into two categories: (1) adjust the curvature of the trajectory which is mainly associated to the smooth motion during self-driving, and (2) optimise the trajectory with cost functions or control methods that take the vehicle model and surrounding obstacles into consideration [16]. While finding the most feasible trajectory in

the first type, arcs, spline curves, polynomial spirals, clothoid curves, and other geometric parameters can be used to form the trajectory; this technique is called ***Interpolation***, which indicates an action of structuring new data in the empty area between two previous identified boundaries. On the other hand, the second class uses numerical functions or control theories to maximise or minimise the objective variables such as the distance to the reference path or surrounding obstacles, the smoothness of the trajectory, the trajectory curvature, etc. so as to obey the kinematic constraints. Both the above two categories can be combined together to calculate a high precision trajectory, however, the computational cost might arise in the meantime.

Interpolation Methodology

While focusing on the trajectory planning of autonomous vehicles, the interpolation methodology attempts to insert a set of new curves within the blank space of the previous known reference points from the path planner in order to enhance the trajectory continuity [17]. Most of the previous researches focus in interpolating a certain type of geometric parameters and assembling all the best trajectory pieces between two points at each time steps to achieve the integrated trajectory [16]. Each of the potential geometric curves will be briefly introduced in the following section.

Lines and Circles

Straight lines and circular shapes are two of the basic elements in geometry and hence enable the trajectory planner to produce a straightforward connection between two adjacent waypoints. Although interpolating this type of geometric curves has several benefits such as low computational power requirement and simple implementation, it will also result in a non-continuous and jerky trajectory. This technique can be found in relative trajectory planning papers [38][39]. Figure 2-13 shows several possible trajectories that are composed of lines and circles.

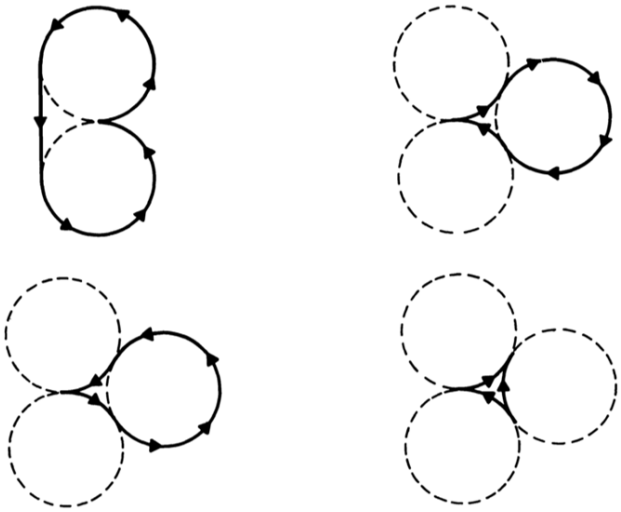

Figure 2-13 Line and Circles [38]**.**

Clothoid Curves

A curve which its curvature is equal to its arc-length is called a Clothoid curve. Therefore, this type of curves can be used to represent the trajectories that have linear variations of their curvatures, ensure the curvature continuity of the trajectory and provide fluent transitions between straight lines and curves. However, the poor smoothness of the curves is the drawbacks of interpolating Clothoid Curves. The detailed information and constraints of implementing Clothoid Curves to the trajectory planning of autonomous vehicles can be found in relevant research [40][41]. The draft diagram of Clothoid Curves is expressed in Figure 2-14.

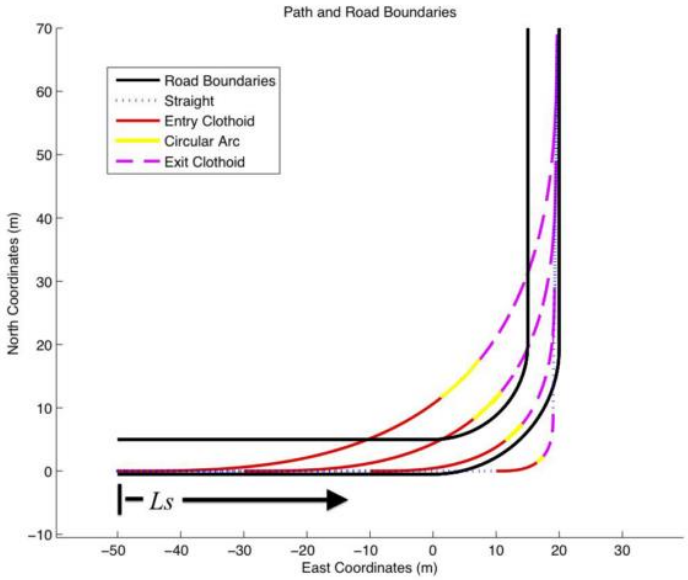

Figure 2-14 The Clothoid trajectories of executing a left turn manoeuvre [40]**.**

Polynomial Curves

Another popular type of geometric curves that has been used in trajectory planning is the Polynomial Curve. For instance, a second order polynomial is refined through considering the error between the current and the target vehicle state [42]; a fourth order polynomial is combined with a dynamic bicycle model so as to monitor the vehicle motion [43]. Polynomial Curves has the characteristic of fitting specific constraints and requirements (e.g. vehicle position, driving velocity, steering angle, trajectory curvature, etc.) at every point along the reference path. In other words, the determined vehicle states at every two adjacent waypoints of the path will assign the proper coefficients of the connection curves. Comparing with other geometric curves, Polynomial Curves requires relatively low power for the computation and is able to guarantee the continuity between two adjacent trajectory pieces. The accuracy of the trajectory can be improved by increasing the order number of the polynomial, but often raises the difficulty of finding the proper coefficients in the meantime. A schematic diagram that utilises a cubic and a quartic polynomials to reach different target positions is presented in Figure 2-15.

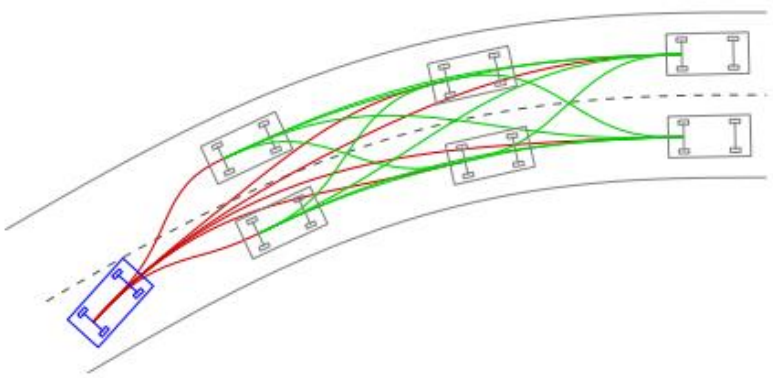

Figure 2-15 A cubic (green) and a quartic (red) polynomials curves [44]**.**

Bezier Curves

Bezier Curves is a type of geometric curves which is based on the Bernstein polynomial, and has the characteristic that its shape is determined by control points. The advantages of applying Bezier Curves to the trajectory planning of autonomous vehicles are similar with utilising Polynomial Curves; both types provide the possibility of the continuous concatenations of curves as well as the low demand of computation power. Nevertheless, the main drawbacks of interpolating Bezier Curves are that the malleability and the time consumption of the planning process become worse and large respectively as the degree of the curves increase. Although raising the degree will bring the above negative effects, high degree Bezier Curves is still treated as one of available solutions for trajectory planning due to the desired performance. A comparison research illustrates that the fifth order curves achieve better smoothness and feasibility than the third order [45]. Figure 2-16 depicts a right turn trajectory planning through interpolating Bezier Curves.

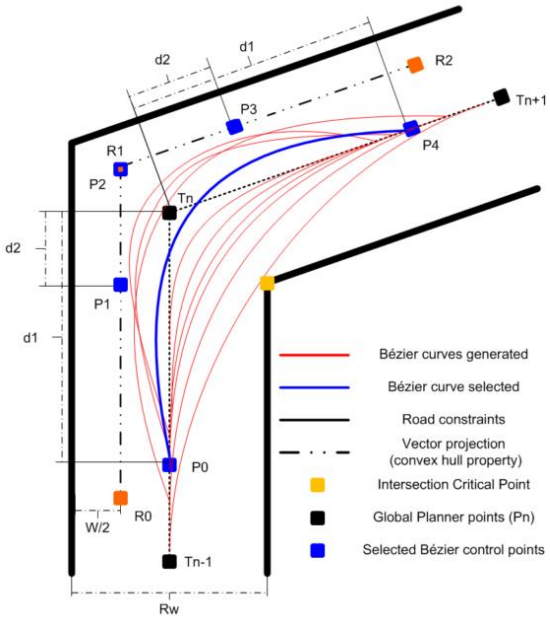

Figure 2-16 Bezier Curves for right turn trajectory planning [46]**.**

Spline Curves

A curve which can be divided into numerous polynomial-defined pieces is called a spline curve. This type of geometric curves is another popular methodology to solve the trajectory planning problem [47][48]. Spline Curves can be seen as the improved version of Polynomial Curves while it is able to generate similar results of higher degree Polynomial Curves without offering the instability; therefore, the low computational cost and the continuity are still retained in Spline Curves interpolations. However, the obtained trajectory might not be optimal if the primary objective is to fit the road constraints. Figure 2-17 shows the variance of a spline curve when a reference knot is changed.

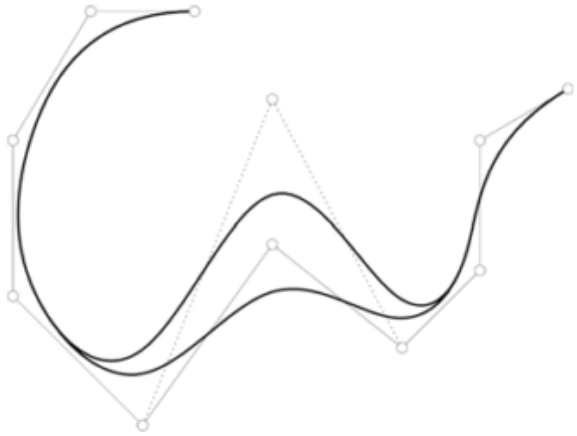

Figure 2-17 Spline Curves [17].

Optimisation Methodology

Apart from the interpolation method, the optimisation methodology aims to maximise or minimise the objective variables of the reference path or trajectory through numerical functions or control engineering techniques.

Function Optimisation

This technique applies one or more cost functions which are associated with the objectives to the reference path and finds the roots of the functions to generate the optimal trajectory. For instance, the lateral offset from the original path, velocity, acceleration and desired behaviour of the host vehicle are concerned in the cost function to obtain the result [49]. The pros of Function Optimisation are that the driving constraints, the surrounding obstacles and the adjacent vehicles can be easily considered in the planning process; but time-consuming is the potential trade-off.

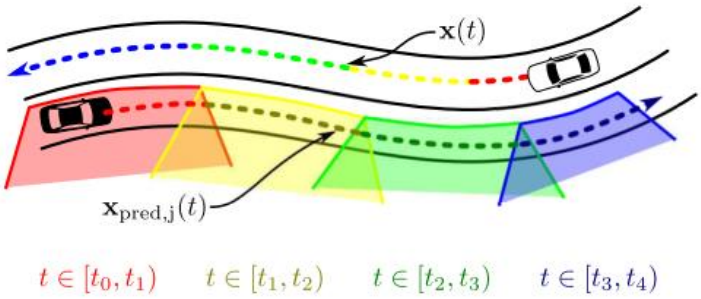

Figure 2-18 Trajectory planning by using a cost function [49].

Model Predictive Control (MPC)

Model Predictive Control (MPC) is another possible methodology to achieve the objective trajectory, which utilises the knowledge of the control engineering and the planning module. Specifically, the dynamic model and the current state of the host vehicle are required to predict the future state and thus the optimal trajectory can be acquired. Recent research combines a linear bicycle model which has linear tyre characteristics with MPC in the trajectory planning stage so as to acquire more comfort trajectory [34]. It is worthwhile mentioning that the performance of MPC is independent to the number of surrounding obstacles but the number of the vehicle model variables will affect the difficulty of optimising the trajectory.

Briefly, trajectory planning is the lowest level of planning for autonomous driving. According to the applied techniques, different essential information such as the vehicle model, the motion constraints, the locations of surrounding obstacles, etc. are required to optimise the piecewise trajectory [10][11].

Constraints and Limitations

One of the common limitations of existing path and trajectory planning techniques is the insufficient performance of obstacles handling which requires precise trajectory or motion predictions of the adjacent obstacles. Since computing and forecasting the traces of the obstacles at each time step require heavy computational cost, numerous related researches often assume the velocity or the acceleration of obstacles are constant. Furthermore, the obstacles are usually represented as simple shapes such as circles and rectangles. Another restriction is that most simple kinematic vehicle models are not able to monitor every detailed performance of the vehicle. The complex models, however, increase the computational power and are inadequate for real-time applications. The similar situation happens to the risk or collision indicators as well.

Also, the information of sensing specific obstacles, surrounding environment or lane boundaries might be blocked by other obstacles or barriers, and will result

in the imprecise perception. In general, the research and development can be categorised as simulations, experiments through model vehicles and the real-world implementations according to the testing environment. However, even with a high degree precision in the first two categories, a good planning performance in the real world is still difficult to be guaranteed These aforementioned constraints might lead to serious errors or inaccuracy manipulations during the motion planning procedure of autonomous vehicles.

2.2 Driving Styles

It is undoubtedly that the development of autonomous vehicles brings a dramatic revolution to the industry of transportation. Although automobile companies more or less encountered accidents during their on-road testing, the failure results cannot stop the pace of progress but indicate the insufficient area which requires further improvements of autonomous functionalities. The recent tragic fatality that happened to one of the Tesla customers while utilising “AUTOPILOT” especially emphasise the lack of mature techniques for guaranteeing passengers’ safety. Investigating and understanding human driver behaviours is one of the possible methodologies not only to enhance the performance and the reliability of self-driving technology but also to raise the drivers’ acceptability and meet their individual driving preference.

On the other hand, most of existed driving assistance systems merely consider the general behaviour of drivers and therefore may not be able to provide personalised functionalities and meet the requirements of individuals. As a result, it is necessary to develop algorithms that are able to detect and predict driver states, analyse and classify driving styles, and estimate intentions of human drivers. Since the preferences, the habits and the emotions of individuals have serious impacts on the driving styles during navigating, recognising different driving styles has been treated as a complex task. Instead of measuring and calculating the driving style straight forward, most previous researches focus on analysing indirect relationships (e.g. energy consumption [50], vehicle efficiency [51], etc.) so as to approach the driving style classification.

2.2.1 Terminologies and General Definitions

Numerous technical terminologies were created in the recent literatures that investigate the relationship among human drivers, environments and vehicle dynamics, such as driving behaviour, driving style, driving pattern, etc. In order to prevent the confusion and clarify the understanding, the individual definitions of these technical terms have to be summarised in advance. In general, ***Driving Pattern*** is closely associated with the road feature, the weather and the handling of the driver, mainly indicates the speed profile, the mean velocity, the acceleration and the deceleration of a vehicle during a driving period. On the contrary, ***Driving Behaviour*** represents the decisions and the manoeuvres of drivers, and particularly aims at the human or the intelligent driver itself rather than the external factors. Another technical term that is related to drivers is ***Driving Skill***. It majorly describes the capability of controlling the vehicle under a specific situation of a human driver, and can be utilised to distinguish basic, average and experienced drivers. On the other hand, ***Driving Condition*** depicts the external situations and limitations of the driving task, for instance, unimpeded or congested traffic, poor or clear visibility, etc. Turning, overtaking, lane changing, braking, acceleration or other possible manoeuvres that happens in a navigation task is called ***Driving Event***.

Driving Style which is the consequence of various factors such as emotion, habit, experience, etc., however, does not have a unified definition and still needs to be further discussed. The attitude and thought of drivers towards a driving assignment, the way to achieve a navigation mission, the aggressiveness potential of drivers, and other associated performances have been utilised to approach the driving style in recent literatures. Furthermore, personal character, age, gender and decision selection have been confirmed as essential factors to distinguish different driving styles, as well as driving history, navigation training and route and vehicle familiarity [52]. Fuel consumption is another possible approach to classify driving styles when driving conventional and fully electric vehicles instead of hybrid electrical ones [51][53]. Different road conditions such as slippery road, motorway, urban street, etc. also affect the performance of drivers [54] and hence the road style has to be precisely

identified before categorising the driving style [55]. It should be noticed that both the environmental conditions and the characteristics of different drivers have significant impacts on the driving style. An elaborate survey has summarised the potential factors that will influence the driving style and are shown in Figure 2-19 [56].

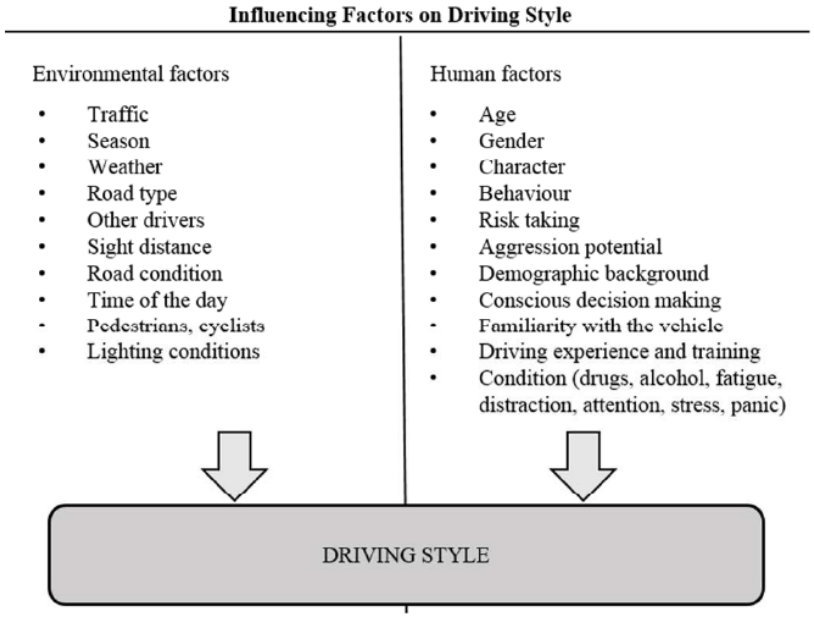

Figure 2-19 Potential factors that will affect driving style [56]**.**

Another human related terminology is ***Human-like***, which is extremely popular in the field of artificial intelligent. The core conception of human-like is to request an autonomy imitating the performance and the response of a real human being. As mentioned in Introduction, equipping the human-like characteristic in a vehicle autonomy is able to provide several outstanding advantages. For instance, increasing the public acceptance to autonomous vehicles, preventing the potential after-effects (e.g. the motion sickness, the unpredictable manipulation, etc.) while riding an autonomous vehicle, and so on. However, human-like functionality might also lead to the concern of driving safety. As a result, the human factor could be considered in autonomous systems if and only if the safety regulation is satisfied.

2.2.2 Driving Style Clustering

Although the influencing factors that mentioned previously can be used to cluster different driving styles, it is impractical to take all of them into account due to the restrictions of realistic situations (e.g. limitations of sensors, in-vehicle implements, computational power, etc.). Different available influencing variables have to be integrated with proper classification algorithms so as to achieve the driving style clustering. Generally, the classes of driver driving style are based on the allocation of the selected features and should be determined in advance of the development of the driving style identification algorithm. Moreover, with the purpose of defining a suitable set of clusters, not only the interaction among influence factors, human drivers, and surrounding traffic participants but also the trade-off between computational cost and clustering precision must be considered [56].

The original concept of driving style classification is mainly based on the recognition of driver patterns that aims to improve driving safety and vehicle efficiency; hence, the clusters of driver driving style in literatures often utilise either of them as the basis. For instance, eight different styles: (1) dissociative, (2) anxious, (3) risky, (4) angry, (5) high-velocity, (6) distress-reduction, (7) patient, and (8) careful are labelled while focusing the correlation between human factors and driving safety [52]; on the other hand, the vehicle efficiency which is acquired from the simulation of energy consumption was employed to indicate the driving style [57]. Apart from the clustering with large number of classes, most literatures prefer to distinguish driving style within two or three classes: (1) aggressive and (2) normal (non-aggressive) [58][59]; or (1) aggressive, (2) moderate and (3) mild [60][61]. The characteristic of aggressive drivers can be assigned to the unsafe performance during operating the vehicle, such as excessive driving velocity, sudden acceleration or braking, insufficient safe margin, etc. On the contrary, mild drivers merely perform gentle and smooth adjustment towards the steering wheel and the throttle. Moderate drivers might involve the features from both aggressive and mild groups but cannot be attributed to any of them explicitly [56].

2.2.3 Classification Algorithms

Based on the determined classes of clustering, available influence variables and the chosen identification technique, the algorithms of classifying driver driving styles can be carried out. The selected algorithm can be evaluated iteratively with different sets of influencing factors in order to deduce the suitable set of input variables and improve the classification performance and precision [56]. In addition, the potential classification algorithms are typically composed of (1) rule-based algorithms and (2) data-driven algorithms while considering the techniques which are utilised in the driving style clustering.

Rule-based Algorithms

The rule-based approach is a relatively simple methodology to achieve driving styles recognition. This method requires a set of predetermined thresholds to validate the specific driving style information (e.g. score, true or false, etc.) which is transferred from the raw driver driving data; hence, it is also named as threshold-based algorithm. For instance, the number of aggressive vehicle operations is counted from a driver within six different driving scenarios: acceleration, braking, left and right lane changing, and left and right turning, so as to evaluate the driving style of the driver [54]. Nonetheless, the standard rule-based algorithms might encounter difficulties and complexities to solve the driving style classification with a large number of input variables. An alternative solution is to apply the fuzzy logic technique since it has the characteristics of comprehensibility, simplicity, robustness and low computational demand [56]. The fuzzy logic driving style clustering can be further combined with the throttle and braking pedal information to advise the driver on the optimal operation of the pedals [53].

Data-driven Algorithms

Although the rule-based and fuzzy logic algorithms are simple to implement, they still have a crucial restriction which is that the predefined thresholds are fixed. This defect, however, can be solved by utilising data-driven algorithms to classify driver driving styles. Moreover, it has additional benefits of better

adaptability and the capability of managing a large amount of data and variables, which substantially popularise data-driven methodologies in solving driving style clustering problems [56]. A dynamic time wrapping technique is employed to identify the essential information which is acquired from the accelerometer, the gyroscope and the magnetometer of the smartphone; and the results are compared with the templates of different driving style so as to detect the aggressive manoeuvres during the driving period [58]. Machine learning is another well-known data-driven approach and also has the ability to classify different driving styles. One of the unsupervised learning techniques (K-means Clustering) to distinguish driving style is applied to the acceleration, the braking and the turning profiles extracted from vehicle Controller Area Network (CAN) bus. The simulation results illustrate that the braking profile is more representative than the other two features while classifying the driver driving style; furthermore, the Support Vector Machine (SVM) which is attributed to supervised learning techniques is also utilised to identify the same data and the outcome provides more constant performance compared with the K-means Clustering technique [62].

Both rule-based and data-driven algorithms have some techniques that can be operated either on-line or off-line to identify driver driving styles. For the on-line implementation, the time frame of data analysing has to be considered properly since the large time window might involve several manoeuvres and cause the absence of details; the small one might be too short to process an entire manoeuvre. It is worthwhile mentioning that none of the classification techniques can be concluded as the optimal solution to distinguish driving styles while the performance is considerably related to the operating conditions. However, according to the characteristics of drivers' driving data and the preference of statistical investigation, data-driven algorithms seem to be more preferable in recent researches [56].

2.3 Lane Change Manoeuvre

Almost all of the potential scenarios that a driver might operate when navigating on the motorway can be disassembled into five elementary manoeuvres: (1)

constant speed driving, (2) acceleration, (3) braking, (4) left lane changing, and (5) right lane changing. The Overtaking scenario is a typical instance which might comprise one or several transitions between adjacent lanes and is happened frequently during motorway driving [63]. For instance, overtaking the front slow vehicle often starts with a constant speed forward driving before either a left or a right lane changing; once the vehicle is shift to the adjacent lane, the acceleration manoeuvre is executed so as to overtake the target vehicle; then, the vehicle performs an opposite lane changing to merge back to the previous lane; ending up with a slight braking manoeuvre to decelerate the driving speed to a proper navigation velocity.

While focusing on the five elementary manoeuvres, the left and the right lane changes are more complicated compared with the other three. In order to execute a safe lane change manoeuvre, a large amount of essential information has to be captured and analysed by the driver or the vehicle autonomy in advance, including relative velocities with surrounding vehicles, available distance and space, traffic environments, etc. [64]. Especially for the autonomous vehicles, the autonomies have to imitate human drivers and obtain crucial information through different sensors and actuators (e.g. LiDAR, Radar, inertial sensors, electric motors, etc.). As a consequence, summarising a concise definition and potential variables of the lane change manoeuvre is indispensable.

2.3.1 Definition and Essential Parameters

Lane changing is one of the typical scenarios that happen generally during a driving task, and is specified as a transfer or lateral control manoeuvre of the ego vehicle from the current driving lane to either the right or the left adjacent lane [64]. Figure 2-20 provides the schematic diagram of a lane change manoeuvre. Nevertheless, there is no unified and agreed description on how to determine vehicle states from the initial point to the target point of a lane change manoeuvre.

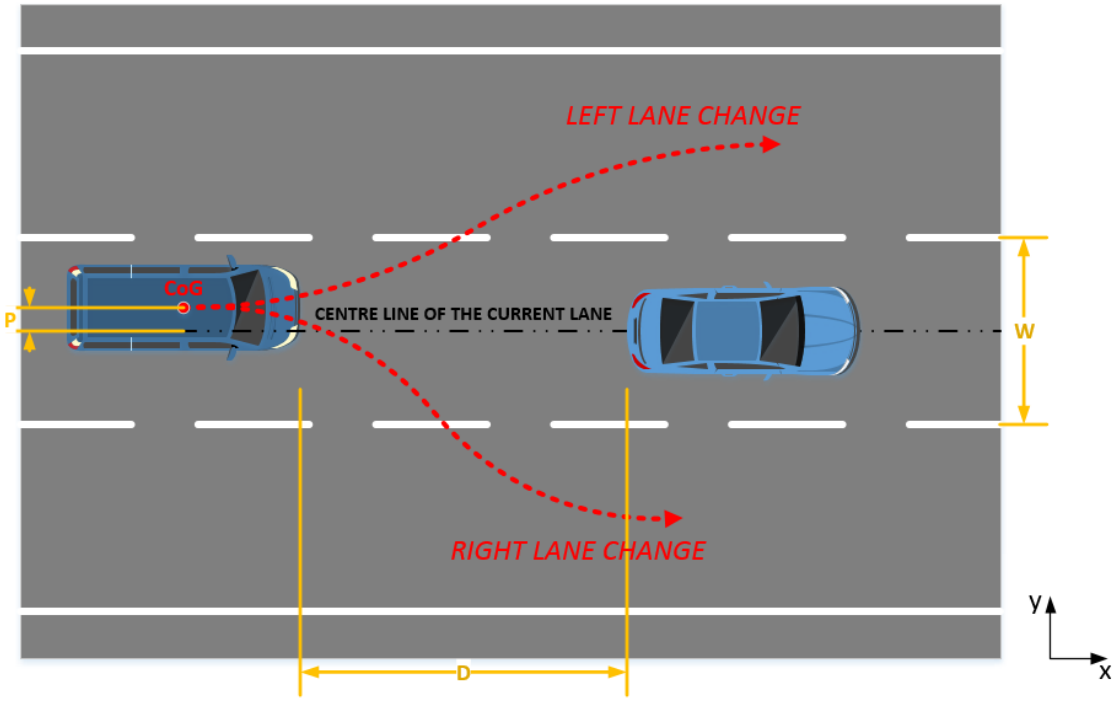

Figure 2-20 Lane change manoeuvre on a three-lane road.

Chee and Tomizuka utilised four different reference trajectories with constant forward velocity and maximum limitations of lateral acceleration and jerk to define the optimal lane change manoeuvre [65][66]. Shiller and Sundar gave the optimal emergency lane changing a definition that the trajectory performs the shortest longitudinal displacement during the lane transition period [67]. On the other hand, Hatipoglu et *al.* defined the end state of a lane change manoeuvre which has to fulfil the conditions: (1) both the lateral velocity and the lateral acceleration have to return zero, and (2) the vehicle lateral displacement has to be equal to the width of lanes; within the assumptions that only the yaw rate and the steering angle of the vehicle can be measured, and the variation of road curvature is remained in a small value [68]. Similarly, Shamir explicitly indicated the initial and the end states of a vehicle while completing a normal lane transition, which can be concluded as the vehicle has to perform the same longitudinal velocity, and zero acceleration and lateral velocity at both the initial and the end points; furthermore, the initial vehicle position has to be shifted a distance that equals the width of lanes in the lateral direction [63]. Table 2-1

presents a concise summary of the variables that were used to determine a lane change manoeuvre in the reviewed literatures.

It can be seen that some of the references applied up to 10 different parameters to describe a lane change manoeuvre, but one of the others merely considered 5 features. Accordingly, the more variables the evaluation takes into account, the higher fidelity the result will have. But its computational cost inevitably becomes expensive. In other words, it is a trade-off between the performance and the cost. Hence, assessing the research objective scrupulously so as to reduce the requirement of the computational power and generate a satisfactory result without losing the essential information is the prior task.

Table 2-1 Essential parameters for lane change manoeuvres.

Parameters	Descriptions	Publications
l_1	Distance from Centre of Gravity (CoG) to the front axle	[65]
l_2	Distance from CoG to the rear axle	[65]
D	Distance to the front vehicle (Clearing distance)	[67][69]
y	Lateral position	[63][65][67][68]
v_y	Lateral velocity	[63][68]
a_y	Lateral acceleration	[66][68]
J	Lateral jerk	[63][65][66]
P	Lateral displacement from CoG to the central line of the initial lane	[66]
x	Longitudinal position	[63][66][67][69]
v_x	Longitudinal velocity	[63][68]
K	Radius of trajectory curvature	[66]
δ	Steering angle of the front wheel	[65][66][67][68][69]
T	Time of the lane change manoeuvre	[63][65][66][67][68][69]
V	Vehicle velocity	[63][65][66][67][69]
A	Vehicle acceleration	[63]
W	Width of the lane	[66][67][68]
ε	Yaw angle	[65][66][67][68]
γ	Yaw rate	[67][68]

2.3.2 Discussion

Chee and Tomizuka defined that the ideal trajectory of a lane change manoeuvre has to guarantee the passenger ride comfort and the transition time. This optimal lane change trajectory is also termed as the virtual desired trajectory (VDT) since it is not materially marked on roads and can be proposed through the trapezoidal lateral acceleration profile. In order to generate a VDT, the vehicle acceleration profile is presumed to be trapezoidal, and the position

of the vehicle while operating the lane change manoeuvre can be acquired through integrating the trapezoidal acceleration profile twice [65]. It should be noted that the potential VDTs can be constructed based on different techniques. To further discuss the optimal VDT for the lane change manoeuvre, the authors analysed and compared four different types of VDT: (1) circular trajectory, (2) cosine trajectory, (3) fifth order polynomial trajectory and (4) trapezoidal acceleration trajectory under the same condition (constant forward velocity and maximum limitations of lateral acceleration and jerk). The trapezoidal acceleration trajectory was claimed as the optimal VDT for a lane change manoeuvre since the passengers' comfort and the duration of the lane changing manoeuvre are the two most crucial considerations [66].

Apart from generating a VDT, another possible methodology to determine the vehicle states is to apply the optimal yaw rate as the reference during the lane change scenario. With the virtual yaw reference, the ideal lane change trajectory can be conducted [68]. A lane change manoeuvre might also be executed to avoid a sudden accident; therefore, a normal comfortable transition might not be feasible in this urgent scenario. Shiller and Sundar proposed an emergency lane change manoeuvre to avoid a front obstacle and identified the boundaries whether the vehicle should operate a lane changing or simply maintain in the original lane and decelerate the speed to lessen the collision damage, based on different initial vehicle velocities. The trajectory optimisation can be focused on minimising the reaction time and the clearing distance (the distance to the front vehicle or obstacle) so as to obtain the optimal emergency lane changing [67].

An extended manoeuvre of the lane changing is the overtaking; Shamir divided it into three phases: (1) a diversion from the current lane to either the left or the right adjacent lane, (2) a straight forward driving in the adjacent lane to overtake the target vehicle, and (3) another transition back to the original lane when overtaking a front slow vehicle. The fifth order polynomial was used to generate the lane change trajectories and these trajectories are optimised through minimising the jerk and the kinematic energy [63]. A more specific overtaking

research that takes different relationships between the ego vehicle and the front vehicle into account is then investigated. Naranjo et *al.* combined the fuzzy logic control methodology which has the capability to imitate the behaviour and the reactions of human drivers with a high accuracy GPS and a wireless communication environment to approach the two lane change trajectories during the overtaking scenario [69].

Although previous publications have investigated the lane change manoeuvre either on motorways or normal roads, the human factor which plays an important role in driving tasks is seldom considered. One of the primary reasons is that the human decision making in complex scenarios is difficult to imitate, for instance, it depends on personal characteristics and could significantly be influenced by the surrounding environment and the time factors. Since the Constant Yaw Rate and Acceleration (CYRA) model which is ordinarily utilised in risk evaluation and trajectory estimation provides accurate performance only in a short period motion but not for a long term behaviour such as an entire process of lane changing (e.g. two to seven seconds), Wen et *al.* developed a parametric approach of predicting lane changing trajectory on motorway. Apart from most of the other mathematical algorithms that focus on finding an optimal path, this methodology takes human factors into account and generates a human-like trajectory of lane changing based on the driving pattern of a specific driver [70]. As a consequence, achieving the human-like lane change for autonomous vehicles will be the next challenge to overcome.

2.4 Model Predictive Control

Model Predictive Control (MPC) is one of the advanced techniques in the control system, which can be dated back to 1980s. Although it has more than 25 years history, this control technique still draws attention in both the academia and the industry in recent years; especially in the field of transportation and power system [71][72][73][74][75][76][77]. Briefly, the system model, the measurements and the system state at the current time step, and the process variable references are the essential factors while operating MPC; and the primary objective of MPC is to calculate a sequence of future control input $\boldsymbol{u}$

with the purpose of optimising the future performance of the targeted system output $\boldsymbol{y}$. This optimisation process is manipulated within a finite range of time steps (i.e. prediction horizon). According to the consideration of both the current system information and the constraints of inputs, outputs and system state, MPC is able to perform the advantage of strong robustness [71][72]. Figure 2-21 indicates the general block diagram of using MPC techniques to control the target system. The purpose of the Internal Model in the model predictive controller block is to monitor and predict the real system behaviour. Therefore, the more identical of the Internal Model to the actual System Model is, the more accurate for MPC to control the real plant will be.

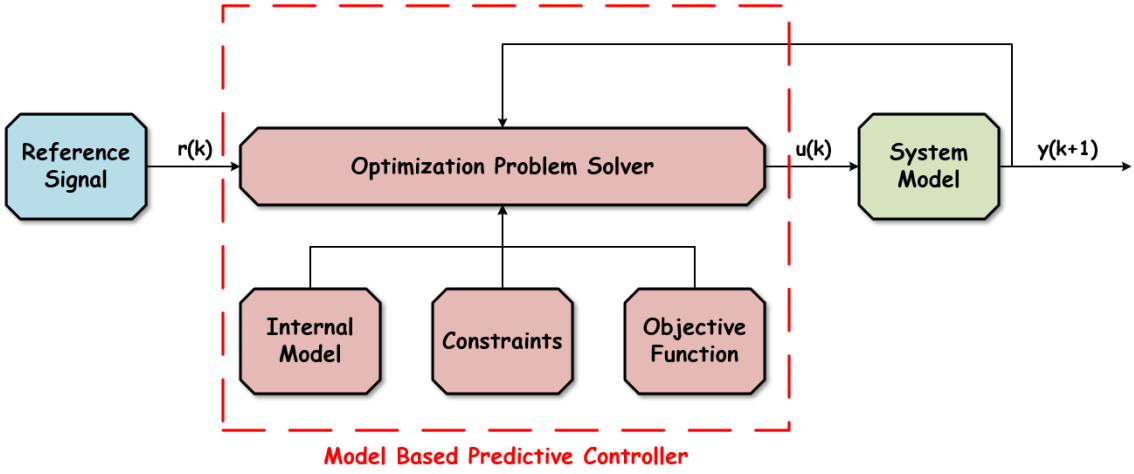

Figure 2-21 The block diagram of a model predictive controller.

In other words, MPC has the capability of anticipating future behaviour of the system and computing the optimal inputs accordingly. This predictive characteristic which cannot be achieved in most traditional control techniques (e.g. PID control, LQR control, etc.), resulting MPC to be one of the effective control techniques while solving motion planning problems of autonomous vehicles. Though comparing to other control techniques, the control progress of utilising MPC might require more processing time to manage real-time problems; the impact of this drawback can be minimised with the availability of fast solving methods and products in the market recently. This chapter

summarises the knowledge of MPC in order to support the design of human-like trajectory planning.

2.4.1 General Discussion

MPC is a model-based control technique and its performance mainly relies on the accuracy of the model of the target system. By minimising the value of the objective function which is also termed as the cost function, MPC is able to generate the optimal control signal to the system. An instance of Single-Input Single-Output (SISO) MPC is shown in Figure 2-22. In order to better understanding the principle and the theory of MPC, several terminologies should be interpreted in advanced.

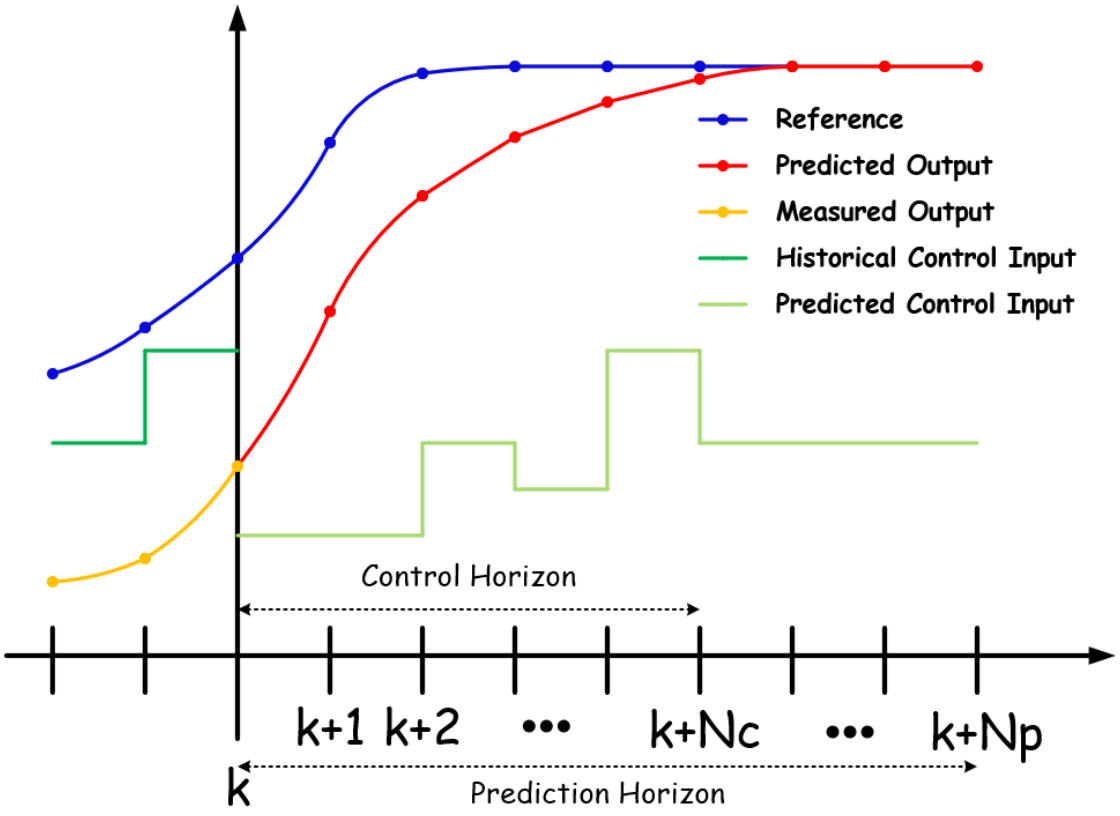

Figure 2-22 A general scheme of discrete SISO MPC.

Moving Horizon Window is a time-dependent window. This horizon window is moveable with a time step basis during the MPC process. For instance, MPC predicts the system behaviour within the prediction horizon window (i.e. from $\boldsymbol{k}$ to $\boldsymbol{k+N_p}$) at current time step $\boldsymbol{k}$; and the window will shift to $(\boldsymbol{k+1})$ to $(\boldsymbol{k+}$

$N_p + 1$) at the next time step $(k + 1)$, where N_p is the constant value that indicates the length of the Prediction Horizon.

Prediction Horizon depicts the period that we would like to estimate for the system future behaviour. The length of Prediction Horizon is N_p and it should be noted that N_p is a number of sample steps rather than a period of time.

Control Horizon indicates the duration (i.e. $k + N_c$) that the manipulate variables are adjustable while estimating the system performance. Beyond the control horizon, the value of the manipulated variables will fix at their last values at time step $k + N_c$ and remain constant until the final time step of the prediction (i.e. $k + N_p$). The length of Prediction Horizon is N_c, where $N_c \leq N_p$. Similar to Prediction Horizon, N_c represents a number of sample steps.

Receding Horizon Control is the most important characteristic of MPC. It only takes the first sample signal from the predicted control sequence as the system actual input and abandons the rest, though the optimal sequence of future control inputs within the Prediction Horizon is already estimated. It should be noted that in order to predict the optimal future control sequence from k to $k + N_p$, the information at the time step k is required and is denoted as the vector $x(k)$. This information $x(k)$ contains numerous system relevant factors, which can be obtained through either estimations or direct measurements.

System Model is a model that describes the properties and the dynamics of the target system, including Transfer Function Model, State Space Model, Zero-Pole-Gain Model, etc.

Internal Model is a linear-time-invariant (LTI) model that has been used in the prediction process of MPC. In general, Internal Model remains the same as System Model; but will be linearized or simplified when the System Model is nonlinear or too complex. Internal Model is essential towards MPC due to the fact that its fitness and quality will affect the predictive control performance. In other words, a precise and consistent future prediction of the system behaviour can be acquired from a well-fitted model.

Control Objective is the requested system behaviour which should be achieved through applying a specific control technique. While utilising MPC methodology, the objective is associated with a function that represents the difference between the actual and the desired system responses; this objective function is also termed as the cost function $\boldsymbol{J}$. By minimising the value of $\boldsymbol{J}$, MPC is able to generate the optimal control sequence within the Prediction Horizon.

Since the brief illustrations of the terminologies that are frequently utilised in MPC have been introduced, the following paragraphs will describe the draft principles and the procedures of manipulating MPC.

In general, MPC is based on a given Internal Model and iteratively executes control optimisations within the Prediction Horizon while considering the system state $\boldsymbol{x}(\boldsymbol{k})$ at cuthe rrent time step $\boldsymbol{k}$. The predicted future system states are denoted as $\boldsymbol{x}(\boldsymbol{k}+1|\boldsymbol{k})$, $\boldsymbol{x}(\boldsymbol{k}+2|\boldsymbol{k})$,…, $\boldsymbol{x}(\boldsymbol{k}+\boldsymbol{N_p}|\boldsymbol{k})$. The objective function is calculated to obtain the optimal future control sequence that minimises its value from $\boldsymbol{k}$ to $\boldsymbol{k}+\boldsymbol{N_p}$; the future control trajectory is denoted by $\boldsymbol{u}(\boldsymbol{k})$, $\boldsymbol{u}(\boldsymbol{k}+\mathbf{1})$,…, $\boldsymbol{u}(\boldsymbol{k}+\boldsymbol{N_p}-\mathbf{1})$. However, only the first control signal $\boldsymbol{u}(\boldsymbol{k})$ from the obtained optimal sequence will be implemented to the System Model and the rest will be neglected. After the first optimisation cycle, the Prediction Horizon is then shifted to the next time step $\boldsymbol{k}+\mathbf{1}$, and the MPC activates a new optimisation cycle while taking the new system state $\boldsymbol{x}(\boldsymbol{k}+\mathbf{1})$ into account so as to generate the new optimal future control sequence from $\boldsymbol{k}+\mathbf{1}$ to $\boldsymbol{k}+\boldsymbol{N_p}+\mathbf{1}$; similarly, only the first control input $\boldsymbol{u}(\boldsymbol{k}+\mathbf{1})$from the new sequence will be inputted to the system.

The above processes are recursively operated as the Prediction Horizon keeps shifting to the next sample time, and therefore MPC is also called Receding Horizon Control. Consequently, MPC has the capability to optimise the current time step while taking the future time steps within a specific period into account, and overcome the system uncertainties which are caused by external disturbance, model-plant mismatch, time variants, etc. under realistic situations.

2.4.2 State Space Model

As mentioned in the previous section, the performance of MPC relies on the model which is intended to monitor and describe the dynamical behaviour of the target system. At the early stage of MPC history, the Finite Impulse Response (FIR) models and the step response models were widely implemented in the control process according to the characteristic of clearly describing the delay of the process time, the response time and the gain; but these models are restricted to stable systems. Transfer function models were later utilised to represent the systems in MPC applications since these models provide a more parsimonious way of describing system dynamics and can be applied to both stable and unstable systems. However, the transfer function MPC is often considered to deliver poor performance in managing multi-variable systems. Apart from the above system models, the state space model draws attention recently as it has the ability to handle the multi-variable system and therefore is used to describe the dynamics of the target system in MPC [72].

Considering the research tasks of this project, the vehicle autonomy is required to execute the entire lane change manoeuvre during motorway driving and the Three-Point Turn under low-speed condition. The control inputs of these manoeuvres are composed of the vehicle velocity, the lateral acceleration, the longitudinal acceleration, the steering angle, the distance to safety boundaries, and other essential driving parameters. As a result, the state space model can be seen as the most suitable solution to describe the system dynamics of a lane change manoeuvre.

Equation 2-1 and Equation 2-2 show the state space representation of a normal LTI System in time-continuous form.

$$\dot{\boldsymbol{x}}(\boldsymbol{t}) = \boldsymbol{A}\boldsymbol{x}(\boldsymbol{t}) + \boldsymbol{B}\boldsymbol{u}(\boldsymbol{t}) \quad \textbf{(2-1)}$$

$$\boldsymbol{y}(\boldsymbol{t}) = \boldsymbol{C}\boldsymbol{x}(\boldsymbol{t}) + \boldsymbol{D}\boldsymbol{u}(\boldsymbol{t}) \quad \textbf{(2-2)}$$

Where $\boldsymbol{x}$ is the system state, $\boldsymbol{u}$ and $\boldsymbol{y}$ are the input and the output parameters, $\boldsymbol{A}$ is the transition matrix, $\boldsymbol{B}$ and $\boldsymbol{C}$ respectively represent the input and the

output matrices, and $\boldsymbol{D}$ is the feedthrough matrix that describes the relationship between the system input $\boldsymbol{u}$ and the system output $\boldsymbol{y}$.

The discrete time version of the state space model is presented in Equation 2-3 and Equation 2-4.

$$\boldsymbol{x(k+1) = A_d x(k) + B_d u(k)} \quad \textbf{(2-3)}$$

$$\boldsymbol{y(k) = C_d x(k) + D_d u(k)} \quad \textbf{(2-4)}$$

Where the subscript $\boldsymbol{d}$ denotes the discrete version of the matrices, and $\boldsymbol{k}$ is the sampling time step.

According to the property of the discrete state space model and the characteristic of Receding Horizon Control, the prediction phase of MPC is based on the information of system state at current time step $\boldsymbol{k}$, which leads to the reasonable assumption that the input signal $\boldsymbol{u(k)}$ at time $\boldsymbol{k}$ has no impact to the system output $\boldsymbol{y(k)}$ at the same time step. Hence, the matrix $\boldsymbol{D_d}$ is assigned to 0, and Equation 2-4 can be rewritten as Equation 2-5.

$$\boldsymbol{y(k) = C_d x(k)} \quad \textbf{(2-5)}$$

2.4.3 Predictive Control

Once the type of the Internal Model has been determined and converted into a discrete form, the next stage is to operate the predictive control; which can be generally divided into two parts: the prediction and the optimisation.

2.4.3.1 Prediction

As mentioned in Equation 2-3, the state of the system $\boldsymbol{x(k+1)}$ at the time step $\boldsymbol{k+1}$ can be obtained based on the current system state $\boldsymbol{x(k)}$ and input $\boldsymbol{u(k)}$. Similarly, the state at the next time step $\boldsymbol{x(k+2)}$ can be predicted according to the same equation, and is derived in Equation 2-6 and Equation 2-7.

$$\boldsymbol{x(k+2) = A_d x(k+1) + B_d u(k+1)} \quad \textbf{(2-6)}$$

$$\boldsymbol{x(k+2) = {A_d}^2 x(k) + A_d B_d u(k) + B_d u(k+1)} \quad \textbf{(2-7)}$$

The predicted iterations will be continued up to the Prediction Horizon, which are N_p steps ahead from current step; as shown in Equation 2-8.

$$\begin{Bmatrix} x(k+1) \\ x(k+2) \\ \vdots \\ x(k+N_p) \end{Bmatrix} = \begin{bmatrix} A_d \\ {A_d}^2 \\ \vdots \\ {A_d}^{N_p} \end{bmatrix} x(k) + \begin{bmatrix} B_d & 0 & \cdots & 0 \\ A_d B_d & B_d & \cdots & \vdots \\ \vdots & \vdots & \ddots & 0 \\ {A_d}^{N_p-1} B_d & \cdots & A_d B_d & B_d \end{bmatrix} \begin{Bmatrix} u(k) \\ u(k+1) \\ \vdots \\ u(k+N_p-1) \end{Bmatrix} \quad \textbf{(2-8)}$$

Furthermore, the estimated output can be found in Equation 2-9.

$$\begin{Bmatrix} y(k+1) \\ y(k+2) \\ \vdots \\ y(k+N_p) \end{Bmatrix} = \begin{bmatrix} C_d & 0 & \cdots & 0 \\ 0 & C_d & \cdots & \vdots \\ \vdots & \vdots & \ddots & 0 \\ 0 & \cdots & 0 & C_d \end{bmatrix} \begin{Bmatrix} x(k+1) \\ x(k+2) \\ \vdots \\ x(k+N_p) \end{Bmatrix} \quad \textbf{(2-9)}$$

2.4.3.2 Optimisation

After the deduction of predicting the future system behaviour (i.e. within the Prediction Horizon) based on the system information at the current time step, MPC algorithm will then compute the sequence of future control input to optimise the reference-following response. Precisely, the optimisation process is to minimise the value of cost function J. Equation 2-10 presents the common formulation of the cost function.

$$J = \sum_{i=1}^{N_p} \left(x(k+i) - x_{ref}(k+i)\right)^T Q(i) \left(x(k+i) - x_{ref}(k+i)\right) + \sum_{i=0}^{N_c-1} \left(u(k+i) - u_{ref}(k+i)\right)^T R(i) \left(u(k+i) - u_{ref}(k+i)\right) \quad \textbf{(2-10)}$$

where N_p is the Prediction Horizon; N_c is the Control Horizon; $x_{ref}(k+i)$ is the reference of the system state; $u_{ref}(k+i)$ is the reference of the manipulated input; and $Q(i)$ and $R(i)$ are the weighting matrices related to the system state

and the manipulated input with time step $\boldsymbol{i}$ ahead from the current time respectively.

Although the product of the optimisation stage is a sequence of control input within the Prediction Horizon: $\boldsymbol{u(k)}$, $\boldsymbol{u(k+1)}$,…, $\boldsymbol{u\left(k+N_p-1\right)}$, only the first one, $\boldsymbol{u(k)}$, will be treated as the optimal signal and inputted to the real system model.

2.4.4 MPC with Constraints

Comparing to some traditional control techniques, MPC has the benefit of considering different types of constraints while controlling the system. Several types of constraints that regularly encountered in applications will be introduced in this subsection.

Constraints on the Amplitude of the Control Variable

In most of the real systems, the value of manipulated variables is restricted within a certain range in order to guarantee the stability, the safety, the acceptable performance, etc. The mathematical form of this constraint is stated in Equation 2-11.

$$\boldsymbol{u^{min} \leq u(k) \leq u^{max}} \quad \textbf{(2-11)}$$

where $\boldsymbol{u^{min}}$ and $\boldsymbol{u^{max}}$ indicate the lower and the upper bounds of control variables respectively.

Constraints on the Control Variable Incremental Variation

Apart from the amplitude constraint of control variables, their rates of changes (i.e. the incremental variation of the control input $\Delta\boldsymbol{u(k)}$ between two different sample steps) are often regulated in the meantime. If the upper limit and the lower limit are assumed as $\Delta\boldsymbol{u^{max}}$ and $\Delta\boldsymbol{u^{min}}$ in a single-input system, the constraint on the control variable incremental variation can be specified in Equation 2-12.

$$\Delta\boldsymbol{u^{min} \leq \Delta u(k) \leq \Delta u^{max}} \quad \textbf{(2-12)}$$

Output and State Variable Constraints

The operation field of the system output can also be constrained, as written in Equation 2-13.

$$\boldsymbol{y^{min} \leq y(k) \leq y^{max}} \quad \textbf{(2-13)}$$

where the upper limit is $\boldsymbol{y^{max}}$ and the lower limit is $\boldsymbol{y^{min}}$.

It is worthwhile mentioning that output constraints are often considered as 'soft' constraints due to the fact that enforcing this type of constraint might lead to large variations in both the control variables and their incremental variations; within this circumstance, the control variables or their incremental variations could violate their own constraints and cause the constraint confliction. In order to solve the problem, a slack variable $\boldsymbol{s_v > 0}$ is added on both the upper and the lower limits in Equation 2-13, as shown in Equation 2-14.

$$\boldsymbol{y^{min} - s_v \leq y(k) \leq y^{max} + s_v} \quad \textbf{(2-14)}$$

For instance, a large slack variable will be selected to solve the conflict problem and relax the output constraints when the control input constraints are more crucial to the system operation.

Similarly, constraints are also available to impose on the state variables if they are measurable or the observer state variables; but these constraints have to be formed as 'soft' constraints according to the same reason as the aforementioned output case.

Constraints in a Multi-Input and Multi-Output Setting

The previous instances are concentrated on SISO systems. MPC constraints are also suitable for Multi-Input and Multi-Output (MIMO) system, but each variable constraint has to be specified independently.

The amplitude constraints of each manipulated variable are shown in Equation 2-15 to 2-17.

$$\boldsymbol{u_1}^{\boldsymbol{min}} \leq \boldsymbol{u_1(k)} \leq \boldsymbol{u_1}^{\boldsymbol{max}} \quad \textbf{(2-15)}$$

$$\boldsymbol{u_2}^{\boldsymbol{min}} \leq \boldsymbol{u_2(k)} \leq \boldsymbol{u_2}^{\boldsymbol{max}} \quad \textbf{(2-16)}$$

$$\vdots$$

$$\boldsymbol{u_m}^{\boldsymbol{min}} \leq \boldsymbol{u_m(k)} \leq \boldsymbol{u_m}^{\boldsymbol{max}} \quad \textbf{(2-17)}$$

The incremental variation constraints of each manipulated variable are stated in Equation 2-18 to 2-20.

$$\Delta\boldsymbol{u_1}^{\boldsymbol{min}} \leq \Delta\boldsymbol{u_1(k)} \leq \Delta\boldsymbol{u_1}^{\boldsymbol{max}} \quad \textbf{(2-18)}$$

$$\Delta\boldsymbol{u_2}^{\boldsymbol{min}} \leq \Delta\boldsymbol{u_2(k)} \leq \Delta\boldsymbol{u_2}^{\boldsymbol{max}} \quad \textbf{(2-19)}$$

$$\vdots$$

$$\Delta\boldsymbol{u_m}^{\boldsymbol{min}} \leq \Delta\boldsymbol{u_m(k)} \leq \Delta\boldsymbol{u_m}^{\boldsymbol{max}} \quad \textbf{(2-20)}$$

Correspondingly, the output and the state variable constraints of a MIMO system can be specified with the same technique if necessary.

Constraints as Part of the Optimal Solution

Since MPC has the characteristic of receding horizon control, all the constraints are taken into account for each Prediction Horizon during the predictive control process, which allows the constraints to be changed at the beginning of each optimisation. Equation 2-21 to 2-22 presents the incremental variation of manipulated input at the future sample steps.

$$\boldsymbol{u^{min}} \leq \boldsymbol{u(k)} \leq \boldsymbol{u^{max}} \quad \textbf{(2-21)}$$

$$\boldsymbol{u^{min}} \leq \boldsymbol{u(k+1)} \leq \boldsymbol{u^{max}} \quad \textbf{(2-22)}$$

$$\vdots$$

Instead of applying the constraints to all the future sample steps, a smaller number of steps is preferred in the occasions that the computational load has to be remained low.

2.5 Project Novelty

The positive impacts of autonomous vehicles have been verified in recent researches, for instance, improving traffic efficiency and current transportation systems, preventing road fatalities that caused by drivers, achieving a better usage of energy, etc. Generally, the imperfection of human drivers can be seen as the origins of the aforementioned enhancements; substituting the role of human drivers in driving tasks is therefore the primary objective for developing the vehicle autonomy. However, most published researches concentrate on generating the performance that is principally based on the vehicle dynamics instead of considering the specific driving preference, which might result in the sensory inadaptation of passengers and bring negative effects to the autonomous vehicle acceptance. As a result, the ultimate goal of autonomous driving is not only to guarantee the safety of driving but also to imitate the behaviour of human drivers. There still exists a wide knowledge gap in achieving human-like autonomous driving.

In the past years, several surveys and researches start to focus on the passengers' comfort and after-effects of using autonomous vehicles. These studies disclose that passengers might have adverse ride experience during a journey with travelling trajectories which are merely based on vehicle dynamics rather than taken individual driving characteristics into account [9][78][79][80]. One of the serious after-effects is the motion sickness, which is caused by the confliction between the visual and the vestibular perceptual systems. Hence, most potential activities while riding in an autonomous vehicle such as reading, watching films, using a smartphone, etc. will undoubtedly lead to the appearance of motion sickness [9]. In order to ease and mitigate the undesired influence, passengers must be able to anticipate the future motion trajectory and the variance of lateral acceleration while cornering, or at least be familiar with it [9][78][79][80].

This PhD research project "HUMAN-LIKE MOTORWAY LANE CHANGE TRAJECTORY PLANNING FOR AUTONOMOUS VEHICLES" tries to connect the cutting-edge technology (i.e. autonomous driving) with individual human

drivers and develop a novel trajectory planning algorithm; so as to enhance and speed up the future transportation automation in both the academia and the industry. An autonomous vehicle is able to perform specific travelling styles to meet the passengers' requirements since its planning methodology is established upon real human drivers' driving data. This user-friendly novelty not only profits the public acceptance but also mitigates the after-effects of riding autonomous vehicles. For instance, passengers might prefer the style with significant variance while they are almost late to their office or appointments; they might choose the mild variance style during the weekend holidays to enjoy the leisure time when travelling with autonomous vehicles. Moreover, the novelty of this project can be treated as the foundation of using machine learning methodologies to achieve personalised autonomous vehicles in the future.

Since the research covers a wide range knowledge, this chapter reviewed the researches that are relevant to this work, including the motion planning, the driving styles, the lane change manoeuvre and the theory of MPC. Staring with introducing the motion planning for autonomous vehicle and specifying the techniques that have been used in each planning stage. With the purpose of adopting human characteristics from real drivers, the driving styles and its classification algorithm were also summarised. Then, the definition and the essential parameters of a lane change manoeuvre that have been studied in the literatures were reviewed. Finally, a discussion for the knowledge of a MPC controller and the general framework of the MPC-based trajectory planning algorithm were presented. By taking the advantage of the above knowledge, a general picture of how to achieve human-like trajectory planning for autonomous vehicles can be constructed. The novelty of this study was emphasised in the meantime, which has the ability to enhance and speed up the future transportation automation in both the academia and the industry.

3 RESEARCH OBJECTIVES & FRAMEWORK

On the basis of the literature survey in four different essential topics: motion planning for autonomous vehicles, driving styles, the lane change manoeuvre and the knowledge of MPC, this section emphasises the research objectives, and illustrates the framework of this PhD project; targeting to develop a novel methodology of human-like trajectory planning under the typical driving scenario: the lane change on the motorway. Hoping the research results will give a significant contribution to future transportation automation.

3.1 Research Objectives

This PhD project will mainly focus on a typical driving scenario: non-emergency lane changing on the motorway. In general, a lane change manoeuvre is triggered by either emergency or non-emergency situations. The former should only consider the safety of the driver and the passengers while executing the lane changing; other concerns (e.g. the ride comfort, the personalisation, etc.) can be sacrificed. On the other hand, a non-emergency motorway lane changing is often caused by overtaking the front vehicle. On the premise of guaranteeing the driving safety, the human preference and characteristic can be taken into account.

The research aims are set as four parts: firstly, the algorithm of vehicle-dynamics-based trajectory planning without considering human factors will be practised and discussed. Through the process, a more solid foundation for the following research can be achieved. In the meantime, the essential parameters which are able to alter the lane changing trajectory will be investigated and nominated. Secondly, design and conduct a rigorous experiment of collecting the performances from different participants; the trajectories and the driving data will be recorded precisely through an in-vehicle sensory system. Thirdly, these records of on-road testing will be analysed and categorised into proper classes. Accordingly, the values of essential trajectory parameters that considers a particular class will be determined so as to construct the off-line constraint table and achieve the human-like trajectory planning. Finally, the

human-like trajectory planning algorithm for the different classifications will be simulated and validated. It should be noticed that the following research contents, figures and examples are based on left-hand traffic regulations (e.g. UK, JP, etc.).

3.2 Project Framework

The motion planning for either mobile robots or autonomous vehicle has been researched and lucubrated and leads to numerous achievable planning techniques. It is necessary to select suitable planning algorithms while considering the scenario of the application. In addition, each technique will require particular information to process, which is strongly related to the experimental instruments. As mentioned previously, the driving scenario for this PhD project is assigned to the lane change manoeuvre on the motorway. Hence, the part which requires corresponding methodologies and algorithms in motion planning is the trajectory planning. On the other hand, the drivers' driving datasets also have need of the statistics analysis.

The methodological approaches of this research project can be primarily divided into two parts, which are the motion planning and the driver behaviour identification. In the motion planning part, the target is to utilise existed planning techniques to generate the vehicle-based trajectory. Since the research scope of this PhD research is focused on the lane change manoeuvre, the output from the Manoeuvre Selection (Decision Making) in the path planning block will be directly assigned to make a lane change instead of other possible manoeuvres (e.g. deceleration, acceleration etc.). On the other hand, the driver behaviour identification part will classify the experimental driving data from different drivers into several styles of driving through statistical techniques. Once the essential parameters of each style towards the lane change on the motorway are solved, the results will be combined with the vehicle-based trajectory in the motion planning part to modify relevant variables' constraints and enable the trajectory planner to achieve human-like lane change trajectories. The project framework can be found in Figure 3-1.

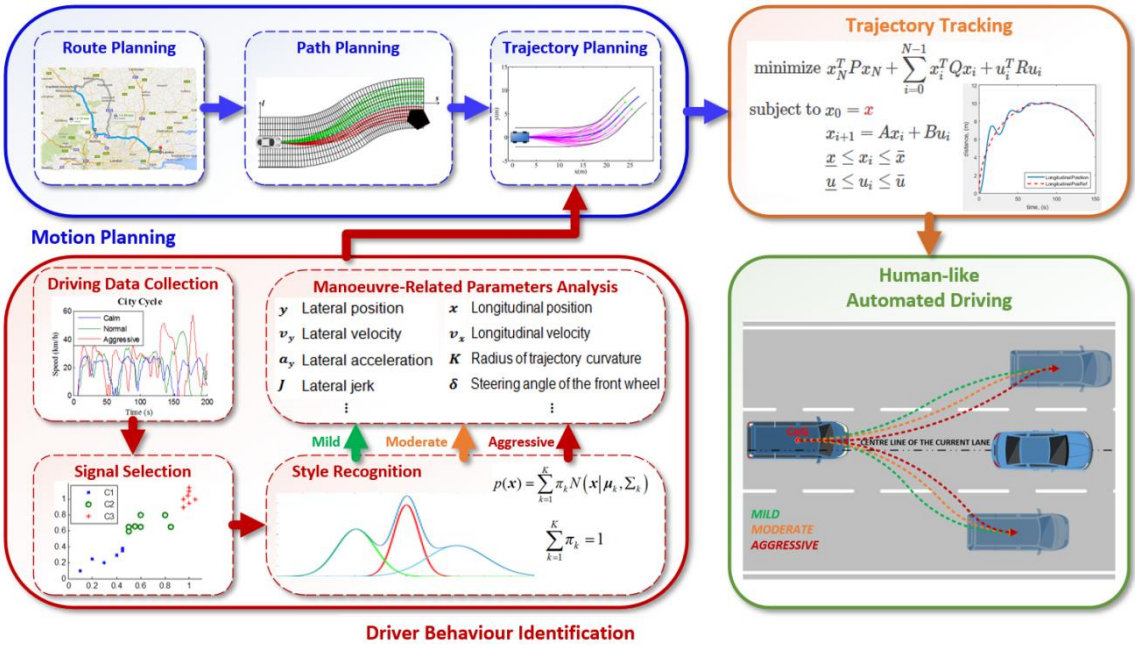

Figure 3-1 The general framework of developing a human-like trajectory planning.

Since this PhD research intends to utilise the parameters from human drivers to approach human-like lane change trajectories, the Model Predictive Control is therefore better than interpolation methodologies. Furthermore, it is able to estimate the future state of the host vehicle and its performance will not be affected by the number of surrounding obstacles, which is one of the challenges for other methodologies solving motorway driving tasks. In another aspect, the driving style classification involves the amount of human driving data and requires precise identification to improve the performance of clustering. As a result, the rule-based algorithm is insufficient in this research project but the problem can be solved by utilising the data-driven method.

This chapter introduced the objectives of this research, and the primary target is to develop a novel approach of achieving human-like trajectory planning for the non-emergency lane changing on the motorway. With the purpose of providing a better understanding to readers, the specific framework was illustrated in the meantime.

4 EXPERIMENTAL DATA COLLECTION

The main purpose of this chapter is to design a rigorous and reliable experiment that is able to contribute the mentioned human factor to the objective of this study. As stated previously, there are many different methods to approach human-like trajectory planning. Since the one that directly refers to real human drivers' driving data is the most convinced tactic, it is considered in this PhD research. So, a number of experiments were designed to collect the driving data from different human drivers. A pre-trial was first operated in order to examine the feasibility of the designed framework and spotlight the potential defects that were observed during the test period. By refining the defects that need to be improved, the main experiment can be eventually carried out to build a human driving database from 12 participants. Instead of the participant's physiologic performance, only the vehicle-dynamic-related parameters (e.g. the duration, vehicle velocity, brake pressure, throttle position, steering wheel angle, acceleration, etc.) will be collected via the professional instruments (e.g. CAN bus reader, IMU, Camera, etc.). The primary reason is that these parameters are able to reflect human characteristics, while a driver merely commands the vehicle to follow his free will through controlling the throttle pedal, the brake pedal and the hand steering wheel. This chapter presents the entire procedure of collecting the driving data from different drivers, as well as the experiment details, the instrument configurations and the participants' information.

4.1 A Pre-Trial

The first version of the driving trial took place on the 9th of May, 2016. Apart from the original goal which was set to record the driving data from a young female driver while she is driving on the motorway; the other vital targets of this trial were to practice the entire test procedure and figure out potential defects that might affect the experiment's precision. The testing route was from Cranfield University to Laindon in the United Kingdom, involving M1 and M25 two motorways and can be referred to as Figure 2-3. The utilised vehicle was Ford Mondeo; an on-board diagnostics (OBD) reader was connected to its OBD port to record the vehicle dynamical signals; two cameras were implemented in

the vehicle to obtain the front and the rear environment information, which are shown in Figure 4-1.

Figure 4-1 Two opposite direction cameras for surrounding environment recording.

The driver did 44 lane changes on M1 and 65 on M25, with totally 109 lane changes during the motorway driving period. In the 109 lane changes, 4 left lane changes were performed under the situation which has only one vehicle in the front, as shown in the upper diagram in Figure 4-2; 11 right lane changes were executed when only one front vehicle is nearby, similar to the scenario shown in the lower diagram in Figure 4-2. The number of left lane changes while no surrounding vehicle is 46 during the entire motorway driving. On the other hand, the right lane change with no surrounding vehicle happened 19 times. The above analysis was fully based on the video footages from the two cameras.

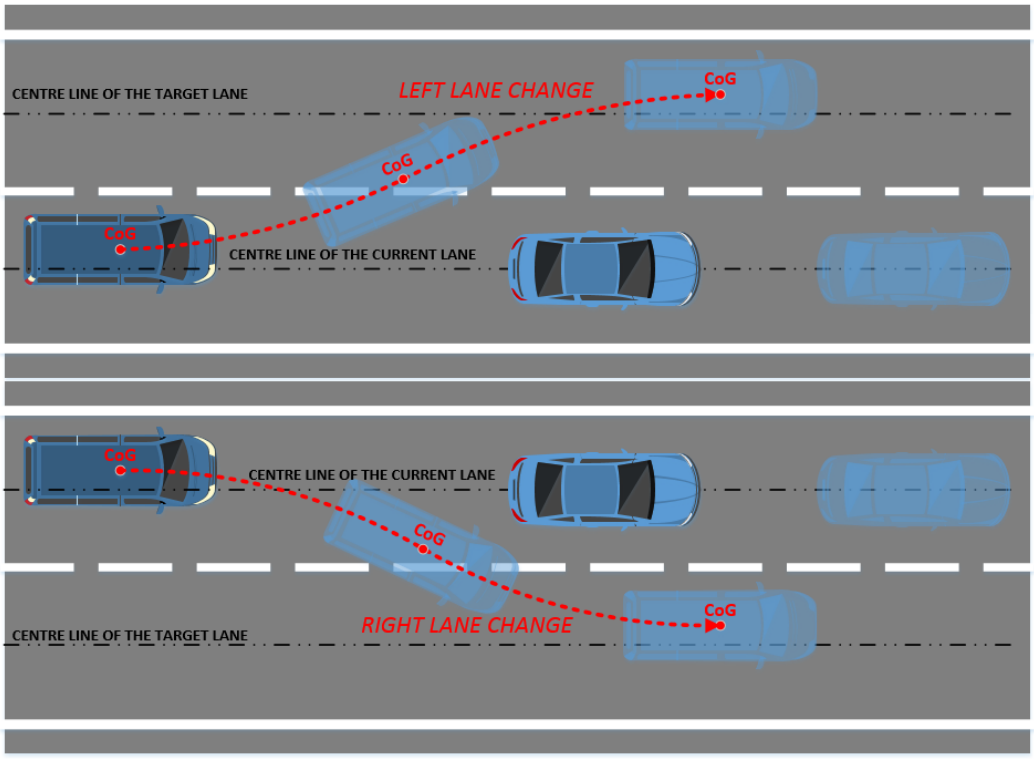

Figure 4-2 Left lane changing and right lane changing with a vehicle in the front.

All the vehicle dynamic data (e.g. vehicle velocity, engine speed, etc.) during the driving experiment was measured by in-vehicle sensors. An external device was connected to the vehicle's OBD port to decode the CAN bus data which contains more than hundreds of channels. However, only a few channels delivered the correct information because of the age of the test vehicle; thus, the process of manual identifying was required. Since the vehicle raw data was in ".mat" format, MATLAB seemed to be the most suitable software to handle the driver driving data. Figure 4-3 gives an example of the steering angle with blue colour and the turn indicator signal with red colour for the No. 83 lane change. It is obvious that all the signals from the vehicle CAN bus are discrete. Moreover, each lane change profile merely occupies a small partition of the entire driving data and is therefore required to be extracted.

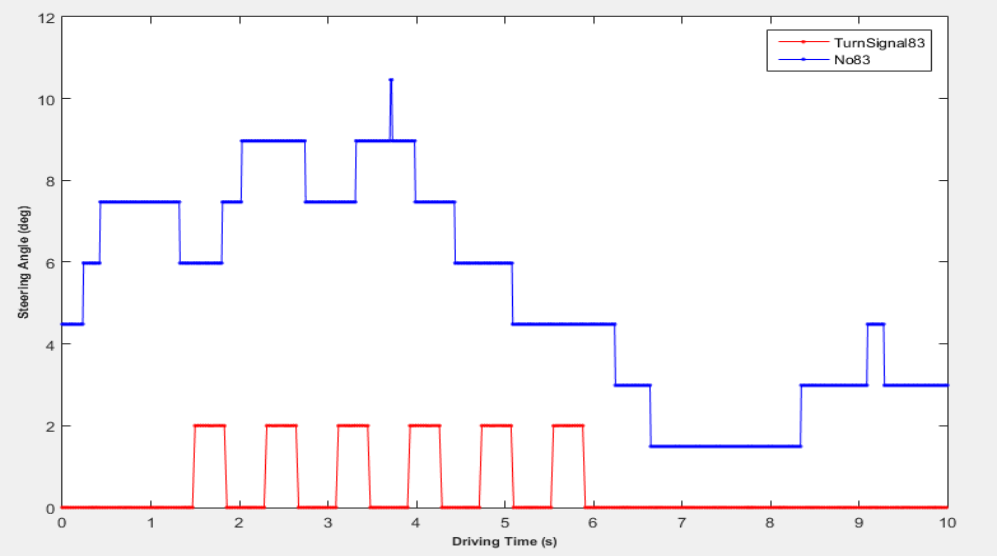

Figure 4-3 The steering and the turn signals of No. 83 lane changing.

With the purpose of extracting all the lane change manoeuvres from the original file, a script was coded within the MATLAB software. It is worthwhile mentioning that the start point of each extraction was based on the first impulse of the turn indicator signal in order to standardise all the lane change manoeuvres. However, this method has the ability to deliver reliable results only if a lane change manoeuvre launches exactly at the same time when the driver switches on the turn indicator, which cannot be guaranteed in the real circumstance.

Although the driving data of this trial wasn't taken into account in the data analysis stage, the experience still contributed a great effort in improving the quality and reliability of the main experiment, which can be summarised as:

1) Where are the ideal positions to mount the instruments in the test vehicle?
    a. In general, the ideal position of installing an instrument is mainly depended on its objectives and requirements. For instance, a camera is used to capture the front environmental information and thus needs to be mounted under the windshield and behind the rear-view mirror; an Inertial Measurement Unit (IMU) targets to measure the dynamics of the vehicle and hence the CoG inside the vehicle is the ideal location; the connection with satellites

affects the performance of a GPS antenna which requires to be installed on the vehicle roof.

2) How to obtain the vehicle dynamic signals if some in-vehicle sensors from the CAN bus are not functional?
    a. An IMU will be the answer, which has the ability to measure the vehicle dynamics and its accuracy is usually better than in-vehicle sensors.
3) How to synchronise the video footage and the recorded vehicle dynamic signals during the driving period?
    a. Due to the limited budget of this PhD research, it is suggested to solve the synchronisation problem through using a pulse generator device and periodically sending a trigger signal to both the video footage and the data logger.

Hence, the proper experiment plan of recording the driving data from different human drivers had been redesigned and is presented in the following sections.

4.2 The Main Experiment

Similar to the pre-trial experiment presented in Section 4.1, the aim of the main experiment is to measure and collect the vehicle dynamic parameters as well as recording the environmental information while different human drivers are operating the test vehicle. The test route was suggested to remain consistent on one particular motorway so as to eliminate the possible influences which are caused by the configuration dissimilarity between different motorways. Furthermore, the length of the test route was considered to be long enough to assure that participants are able to generate sufficient data. Hence, the return trip between Cranfield University and Rugby through M1 motorway was selected as showed in Figure 4-4, which involves 92 km of motorway and 12 km of country road. Although the objective driving scenario in this PhD research is the lane change on a motorway, the driving data within the rural area was also recorded so that the experimental data can be referred to or utilised by future research projects.

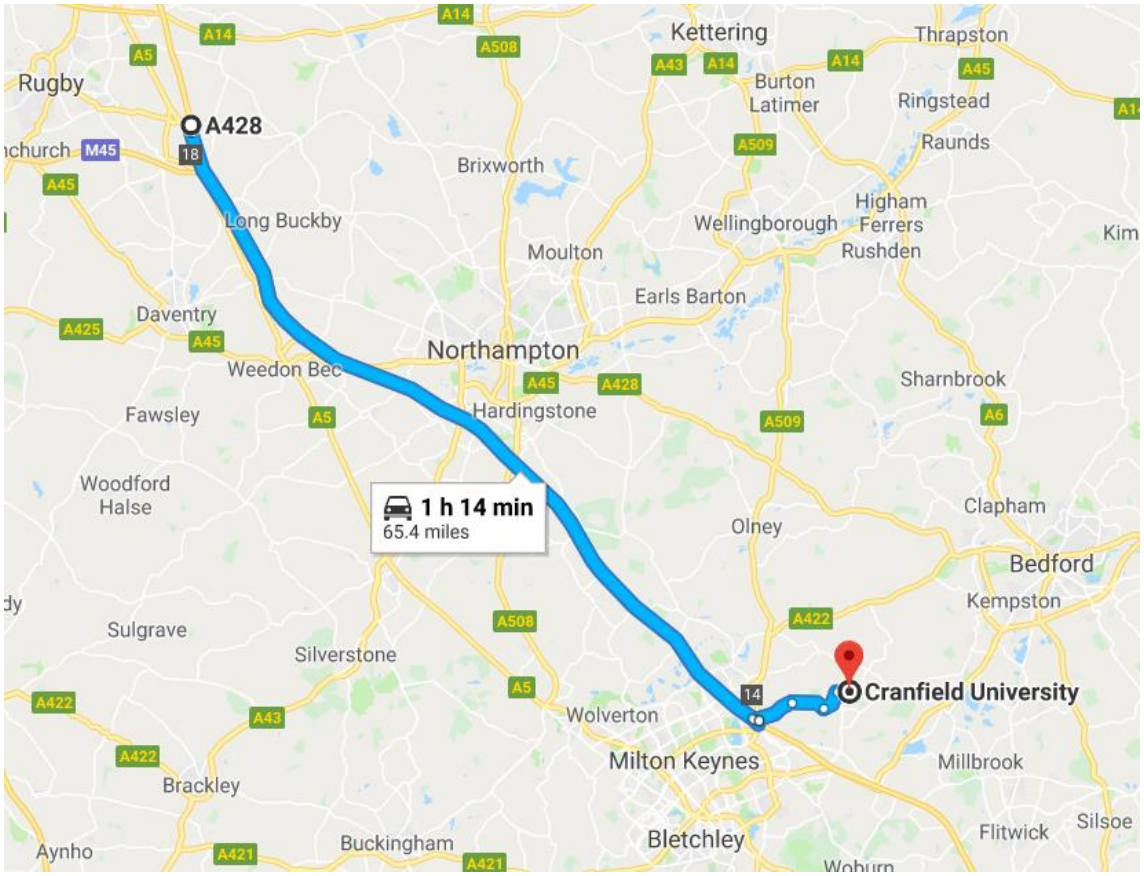

Figure 4-4 The route from Cranfield to Rugby.

With the purpose of distinguishing between the motorway and the urban lane changes, the traffic condition on the motorway in this research was assumed to be light. Hence, the time slot of the experiment was arranged within the off-peak hours (i.e. between 10 am and 3 pm) during weekdays to avoid the traffic congestion on the motorway. The risk assessment, the ethic approval and the participant consent forms were completed before the trials in order to minimise the possibility of accidents and protect the participants' personal data. The first trial took place in June 2018 and the last one was done in October 2018, a total of 12 different participants contributed their effort to this experiment. The following sections present the test platform, the applied instruments, the configuration, the installation layout and the participants' information. The designed instruction manual for the experiment can be found in Section 4.2.4.

4.2.1 Experiment Platform and Instruments

The experiments were conducted as part of an industrial project, called CogShift, which is one of the UK government investments in the field of autonomous vehicles, and it is focused on developing a safe, smooth and instant transition between autonomous driving and manual driving modes. The project is performed by a consortium of different partners including Cranfield University, Jaguar Land Rover and other organisations. A prototype Land Rover Discovery 2017 was used as the test platform in this PhD research that is illustrated in Figure 4-5. One good reason of selecting this vehicle instead of other was that Jaguar Land Rover shared its CAN bus decoder file; so that all the channels from the CAN bus can be identified, extracted and recorded.

Figure 4-5 The test vehicle Land Rover Discovery 2017.

Nowadays, modern car manufacturers implement numerous sensors in their vehicles. These sensors are able to observe the vehicle states and monitor the condition of each component. Although most vehicle dynamic signals have been covered by the in-vehicle sensors, additional GPS and IMU were still required in this experiment; not only to complement the absent information (i.e. the global position of the vehicle in this research) but also to enhance the

precision. The primary reason is that most of the manufacturers concern the production cost and could not provide high accuracy sensors. Moreover, even though the vehicle position can be obtained through integrating the vehicle velocity from the CAN bus, the integration results still contain magnified deviations due to the information distortion and the ordinary accuracy of the commercial in-vehicle sensors. The professional instruments (i.e. IMU and GPS) are thus indispensable. It should be noted that the precision of the vehicle dynamic data dramatically influences the performance of both trajectory planning and driver driving data analysing. To fulfil the above requirements, Racelogic VBOX which is accessible in Cranfield Advanced Vehicle Engineering Centre was then utilised. Racelogic VBOX is an integrated suite of data acquisition instruments that contains a data logger, an IMU, GPS receivers and other compatible modules, providing the log rate up to 20 Hz and the positional accuracy of 40 cm. Figure 4-6 demonstrates the Racelogic VBOX suite.

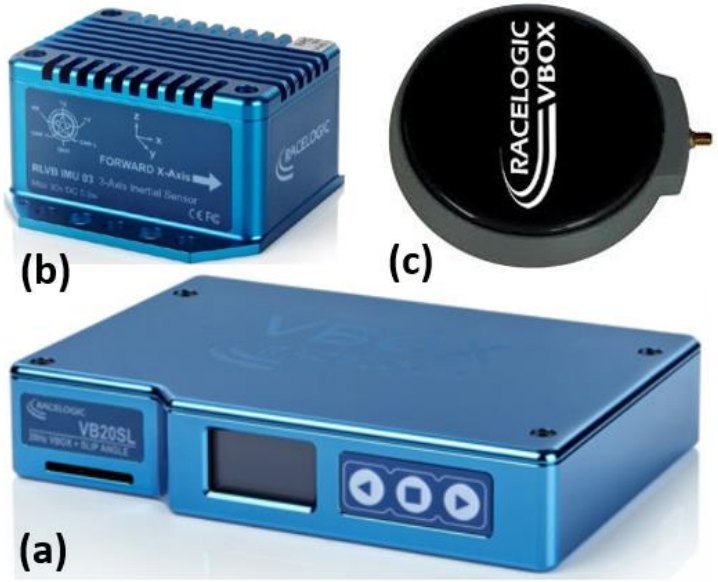

Figure 4-6 Racelogic VBOX: (a) Data Logger, (b) IMU and (c) GPS Antenna.

On the other hand, the surrounding environment information is another essential influence for motion planning, including the message of the distance to the obstacles, the relative speed with adjacent vehicles, the lane boundaries,

etc., which should be captured by the perception system for further analysis. This process not only helps the vehicle autonomy to construct a digital world model but also enables the motion planner to evaluate the most appropriate action under the current situation. Furthermore, it was assumed that the traffic condition will also alter the driver's response and performance towards particular driving manoeuvres. To validate the assumption and gather the environmental data during each driving test, a Logitech camera (i.e. C920 HD PRO WEBCAM) which is able to generate detailed Full HD video was mounted in the test vehicle.

Since the vehicle dynamic signals and the environment information were recorded from two isolated devices, the difficulty of synchronising these two data had to be overcome before post-processing. The time scale of vehicle dynamic signals can be calibrated by VBOX GPS modules while recording, but the time scale of the camera's videos was based on the clock from the laptop workstation. Therefore, the captured video would inevitably have a small time-shifting when the workstation is not connected to the Internet. To minimise the time-shifting effect and ensure the synchronisation between the video footage and the driving data, an Arduino Uno board was used in the experiment. It can be understood as a small processor which has the ability to store and execute user's pre-programmed scripts. The methodology of synchronisation was to request Arduino Uno sending an electric pulse to both a light-emitting diode (LED) and the Racelogic VBOX data logger every $\mathbf{20}$ s. Then, the state of LED and the environment information were simultaneously captured by the camera during the driving test so that the obtained video and the recorded driving data could be synchronised based on the pulse signal. The pictures of the utilised camera and Arduino Uno can be found in Figure 4-7.

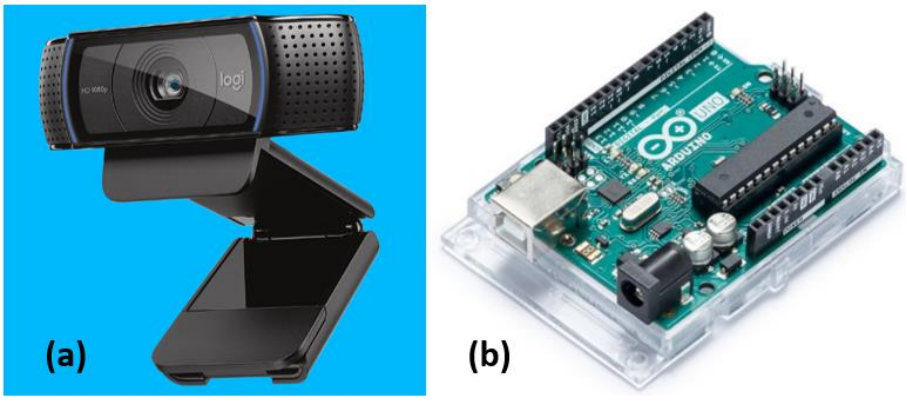

Figure 4-7 (a) Logitech C920 Webcam and (b) Arduino Uno.

4.2.2 Instruments Configuration and Installation Layout

As stated in the previous section, the purpose of in-vehicle sensors is to supervise and transmit the conditions of vehicle components. Generally, these obtained sensor signals are gathered and can be read from the vehicle CAN bus through its OBD port. However, the OBD port of the Discovery in this experiment didn't provide the CAN bus information. In order to achieve the CAN signal extraction, a cable was first wired directly to the CAN High and CAN Low wires and connected to the VBOX data logger. But this action ended up with that numerous intrusive signals were unintentionally broadcasted onto the CAN bus, and caused both the distortion of the original data and several warning signs to appear on the vehicle dashboard. Hence, an alternative CAN interface which is compatible with Racelogic VBOX was then applied.

Figure 4-8 shows the schema of the instruments' configuration for the experiment. The CAN bus interface, the IMU and the GPS antenna first inputted the valuable signals. Then, the VBOX Data Logger integrated all the channels and the electric pulse from Arduino Uno into a comprehensive driving data. In the meantime, the camera continuously captured the images of the environmental information and the flash of the LED that was triggered by the same electric pulse from Arduino Uno, and transferred these images into the video format. Finally, the obtained driving data and the recorded videos were stored in the workstation for the post-processing and analysis. An electrical diagram is also presented in Figure 4-9.

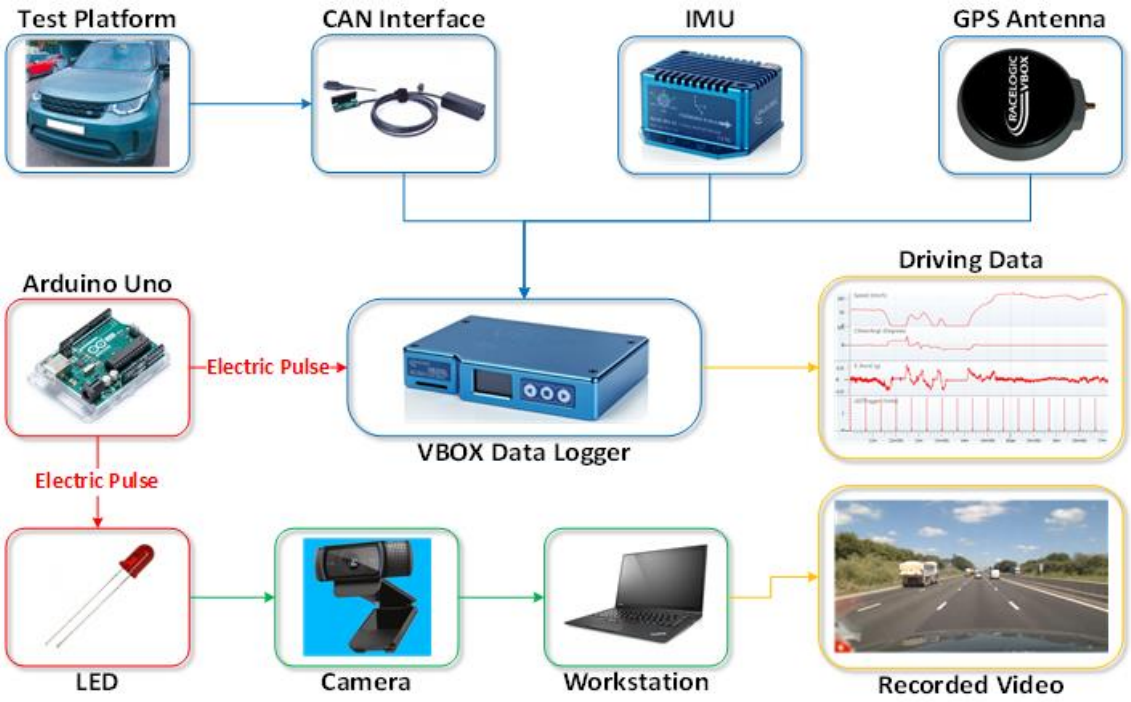

Figure 4-8 The schema of the experiment instruments

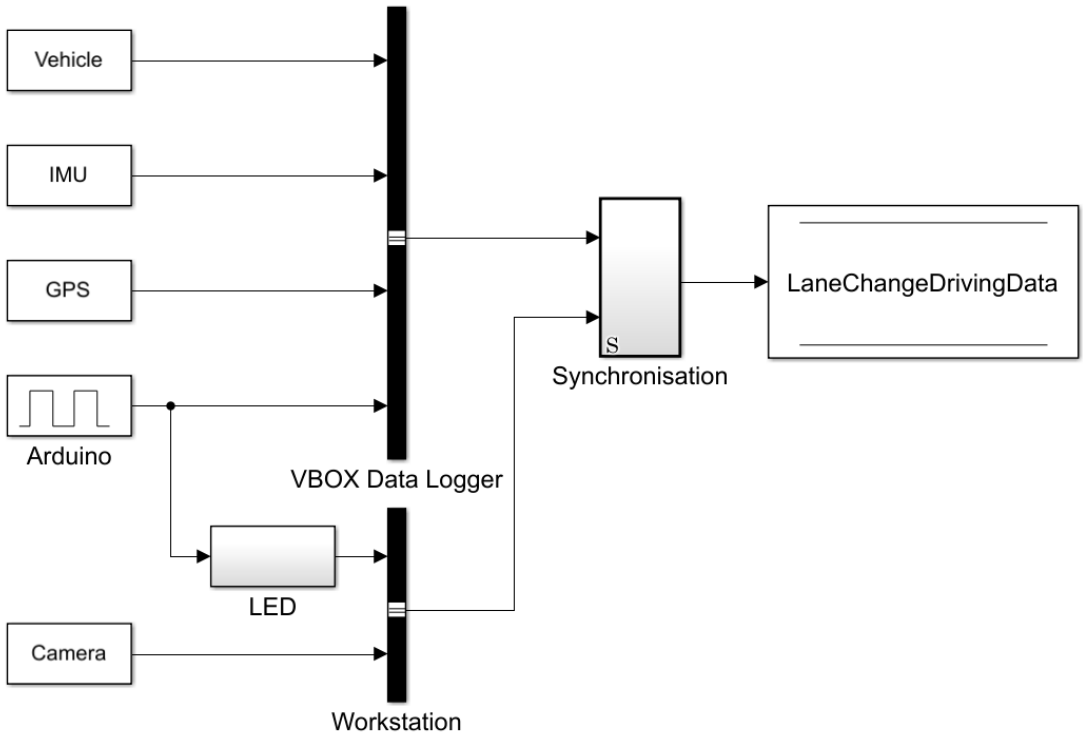

Figure 4-9 The electrical diagram of the experiment instruments

Since the trials contained the high-speed driving scenarios on the motorway, it is extremely important to ensure the utilised instruments were installed securely; not only to assure the accuracy of the sensor measurements but also to prevent the possible accidents which are caused by the device dropping due to the high-frequency vibration and the wind resistance. The installation layout of the applied instruments is presented in Figure 4-10. The GPS antenna was fitted on the vehicle roof through the strong magnetic force and the IMU was mounted at the CoG inside the vehicle. The Camera was set to face forward to record the front image during driving. Both the Camera and the LED were attached under the windshield and behind the rear-view mirror so as to avoid blocking the driver's sight, which can be seen in Figure 4-11.

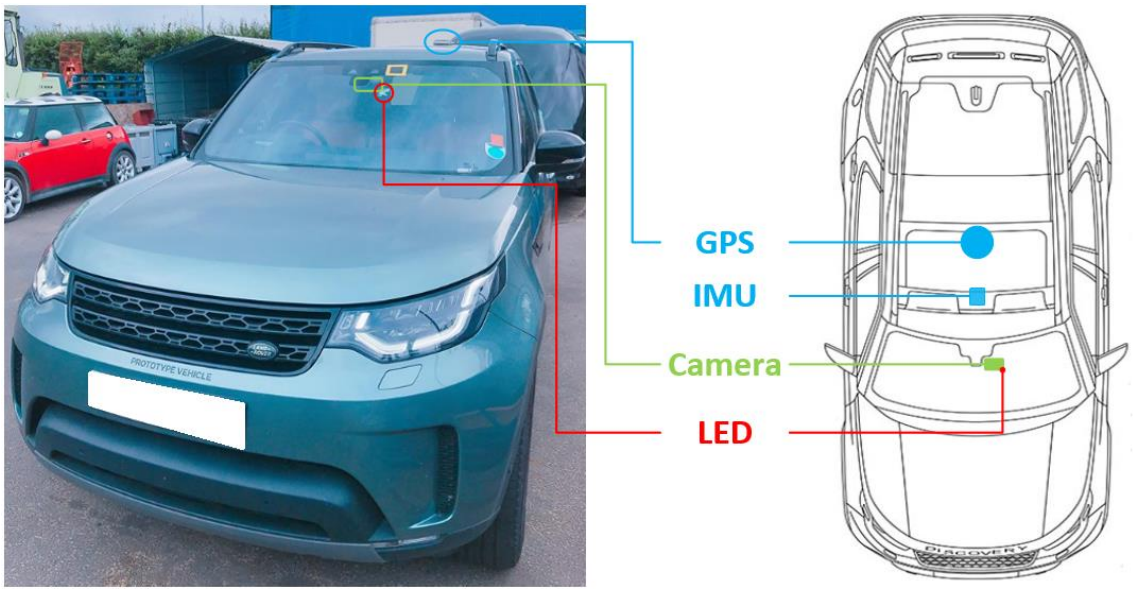

Figure 4-10 The installation layout of the experiment instruments

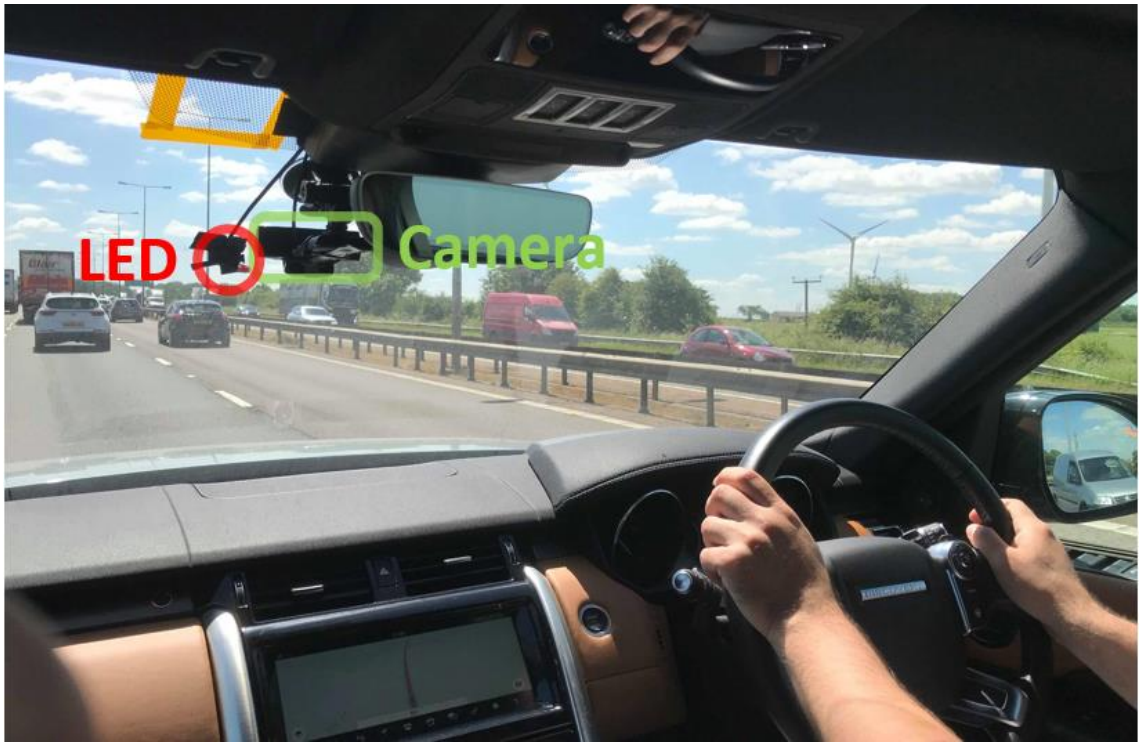

Figure 4-11 In-vehicle view.

4.2.3 Participants

The principle of data analysis is to explore the hidden information from the objective database. Generally, more data provides more precise outcomes, but it inevitably consumes additional time and resources. In order to make a proper trade-off and obtain valuable and acceptable driving patterns, the participants who attended this experiment and generate the driving data had to be chosen wisely and reasonably.

Firstly, the experiment consisted of hours of driving tasks and was planned to be carried out in the United Kingdom; therefore, a valid UK driving license had to be owned by each participant. Moreover, the requirements of the minimum length of having the UK driving license was bounded to 1 year and the minimum frequency of driving per week was set to 4 days; with the intention of excluding the driving data from novice drivers which might degrade the analysis results. Secondly, the trial route involved both motorways and country roads, which are outside the campus. To assure the safety during the test period, the drivers had to be covered by the university's insurance. All participants were selected from

the staffs in Cranfield Advanced Vehicle Engineering Centre. Lastly, the gender of the participants might have different responses while facing the same driving condition, which will undoubtedly affect the analysis outcomes. With the purpose of eliminating this possible consequence and obtain consistent driving data, all the participants have to be the same gender. Since male staffs had a majority in Cranfield Advanced Vehicle Engineering Centre, male drivers were nominated as the participants in this PhD research.

To balance the mentioned trade-off between the size of the database and the consumed resources, the number of participants was finally determined as 12. On the other hand, each participant took a short questionnaire before the trial, providing some information which might be useful for the data analysis in the later stage or the future research. These details were summarised and can be found in Table 4-1. Again, the objective of this experiment is to record the driving data that is performed by real human drivers. By adopting the human characteristics from the recorded driving data, the vehicle autonomy is able to deliver human-like driving. As mentioned in the literature review, trichotomy is a common method to distinguish the driving styles. Mild, Moderate and Aggressive are termed to indicate the positivity of the drivers during the driving period.

Table 4-1 Participant information

Driver No.	Age	Length of Having UK Driving License	Frequency of Driving per Week	Self-evaluation Driving Style
1	42	8 Years	7 Days	Mild
2	40	22 Years	5 Days	Moderate
3	50	33 Years	7 Days	Moderate
4	36	1.5 Years	7 Days	Moderate
5	49	6 Years	7 Days	Moderate
6	52	34 Years	7 Days	Moderate
7	39	12 Years	7 Days	Moderate
8	35	8 Years	7 Days	Aggressive
9	48	31 Years	7 Days	Moderate
10	41	22 Years	7 Days	Mild
11	58	40 Years	4 Days	Moderate
12	26	7 Years	4 Days	Moderate

4.2.4 Experiment Instruction Manual

- **Objectives**: The aim of this experiment is to measure and collect the vehicle dynamic and driver's parameters while operating lane changes on the motorway.
- **Instruments**: (1) Racelogic VBOX Data Logger, (2) High precision GPS Antenna, (3) Inertial Measurement Unit (IMU), (4) CAN Bus Interface, (5) Arduino Uno, (6) LED, (7) SD Card, (8) Full HD Camera, (9) Laptop Workstation.
- **Place**: On a motorway during off-peak hours. (i.e. M1 motorway, from Cranfield to Rugby and the length is around 28.6 miles on the motorway). The route is shown in Figure 4-4.
- **Vehicle**: Land Rover Discovery 2017.
- **Participants and Supervisor**: 13 people in total; 12 male drivers who are eligible to drive the test vehicle, has a valid UK driving license more than 1 year and at least drives 4 days per week; 1 person to supervise the data recording process and instruct the driver to follow the experiment procedures.
- **Procedures**:
    I. Before starting the experiment, double check that all the instruments are functional and have enough electricity to support the experiment.
    II. Install all the instruments on the vehicle correctly as shown in Figure 4-10.
    III. Set up and install the video recording equipment: the camera is placed above the vehicle dashboard and face forward to record the front image during driving.
    IV. Select one of the participants and note down his age, the age of having the UK driving license, and the self-assessed driving style. Request him to complete the participant consent form.
    V. Inform the participant that he has to drive the vehicle from Cranfield to Rugby and return back to Cranfield through M1 motorway.

VI. Once the above steps have been confirmed, both the participant and the supervisor should enter into the test vehicle. The participant is then allowed to start the engine and the supervisor rechecks whether all the instruments are functional or not.

VII. The experiment begins when the supervisor presses the data collecting button. The participant is then eligible to drive to Rugby and return back based on the determined route and according to his own driving preference.

VIII. Once the test vehicle arrives back to Cranfield University, the participant has to find a place to stop and park the vehicle. The supervisor presses the button to stop the data collection so as to name and save both the driving data and the recorded video.

IX. Repeat the experiment until all 12 participants complete the experiment.

- **Note**: The log rate of the VBOX data logger was set to its maximum capability that is 20 Hz. The measured dynamic parameters of the test vehicle during the experiment are stated in Table 4-2.

Table 4-2 The parameters that have to be measured in the motorway lane change experiment.

T	**Duration**
v	**Velocity**
P_{brake}	**Brake Pressure**
$P_{throttle}$	**Throttle Position**
E_{spd}	**Engine Speed**
I_{turn}	**Turn Indicator**
$\delta_{handraw}$	**Raw Hand Steering Wheel Angle**
γ_{yaw}	**Yaw Rate**
a_x	**Longitudinal Acceleration**
a_y	**Lateral Acceleration**

In order to obtain the reliable human driving data, the method that directly refers to drivers' performance is recommended. The experiments were therefore designed in accordance with this convinced tactic. The first one was implemented to examine the feasibility of the designed framework and spotlight

the potential defects that were observed during the test period. These insufficiencies were improved before conducting the main experiment, which involves 12 different male drivers. Their driving data and the front environmental information can be recorded in the Racelogic data logger. In other words, the main experiment provides the raw message of human driving characteristics to the human-like trajectory planning algorithm, which requires further refinement. The participants' information, the entire procedure of collecting the driving data, the experiment details, and the instrument configurations were also detailed in this chapter.

5 HUMAN DRIVING DATA ANALYSIS

Since the participants' driving data has been successfully collected in the experiment, this chapter focuses on filtering the irrelevant signals and mining the human characteristics that are hidden in the essential features. Starting with introducing the knowledge of the data statistics and applying the linear correlation and the histogram with the kernel distribution fitting technique to the recorded signals for right lane changes, so as to remove those irrelevant ones. The remaining signals (i.e. the vehicle velocity $\boldsymbol{v}$, the hand steering wheel angle $\boldsymbol{\delta_{handreal}}$, the longitudinal acceleration $\boldsymbol{a_x}$, the rate of hand steering $\boldsymbol{\gamma_{handsteer}}$ and the rate of longitudinal accelerating $\boldsymbol{\gamma_{longAcc}}$) are able to construct a multi-dimension structure. Through inputting the driving datasets which are generated by different participants into the structure, the performance and the pattern of the human drivers can be observed. Since the driving style is still a vague concept and does not have a unified definition, this research considers the overall variance (i.e. from each sample point to the centroid of the driving data) as an index for driving style clustering. Then, the boundary values of the signals which correspond to each nominated driving style are calculated so as to build the off-line constraints table for the human-like trajectory planning. On the other hand, the original driving data is grouped based on three different surrounding traffic conditions and the differences between the groups are analysed, with the purpose of validating the assumption that the traffic condition could affect drivers' performance. It should be highlighted that the main contribution of this chapter is to investigate the marginal values of three different driving styles based on the real human driving data which is collected in the on-road driving experiment.

Although the factor of human drivers plays a critical role in the human-like trajectory planning, the direct measurement towards participants (e.g. the force that the driver applies on the hand steering wheel, the level of concentration, etc.) was not considered in this PhD research. The primary reason is that the human driver is able to examine the environmental information and command the vehicle to follow his free will through controlling the throttle pedal, the brake

pedal and the hand steering wheel; in other words, these three actuators have the ability to transmit the personal characteristics of the human driver to the vehicle. Hence, recording the vehicle dynamic signals instead of measuring the participant's physiologic performance was the adoptive approach in the experiment. While considering the lane change manoeuvre, both lateral and longitudinal related vehicle dynamic signals had to be taken into account. Table 4-2 shows the parameters that were selected to be recorded by the mentioned in-vehicle instruments in the experiment. These variables contain vital information of the participants and were considered as the potential factors of distinguishing different driving styles.

The raw signal of the hand steering wheel angle $\boldsymbol{\delta_{handraw}}$ was initially considered as the index of extracting each lane change on the motorway from the original driving data. However, due to the fact that most participants merely inputted small angles to the hand steering wheel to complete lane changes on the motorway, it was impossible to apply a threshold-filtered script to automatically detect both the starts and the ends of lane change manoeuvres. As a consequence, the synchronised video had to be analysed along with the driving data. The methodology of identifying lane change manoeuvres was to examine the recorded video footages frame by frame and measure the distance to the left lane boundary. Once the value of the distance starts to grow from the average value before the lane change, it represents the start of the lane change manoeuvre. Similarly, when the value of the distance to the left lane boundary of the target lane is no longer increase comparing with the average value after the lane change, it indicates the end of the lane change manoeuvre.

Since the test route, M1 motorway, is not completely straight and it consists of a number of partitions with small curvature, the driver has to slightly and constantly amend the angle of the hand steering wheel to maintain the vehicle staying inside a driving lane. This behaviour will inevitably affect the observed data and leads to the fact that the recorded hand steering wheel angle contains two portions of the steering. In order to minimise this impact, the raw signal of the hand steering wheel angle $\boldsymbol{\delta_{handraw}}$ was calibrated after each lane change

extraction. Via subtracting the average value of $\boldsymbol{\delta_{handraw}}$ within $\mathbf{5}$ s before the start of each lane change, the real signal of the hand steering wheel angle $\boldsymbol{\delta_{handreal}}$ that causes the lane change manoeuvre can be acquired. The renewed version of the selected signals for the data analysis are summarised in Table 5-1.

Table 5-1 The signals that were considered in driving data analysis.

$\boldsymbol{T}$	**Duration**
$\boldsymbol{v}$	**Velocity**
$\boldsymbol{P_{brake}}$	**Brake Pressure**
$\boldsymbol{P_{throttle}}$	**Throttle Position**
$\boldsymbol{E_{spd}}$	**Engine Speed**
$\boldsymbol{I_{turn}}$	**Turn Indicator**
$\boldsymbol{\delta_{handreal}}$	**Real Hand Steering Wheel Angle**
$\boldsymbol{\gamma_{yaw}}$	**Yaw Rate**
$\boldsymbol{a_x}$	**Longitudinal Acceleration**
$\boldsymbol{a_y}$	**Lateral Acceleration**

According to the published Highway Code Rule 267-268 from the UK Department for Transport, a vehicle is prohibited to overtake by moving to a left lane on the motorway. This regulation indicates the qualitative difference between the right lane change and the left one. Hence, these two directions were assumed to have different performance and should be analysed separately and the following contents will focus on the right lane change. Moreover, it is worthwhile mentioning that most participants performed at least one lane change that crossed multiple lanes on the motorway during the driving tests. This particular lane change with large lateral travelling distance is not recommended due to its potential hazard, and would also decrease the accuracy of results. Therefore, only single-lane changes were investigated in this study. Yet again, the lane change sorting was achieved through examining the video footages that captured the environmental information while the participant was driving. Table 5-2 states the numbers of both right and left lane changes that were performed by each participant in the experiment.

Table 5-2 The detailed number of the lane changes that were implemented by the drivers on M1 motorway.

Driver No.	Number of Right Lane Changes	Number of Left Lane Changes	Total Lane Changes
1	16	17	33
2	26	30	56
3	40	41	81
4	29	26	55
5	28	22	50
6	26	29	55
7	7	8	15
8	31	34	65
9	24	29	53
10	15	14	29
11	16	18	34
12	12	13	25
	270	**281**	**551**

The driving experiment provided a number of candidate signals to describe how the participants completed the lane change manoeuvre on the motorway. Although the number of available signals is 10 in total, not all of them can be used to construct the vehicle model in the latter trajectory planning algorithm. With the purpose of filtering out the irrelevant factors and narrowing down the range, several data analysed techniques were utilised.

5.1 Data Statistics

Statistics is one of the important branches in mathematics and can be seen as the integration of the assembly, the organisation, the analysis and the presentation of the target data. A good quality of the statistics outcome can be guaranteed if and only if the processes of all parts are treated scrupulously. Hence, numerous techniques and algorithms were nominated since the 18th century. The primary objective of statistical techniques is to mine the valuable information that is hidden behind the numbers. This section introduces the techniques which is utilised to analyse the human drivers' driving data.

5.1.1 Linear Correlation

Linear correlation is a mathematical phrase describes the strength of a linear association. It is a common but useful statistic technique to identify whether the two variables have a linear relationship with each other. In other words, one variable can be straightforwardly predicted to have a certain constant variance while giving a change to the other if a strong linear correlation exists between these two variables [81]. To quantify and express the degree of variables' correlation, numerous correlation coefficients were developed, often symbolised as $\boldsymbol{\rho}$ or $\boldsymbol{\gamma}$. The most well-known one is the Pearson correlation coefficient (i.e. Pearson's $\boldsymbol{\gamma}$), which numerical measures only the linear relationship instead of others between the target variables. The calculation of Pearson correlation coefficient is shown in Equation 5-1.

$$\boldsymbol{\rho_{X,Y}} = \boldsymbol{corr}(\boldsymbol{X},\boldsymbol{Y}) = \frac{\boldsymbol{cov}(\boldsymbol{X},\boldsymbol{Y})}{\boldsymbol{\sigma_X \sigma_Y}} \quad \textbf{(5-1)}$$

where $\boldsymbol{\rho}$ is the population correlation coefficient, $\boldsymbol{X}$ and $\boldsymbol{Y}$ are the two variables, $\boldsymbol{corr}$ is the alternative representation of the correlation coefficient, $\boldsymbol{cov}$ is the covariance, measuring the joint variability of $\boldsymbol{X}$ and $\boldsymbol{Y}$, $\boldsymbol{\sigma_X}$ and $\boldsymbol{\sigma_Y}$ are the standard deviations of $\boldsymbol{X}$ and $\boldsymbol{Y}$ respectively.

The value of Pearson correlation coefficient ranges between $-\mathbf{1}$ and $\mathbf{1}$; the former implies the instance of a perfect negative linear correlation (i.e. $\boldsymbol{Y}$ decreases while $\boldsymbol{X}$ increases) and the latter indicates the perfect positive one (i.e. $\boldsymbol{Y}$ increases while $\boldsymbol{X}$ increases). If $\boldsymbol{X}$ and $\boldsymbol{Y}$ are uncorrelated, the value of the correlation coefficient will equal to $\mathbf{0}$. To better understand the correlation coefficient, a visualised chart which presents different coefficient values between $\boldsymbol{X}$ and $\boldsymbol{Y}$ datasets is shown in Figure 5-1.

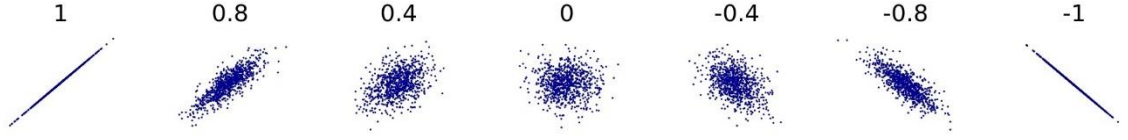

Figure 5-1 Different values of Pearson correlation coefficient between two datasets [82]**.**

5.1.2 Histogram Distribution

Apart from the linear correlation which focuses on distinguishing the relationship between variables, another important technique of statistics is the histogram. This technique concentrates on evaluating one particular variable itself. It is able to assist users to understand the structure of the numerical data and visualise its distribution. To present the histogram of a variable, the full range of the variable has to be first divided into a sequence of consecutive and non-overlapping intervals, which are also known as “Bins”. Then, the values of the variable that belong to each bin are counted and its histogram can be conducted. Figure 5-2 demonstrates an instance of the histogram with the number of bins is set to 20, where the x-axis is the numerical variable (i.e. vehicle velocity) and the y-axis are the frequencies of the intervals.

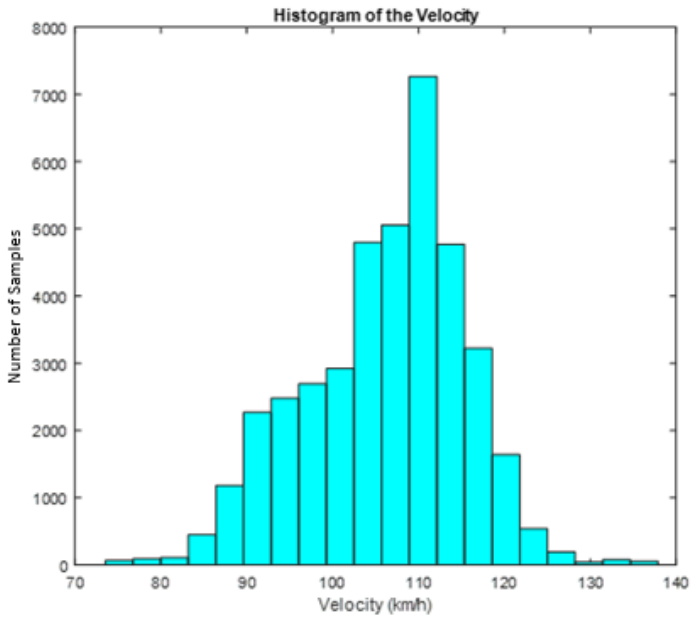

Figure 5-2 An instance of the histogram.

It should be noted that the bins have to be adjacent in order to contain complete information and their widths are often but not necessary to be equal. Another adjustable parameter is the number of bins, which mainly depends on the feature of the variable that is desired to reveal and therefore has no optimal solution. Generally, the higher number of bins can provide a more detailed

behaviour of the variable but might also be drowned by the noise. Equation 5-2 illustrates the mathematical formula of the histogram:

$$\boldsymbol{f} = \sum_{\boldsymbol{i=1}}^{\boldsymbol{k}} \boldsymbol{h_i} \tag{5-2}$$

where $\boldsymbol{h_i}$ is the subset of the histogram, $\boldsymbol{k}$ is the assigned number of bins and $\boldsymbol{f}$ is the total number of frequencies (i.e. full observation).

While constructing a histogram of the particular variable, an additional function which is called “distribution fitting” is often applied to it. Not only to smooth the data between intervals, but also to precisely reflect and present the distribution of the target variable. A kernel distribution fitting was applied to the previous instance of the histogram and can be found in Figure 5-3.

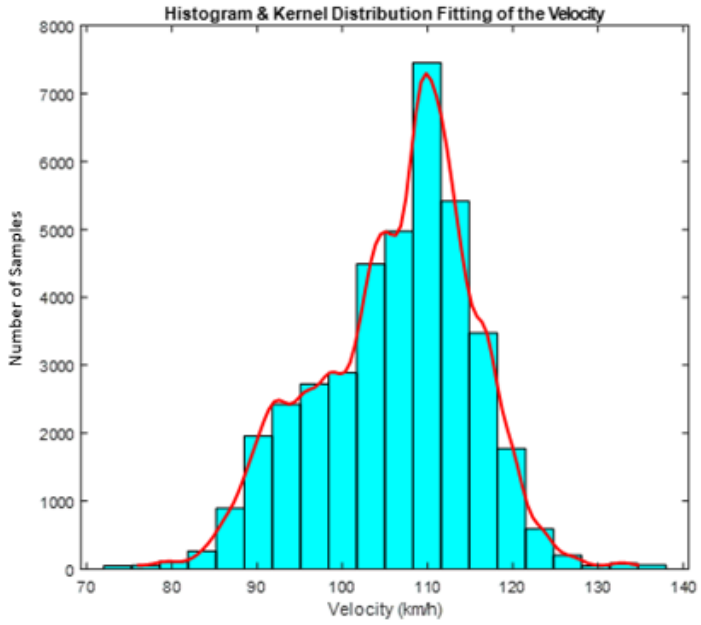

Figure 5-3 The histogram with kernel distribution fitting.

5.2 Linear Correlation and Histogram Distribution for Right Lane Changes

By calculating the Pearson correlation coefficients of the 10 measured signals in the driving experiment, the linearly related pairs can be evaluated. Due to the fact that all the signals were obtained from the real driving tests, the measured data inevitably has minor deviations. Hence, the coefficients with their absolute values greater than $\mathbf{0.6}$ are highlighted. The result of the Pearson correlation analysis is presented in Table 5-3, showing that there are two linear correlated groups among the 10 signals. One is the throttle position $P_{throttle}$ and the longitudinal acceleration a_x. The other is the real hand steering wheel angle $\delta_{handreal}$, the yaw rate γ_{yaw} and the lateral acceleration a_y. This outcome is also proved by the theory of vehicle dynamics [83] and reveals that the signals within each group possess the same human characteristic. As a result, selecting a representative feature of a linear correlated group and eliminating the rest will not lose any useful information of the human driving characteristics. Moreover, the required computational cost of the human-like trajectory planning algorithm in the latter stage can be reduced in the meantime.

Table 5-3 Pearson correlation coefficients of the measured signals.

	T	v	P_{brake}	$P_{throttle}$	E_{spd}	I_{turn}	$\delta_{handrea}$	γ_{yaw}	a_x	a_y
T	1	0.08	0.02	-0.18	-0.09	-0.55	0.51	-0.43	-0.15	0.38
v	**0.08**	1	-0.0274	-0.09	0.36	-0.10	0.17	-0.12	-0.18	0.13
P_{brake}	**0.02**	**-0.03**	1	-0.12	-0.03	-0.01	-0.00	0.01	-0.17	-0.00
$P_{throttle}$	**-0.18**	**-0.09**	**-0.12**	1	0.17	0.18	-0.14	0.08	0.74	-0.10
E_{spd}	**-0.09**	**0.36**	**-0.03**	**0.17**	1	0.05	0.08	-0.05	0.22	0.04
I_{turn}	**-0.55**	**-0.10**	**-0.01**	**0.18**	**0.05**	1	-0.56	0.46	0.14	-0.43
$\delta_{handrea}$	**0.51**	**0.17**	**-0.00**	**-0.14**	**0.08**	**-0.56**	1	-0.75	-0.09	0.67
γ_{yaw}	**-0.43**	**-0.12**	**0.01**	**0.08**	**-0.05**	**0.46**	**-0.75**	1	0.03	-0.66
a_x	**-0.15**	**-0.18**	**-0.17**	**0.74**	**0.22**	**0.14**	**-0.09**	**0.03**	1	-0.04
a_y	**0.38**	**0.13**	**-0.00**	**-0.10**	**0.04**	**-0.43**	**0.67**	**-0.66**	**-0.04**	1

Figure 5-4 shows the recorded driving data for $\mathbf{270}$ right lane changes performed by the $\mathbf{12}$ participants on the motorway; the property of linear correlation can be observed between the above mentioned signals. It should be noted that the negative value of $\boldsymbol{\delta_{handreal}}$ means right steering, the negative value of $\boldsymbol{a_y}$ indicates right accelerating and the positive value of $\boldsymbol{\gamma_{yaw}}$ depicts clockwise rotating; these signs are based on the VBOX data logger's original configuration.

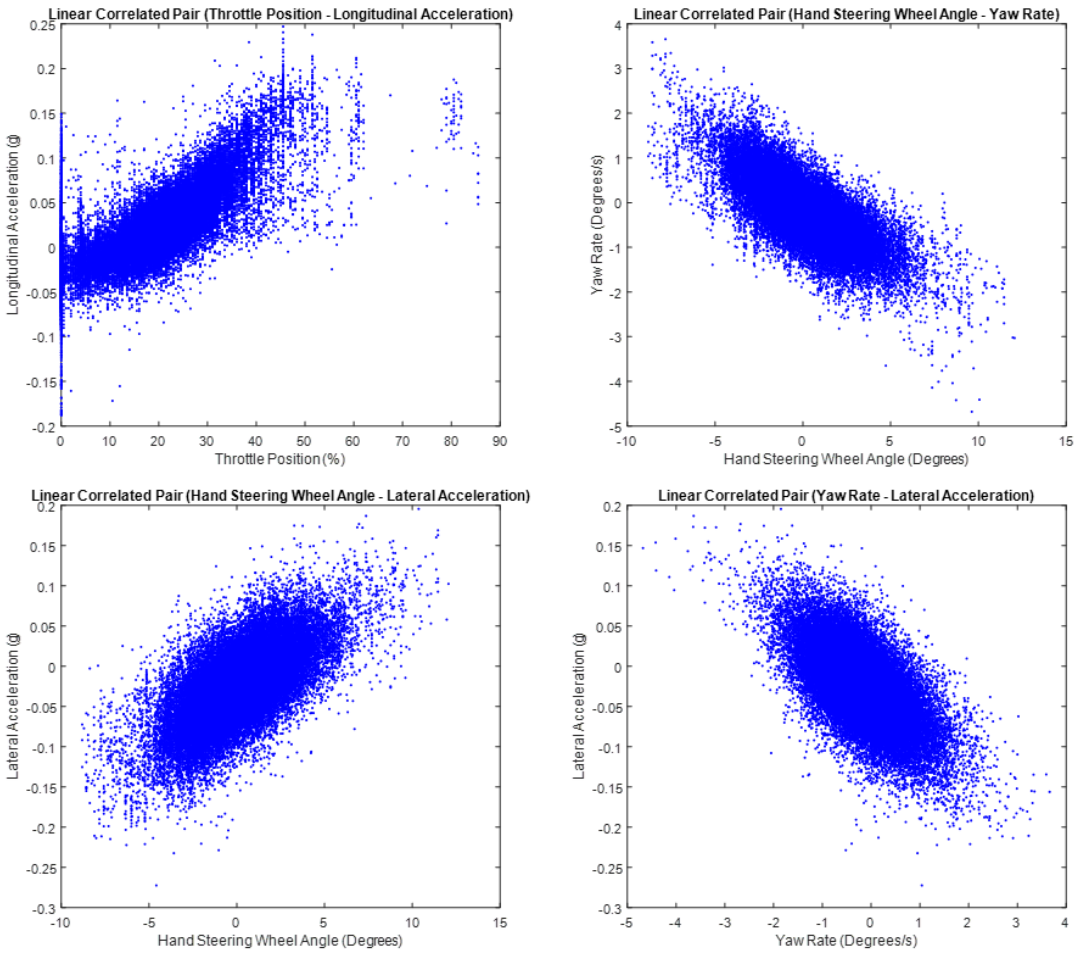

Figure 5-4 Linear correlated signals extracted from the right lane change driving data.

As discussed in the previous section, each related signal group will have the same proportionate variance while giving a change to them. Therefore, all signals within the same group will provide the identical characteristic of the driving style. Hence, selecting one signal to represent the performance of the

group and neglecting others is a reasonable process, not only to preserve the original information but also to reduce the complexity of distinguishing the essential factors of the driving styles. Considering the vehicle model that will be utilised later for simulations, the longitudinal acceleration $\boldsymbol{a_x}$ and the real hand steering wheel angle $\boldsymbol{\delta_{handreal}}$ seemed to be the ideal representatives for the two linear correlation groups.

On the other hand, the engine speed $\boldsymbol{E_{spd}}$ would have a strong linear correlation with the throttle position $\boldsymbol{P_{throttle}}$ and the longitudinal acceleration $\boldsymbol{a_x}$ if and only if the vehicle remains in the same gear. However, the computational result in Table 5-3 shows $\boldsymbol{E_{spd}}$ merely slight linear correlated with $\boldsymbol{P_{throttle}}$ and $\boldsymbol{a_x}$. The primary reason appears to be that the test vehicle is automatic and some of the recorded lane changes contain the automated gear shifting which caused the sudden increments and drops of $\boldsymbol{E_{spd}}$. Hence, the signal of engine speed in this experiment couldn't transmit the characteristics of driving styles with identical baseline and was filtered. Furthermore, the duration $\boldsymbol{T}$ can be understood as an incremental variable which starts from $\boldsymbol{0}$ when a lane change is initiated and resets to $\boldsymbol{0}$ when the manoeuvre is ended; counting the time consumption while a participant is changing between lanes. This leads to the fact that only the maximum value within each lane change carries useful message and has to be treated separately.

Although the correlation coefficients provide the index of grouping the linear related signal pairs for the representative feature selection, the remaining $\boldsymbol{5}$ signals (i.e. the brake pressure $\boldsymbol{P_{brake}}$, the turn indicator $\boldsymbol{I_{turn}}$, the vehicle velocity $\boldsymbol{v}$, the hand steering wheel angle $\boldsymbol{\delta_{handreal}}$ and the longitudinal acceleration $\boldsymbol{a_x}$) might still consist of the irrelevant ones which do not contribute valuable information for achieving human-like lane change control. As a result, the histograms with a distribution fitting of the remaining signals were then examined.

The histogram of the brake pressure $\boldsymbol{P_{brake}}$ is shown in Figure 5-5. The value of $\boldsymbol{P_{brake}}$ remains $\boldsymbol{0}$ for more than $\boldsymbol{99}\%$ of the time, illustrating that all the

participants rarely apply the braking pedal while changing to the right lane. This observation reveals that $\boldsymbol{P_{brake}}$ is an irrelevant signal of mining the characteristics of human drivers towards the right lane change manoeuvre and thus can be eliminated.

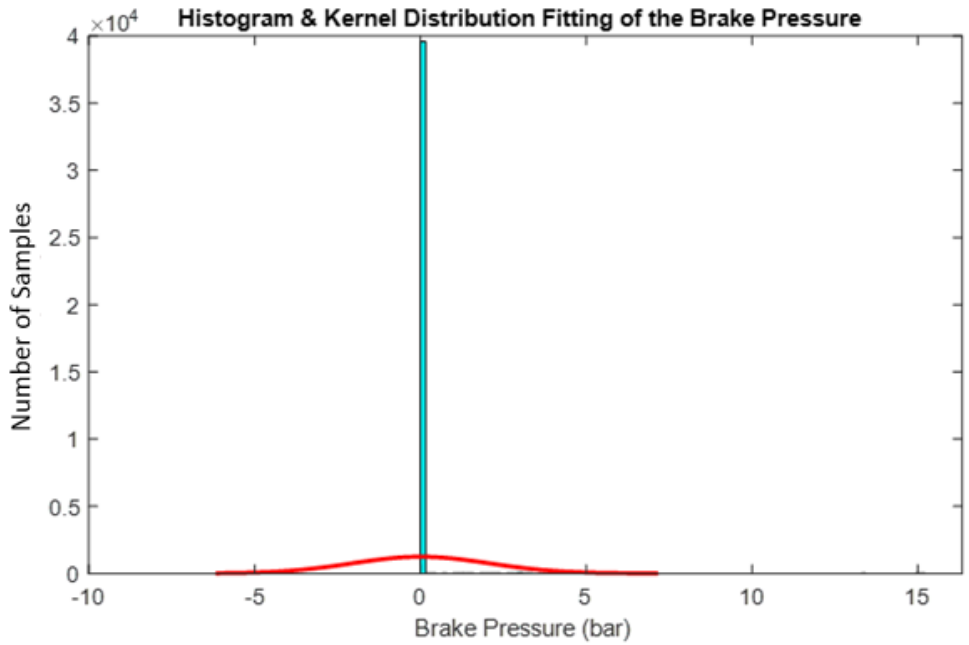

Figure 5-5 Histogram of the Brake Pressure for the right lane changes on the motorway.

Figure 5-6 presents another histogram of the turn indicator $\boldsymbol{I_{turn}}$. The value becomes $\mathbf{1}$ or $\mathbf{0}$ when the turn indicator is switched on or off respectively. From the chart, it is obvious that the turn indicator was not always activated during the periods of changing to the right lane; the inactivate duration was even larger than the other (i.e. the indicator was switched on). This observation highlights the potential safety issue that is performed by human drivers, which can be further researched in the future work. However, this signal does not have the ability to alter the vehicle's lane change trajectory which is the primary concern of this research. Hence, $\boldsymbol{I_{turn}}$ was eventually screened out.

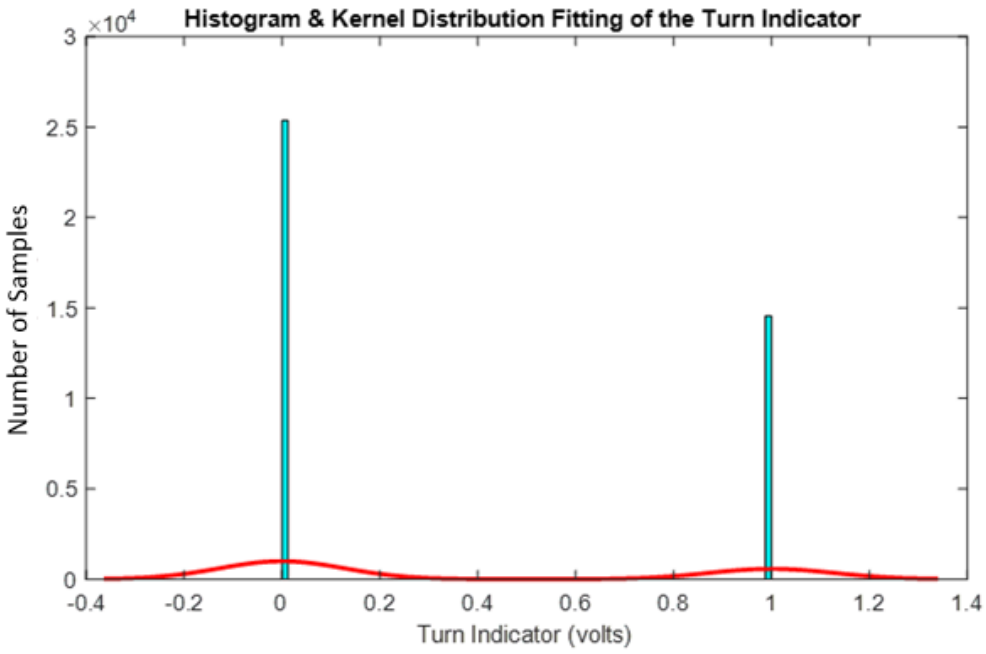

Figure 5-6 Histogram of the Turn Indicator for the right lane changes on the motorway.

The histograms of the rest $\mathbf{3}$ signals which are the vehicle velocity $\boldsymbol{v}$, the hand steering wheel angle $\boldsymbol{\delta_{handreal}}$ and the longitudinal acceleration $\boldsymbol{a_x}$ are presented in Appendix B.1, showing the valuable information of right lane change manoeuvres that were performed by the $\mathbf{12}$ participants. Apart from the above signals which can be measured directly from the in-vehicle sensors and the Racelogic VBOX suite, another $\mathbf{2}$ post-processing signals were put into consideration in the meantime. These signals are the rate of hand steering $\boldsymbol{\gamma_{handsteer}}$ and the rate of longitudinal accelerating $\boldsymbol{\gamma_{longAcc}}$, which provide the instantaneous variation of $\boldsymbol{\delta_{handreal}}$ and $\boldsymbol{a_x}$ that cannot be obtained directly from the Racelogic VBOX suite. Their histograms can also be found in Appendix B.1.

5.3 Driving Style Classification for Right Lane Changes

As the essential features (i.e. the vehicle velocity $\boldsymbol{v}$, the hand steering wheel angle $\boldsymbol{\delta_{handreal}}$, the longitudinal acceleration $\boldsymbol{a_x}$, the rate of hand steering $\boldsymbol{\gamma_{handsteer}}$ and the rate of longitudinal accelerating $\boldsymbol{\gamma_{longAcc}}$) that deliver the human driving characteristics have been determined in the previous section.

The next step is to distinguish different driving styles based on these signals' data. Again, the literature review in Chapter 2 specifies that there is no standard criteria of defining the driving styles. By taking the generic principles of both the academia and the industry, this PhD research targets at trisecting the entire driving data into 'Aggressive', 'Moderate' and 'Mild'. The amplitude of the variance of each sample point to the centroid of the overall recorded data was identified as the index of classification. From the physical point of view, this classification principle indicates that 'Aggressive' driving style contains relatively drastic manipulations while comparing with the average performance of all the human drivers, and 'Mild' is on the contrary.

In general, the Gaussian distribution is a common probability model to describe an unknown factor and is also known as the normal distribution. Since the participants in the driving tests were chosen randomly and the number of recorded right lane changes are $\mathbf{270}$ with more than $\mathbf{39900}$ sample points, it is reasonable to assume that these samples cover all three driving styles and their distribution are normal (i.e. Gaussian distribution). Ideally, this assumption is true when the number of participants is large enough. On the basis of this reasonable assumption, the standard deviation of the Gaussian distribution model was used to define the boundaries of different driving styles in the research. Figure 5-7 shows a typical Gaussian distribution model and illustrates the ranges of the driving styles. Referring to the generality, the values of $\pm\boldsymbol{\sigma}$ and $\pm\mathbf{2}\boldsymbol{\sigma}$ were set to be the boundaries of Mild and Moderate styles respectively, and the value of $\pm\mathbf{4}\boldsymbol{\sigma}$ are the boundaries of Aggressive style in the classification, where $\boldsymbol{\sigma}$ is the standard deviation. One reason of selecting $\pm\mathbf{4}\boldsymbol{\sigma}$ instead of $\pm\mathbf{3}\boldsymbol{\sigma}$ for Aggressive boundaries is that $\pm\mathbf{3}\boldsymbol{\sigma}$ only contains $\mathbf{99.73}\%$ of the data and the rest $\mathbf{0.27}\%$ will be missed out. Another reason is that the test data will inevitability have several extreme values which are caused by either the environmental error or the random noise. The range of $\pm\mathbf{4}\boldsymbol{\sigma}$ covers $\mathbf{99.99}\%$ of the data and has the ability to truncate those extremes but preserve the valuable information.

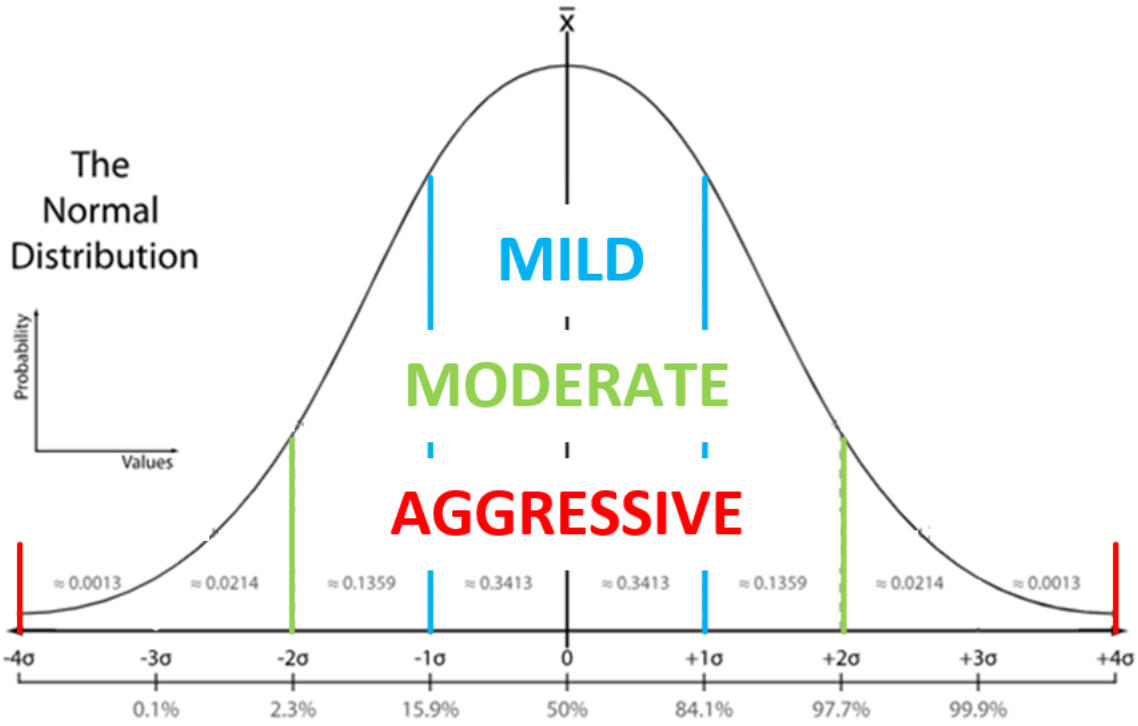

Figure 5-7 The Gaussian distribution model for driving styles classification.

Based on the classification in Figure 5-7, it can be found that Aggressive driving style occupies the widest range and includes both the Moderate and Mild driving styles. In other words, these driving styles are not isolated with each other and both Moderate and Mild are the subsets of Aggressive driving style. This approach aligns with the fact that an aggressive human driver does not always act aggressively, and his performance sometimes belongs to either Moderate or Mild driving style. Specifically, a driving profile without violating the Mild boundaries is called Mild driving. A manoeuvre which has part of the driving exceeds the Mild boundaries but remains inside the Moderate boundaries is nominated as Moderate driving. A more drastic manipulation that transcends the Moderate boundaries is treated as Aggressive.

The experiment provides $\mathbf{270}$ right lane changes with $\mathbf{39920}$ sample points in total. Though each sample point is able to deliver the information of all the recorded signals, only five of them that were determined in the previous section are considered as the valuable factors for the driving style classification. Since the data pool is a multi-dimensional spectrum with different units, the real

values of the selected signals have to be normalised between $\mathbf{0}$ and $\mathbf{1}$. By transforming each sample point to the distance to the centroid of the overall driving data and fitting to the Gaussian distribution model, the values of multiple standard deviations (i.e. the boundaries of Mild, Moderate and Aggressive driving styles) can be acquired. These values are then transformed back to the original domains of the signals so as to indicate their real values.

Table 5-4 The boundary values of the vital signals for different styles of right lane change.

Lane Change Style	Boundary	$v\ (km/hr)$	$\delta_{handreal}\ (Degrees)$	$a_x\ (m/s^2)$	$\gamma_{handsteer}\ (Degrees/s)$	$\gamma_{longAcc}\ (m/s^3)$
Mild	Lower	**91.1**	**- 4.7**	**- 0.76**	**- 26.3**	**- 14.6**
	Upper	**121.2**	**5.1**	**1.23**	**27.0**	**14.6**
Moderate	Lower	**82.2**	**- 7.6**	**- 1.36**	**- 42.1**	**- 23.2**
	Upper	**130.1**	**8.0**	**1.82**	**42.8**	**23.2**
Aggressive	Lower	**61.7**	**- 14.2**	**- 2.71**	**- 78.4**	**- 43.1**
	Upper	**150.6**	**14.6**	**3.18**	**79.1**	**43.1**

The classification results can be viewed in Table 5-4, specifying both the lower and the upper boundaries of the vehicle velocity v, the hand steering wheel angle $\delta_{handreal}$, the longitudinal acceleration a_x, the rate of hand steering $\gamma_{handsteer}$ and the rate of longitudinal accelerating $\gamma_{longAcc}$ for Mild, Moderate and Aggressive driving styles.

5.4 The Effect of Traffic Flow on Right Lane Changes

Although the driving tests were carried out within the off-peak hours to avoid traffic congestions on the motorway, the appearance of surrounding vehicles during each lane change was still the factor that could not be controlled. In other words, the recorded lane changes were performed by the participants under different circumstances. It was assumed that different environmental conditions

might alter the response and performance of human drivers. The video footages that were captured by the camera in the experiment stores the environmental information during the driving, providing a chance to validate this assumption and investigate the influence of different traffic conditions on the lane change manoeuvre.

This section mainly focuses on inspecting the differences between the driving lanes and the front and the right environmental conditions. The investigation can be divided into three cases: (1) change between Normal Speed Lanes & change from Normal Speed Lane to Overtaking Lane, (2) with or without a front vehicle on the current driving lane and (3) with or without a vehicle on the destination lane. Figure 5-8 is showing a schematic diagram of one possible surrounding condition while initiating a right lane change manoeuvre, where the two green lanes are named as “Normal Speed Lane”, the purple lane is so-called “Overtaking Lane”, the white minivan is the ego vehicle, the yellow sedan is the front vehicle on the same lane with the ego vehicle, and the orange SUV (Sports Utility Vehicle) is the vehicle on the target lane.

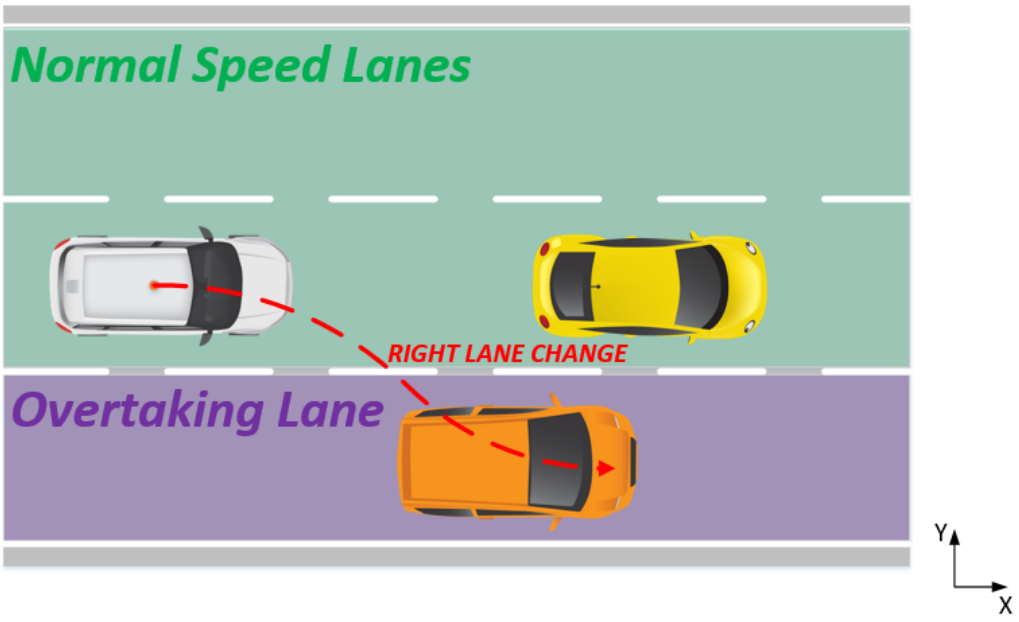

Figure 5-8 The schematic diagram of the right lane change manoeuvre.

5.4.1 Lane Change between Normal Speed Lanes & Lane Change from Normal Speed Lane to Overtaking Lane

From the regulation which is laid down by the UK Department for Transport, the rightest lane on the motorway is the lane for the relatively high-speed driving and the overtaking, also known as “Overtaking Lane”. The rest lanes on the left of the Overtaking Lane are noted as “Normal Speed Lanes”. In accordance with this identification, the recorded $\mathbf{270}$ right lane changes were clustered into two groups. One is the right lane change between Normal Speed Lanes and the other is the right lane change from Normal Speed Lane to Overtaking Lane. Their amounts are $\mathbf{120}$ and $\mathbf{150}$ respectively.

Figure 5-9 plots the sample points of these two groups while considering the three measured signals (i.e. the vehicle velocity $\boldsymbol{v}$, the hand steering wheel angle $\boldsymbol{\delta_{handreal}}$, and the longitudinal acceleration $\boldsymbol{a_x}$), where the blue colour indicates the right lane change between Normal Speed Lanes and the red colour represents the right lane change from Normal Speed Lane to Overtaking Lane. It is obvious that the red group has a higher average velocity than the blue group, which aligns with the common sense that a driver often increases the vehicle’s velocity to change to Overtaking Lane. However, it is hard to identify the differences for $\boldsymbol{\delta_{handreal}}$ and $\boldsymbol{a_x}$. On the other hand, the figure shows the enormous overlap between the two different conditions of the right lane changes.

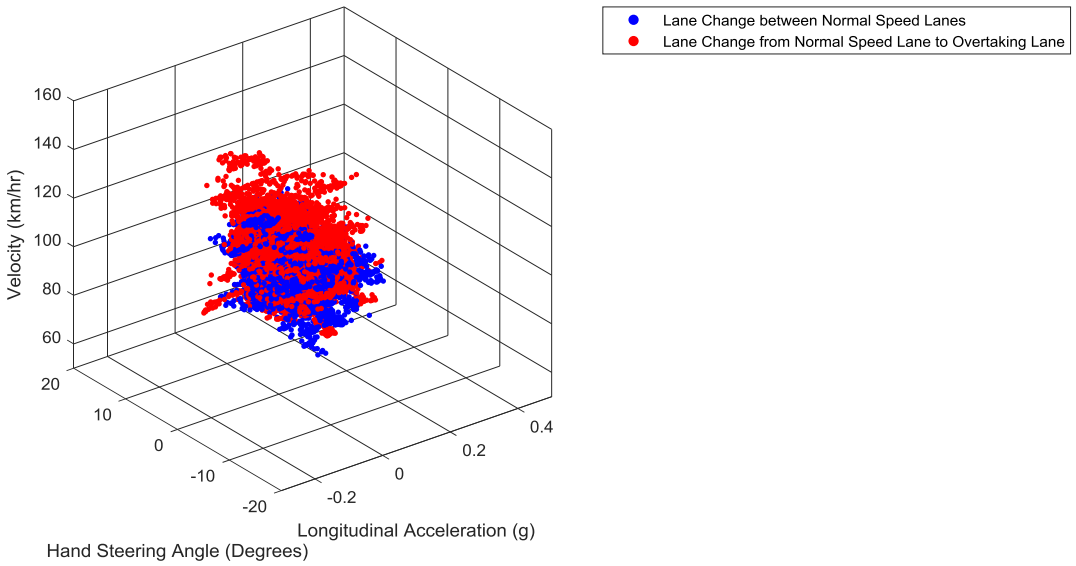

Figure 5-9 The comparison of the measured signals of case 1.

Table 5-5 The boundary values and the variances compared to Table 5-4 of the right lane change between Normal Speed Lanes.

Driving Style	Boundary / Variance	v (km/hr)	$\delta_{handreal}$ (Degrees)	a_x (g)	γ_{steer} (Degrees/s)	$\gamma_{longAcc}$ (g/s)
Mild	Lower	88.9	- 5.3	- 0.0655	- 22.7	- 1.4880
	Variance	- 2.49%	- 12.51%	+ 16.03%	+ 13.62%	- 0.01%
	Upper	119.3	5.3	0.1116	23.4	1.4884
	Variance	- 1.58%	+ 5.51%	- 11.00%	- 13.26%	+ 0.13%
Moderate	Lower	79.9	- 8.4	- 0.1176	- 36.3	- 2.3645
	Variance	- 2.80%	- 10.81%	+ 14.97%	+ 13.80%	+ 0.24%
	Upper	128.3	8.5	0.1638	37.0	2.3648
	Variance	- 1.44%	+ 6.44%	- 11.79%	- 13.56%	- 0.17%
Aggressive	Lower	64.7	- 13.7	- 0.2061	- 59.4	- 3.8527
	Variance	+ 4.80%	+ 3.62%	+ 25.54%	+ 24.29%	+ 12.37%
	Upper	143.5	13.8	0.2523	60.0	3.8531
	Variance	- 4.74%	- 5.63%	- 22.18%	- 24.07%	- 12.33%

Table 5-5 and 5-6 present the classification results with the same procedure in Section 5.3 for the change between Normal Speed Lanes and the change from Normal Speed Lane to Overtaking Lane correspondingly. The variances of the boundaries of the driving styles compared to the values of the overall driving data in Table 5-4 are also presented. It can be seen that within the condition of changing between Normal Speed Lanes, the participants performed: relative slow speed; overall large hand steering wheel angle so that the boundaries for Mild and Moderate styles are expanded; comparative small longitudinal acceleration and rate of hand steering and lead to their boundaries for all three driving styles are narrowed down; and compact rate of longitudinal accelerating for Aggressive style. Within the condition of changing from Normal Speed Lane to Overtaking Lane, the velocity of vehicle is increased and the boundaries are shifted to the positive direction; the hand steering wheel angle becomes condensed, showing relatively small steering value was applied; the distributions of the rest signals are similar to the overall driving data.

Table 5-6 The boundary values and the variance compared to Tabel 5-4 of the right lane change from Normal Speed Lane to Overtaking Lane.

Driving Style	Boundary / Variance	v (km/hr)	$\delta_{handreal}$ (Degrees)	a_x (g)	$\gamma_{handsteer}$ (Degrees/s)	$\gamma_{longAcc}$ (g/s)
Mild	Lower	93.1	- 4.4	- 0.0771	- 26.2	- 1.4831
	Variance	+ 2.15%	+ 6.17%	+ 1.15%	+ 0.36%	+ 0.32%
	Upper	122.4	5.0	0.1254	26.9	1.4805
	Variance	+ 0.98%	- 1.15%	0%	- 0.37%	- 0.40%
Moderate	Lower	83.9	- 7.4	- 0.1409	- 42.9	- 2.4154
	Variance	+ 2.02%	+ 2.96%	- 1.88%	- 1.90%	- 1.90%
	Upper	131.6	8.0	0.1892	43.6	2.4128
	Variance	+ 1.15%	+ 0.09%	+ 1.88%	+ 1.85%	+ 1.85%
Aggressive	Lower	64.0	- 13.7	- 0.2783	- 78.9	- 4.4262
	Variance	+ 3.66%	+ 3.42%	- 0.54%	- 0.67%	- 0.68%
	Upper	151.5	14.3	0.3266	79.6	4.4236
	Variance	+ 0.59%	- 1.74%	+ 0.74%	+ 0.66%	+ 0.65%

5.4.2 Lane Change with or without a Front Vehicle on the Current Driving Lane

Another case study is to consider the appearance of the front vehicle while initiating the right lane change manoeuvre. In the driving dataset, $\mathbf{84}$ right lane changes were activated with a front vehicle on the current driving lane and $\mathbf{186}$ were executed without a front vehicle on the current driving lane. Figure 5-10 demonstrates the right lane change driving data of the three measured signals (i.e. the vehicle velocity v, the hand steering wheel angle $\delta_{handreal}$, and the

longitudinal acceleration $\boldsymbol{a_x}$) for these two groups, where the blue colour indicates the condition with a front vehicle and the red colour is without a front vehicle. Similarly, the red colour has higher velocities compared to the blue group, which supports the fact that human drivers often apply lower speed to avoid collision and ensure driving safely when a vehicle is driven in the front. Apart from $\boldsymbol{v}$, both $\boldsymbol{\delta_{handreal}}$ and $\boldsymbol{a_x}$ do not provide clear differences but merely highlight the large percentage of the overlap between the two mentioned conditions.

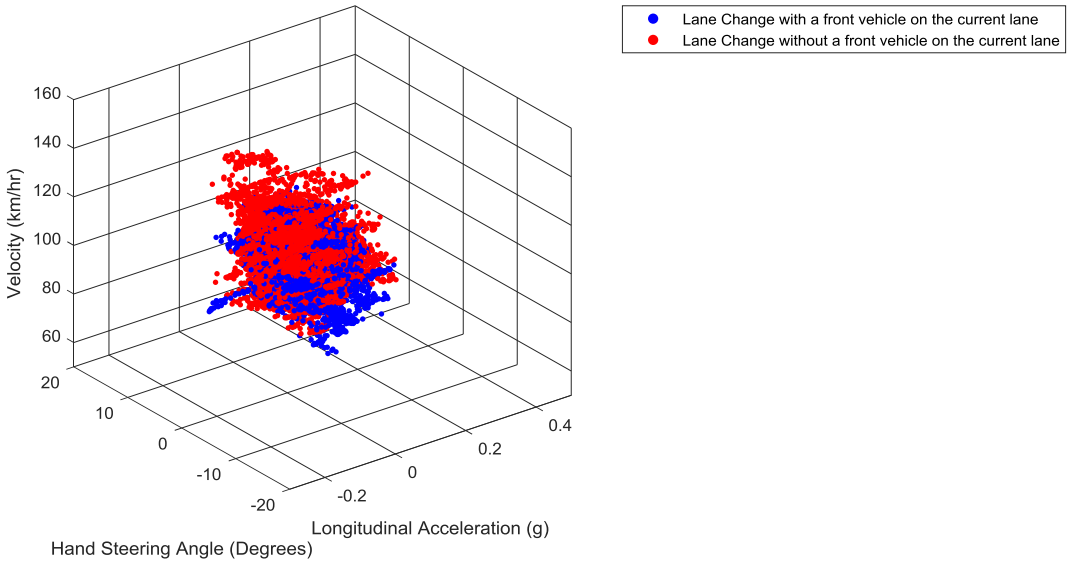

Figure 5-10 The comparison of the measured signals of case 2.

Table 5-7 The boundary values and the variance compared to Tabel 5-4 of the right lane change with a front vehicle on the current driving lane.

Driving Style	Boundary / Variance	v (km/hr)	$\delta_{handreal}$ (Degrees)	a_x (g)	$\gamma_{handsteer}$ (Degrees/s)	$\gamma_{longAcc}$ (g/s)
Mild	Lower	89.5	- 5.3	- 0.0898	- 22.1	- 1.3547
	Variance	- 1.77%	- 12.05%	- 15.13%	+ 16.01%	+ 8.95%
	Upper	119.4	5.6	0.1619	22.8	1.3546
	Variance	- 1.52%	+ 9.82%	+ 29.11%	- 15.42%	- 8.87%
Moderate	Lower	80.5	- 8.5	- 0.1656	- 35.6	- 2.1706
	Variance	- 2.05%	- 12.24%	- 19.74%	+ 15.42%	+ 8.43%
	Upper	128.4	8.8	0.2377	36.3	2.1705
	Variance	- 1.36%	+ 10.82%	+ 28.00%	- 15.06%	- 8.38%
Aggressive	Lower	66.5	- 13.6	- 0.2836	- 56.7	- 3.4407
	Variance	+ 7.78%	+ 4.53%	- 2.46%	+ 27.72%	+ 21.74%
	Upper	142.4	13.9	0.3557	57.4	3.4406
	Variance	- 5.48%	- 4.88%	+ 9.72%	- 27.42%	- 21.72%

To further analyse the distribution variance between the two groups and the complete driving data, the same calculation was applied; and the results are stated in Table 5-7 and 5-8. The former table indicates that with a front vehicle on the current driving lane, the overall velocity is slightly reduced so as to avoid possible collisions. Both the boundaries of the hand steering wheel angle and the longitudinal acceleration are expanded but not for the Aggressive hand steering wheel angle's boundaries. And both the rate of hand steering and rate of longitudinal accelerating are more compact to the centroid of the driving data, displaying that the instantaneous inputs which the participants applied to the host vehicle are small and stable. The other table shows the results for the group without a front vehicle. It can be found that the trend of the vehicle

velocity is slightly increased and condensed; the longitudinal acceleration is gently shifted to the negative direction and the upper boundaries are smaller than the previous group, which illustrates that the participants did not apply large throttle input to the vehicle; and the distributions of the hand steering wheel angle, the rate of hand steering and the rate of longitudinal accelerating are similar to the overall driving data with less than $\pm 2\%$ variances of the driving styles' boundaries.

Table 5-8 The boundary values and the variance compared to Tabel 5-4 of the right lane change without a front vehicle on the current driving lane.

Driving Style	Boundary / Variance	v (km/hr)	$\delta_{handreal}$ (Degrees)	a_x (g)	$\gamma_{handsteer}$ (Degrees/s)	$\gamma_{longAcc}$ (g/s)
Mild	Lower	93.0	- 4.7	- 0.0828	- 26.4	- 1.4928
	Variance	+ 1.98%	+ 0.01%	- 6.15%	- 0.36%	- 0.34%
	Upper	120.9	5.1	0.1194	27.0	1.4909
	Variance	- 0.25%	+ 0.60%	- 4.78%	+ 0.27%	+ 0.30%
Moderate	Lower	84.6	- 7.6	- 0.1429	- 42.3	- 2.3795
	Variance	+ 2.94%	- 0.19%	- 3.33%	- 0.41%	- 0.39%
	Upper	129.2	8.0	0.1795	42.9	2.3776
	Variance	- 0.70%	+ 0.55%	- 3.34%	+ 0.35%	+ 0.37%
Aggressive	Lower	65.1	- 14.4	- 0.2844	- 79.7	- 4.4667
	Variance	+ 5.41%	- 1.51%	- 2.75%	- 1.61%	- 1.60%
	Upper	148.8	14.8	0.3210	80.3	4.4648
	Variance	- 1.21%	+ 1.67%	- 0.99%	+ 1.57%	+ 1.59%

5.4.3 Lane Change with or without a Vehicle on the Destination Lane

The last analysis is to discover the influence towards the right lane change manoeuvre of whether a vehicle is driven near to the host vehicle on the destination lane or not. The number of the right lane changes with a vehicle on

the destination lane is $\mathbf{105}$ and without a vehicle on the destination lane happened $\mathbf{165}$ times. The sample points of these two types of right lane changes while considering the three measured signals (i.e. the vehicle velocity $\boldsymbol{v}$, the hand steering wheel angle $\boldsymbol{\delta_{handreal}}$, and the longitudinal acceleration $\boldsymbol{a_x}$) were plotted in Figure 5-11, where the driving data with a vehicle and without a vehicle on the destination lane are marked with the blue colour and with the red colour separately. Similar to the previous cases, the red group performs higher driving speed than the blue one; this observation corresponds to the circumstance that drivers often remain or slightly reduce the vehicle velocity and wait until the vehicle on the destination lane finishes the passing manoeuvre so as to prevent entering into the hazard zone while shifting to the target lane. The remaining signals $\boldsymbol{\delta_{handreal}}$ and $\boldsymbol{a_x}$ present vague variances and show a wide range of overlap of these two groups.

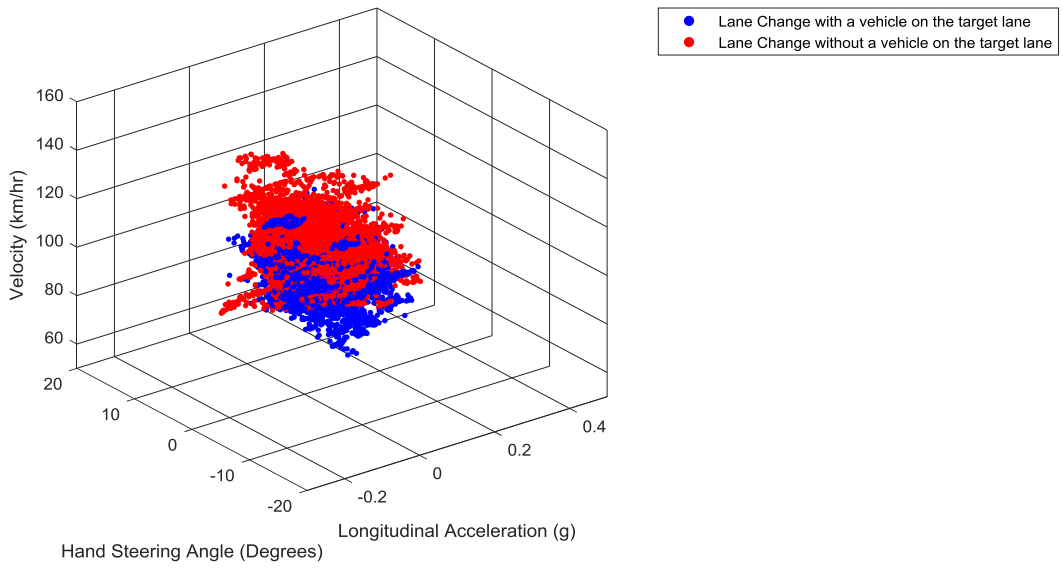

Figure 5-11 The comparison of the measured signals of case 3.

The driving style classifications of both with and without a vehicle which is driven near the host SUV on the destination lane can be found in Table 5-9 and 5-10. Within the condition that there is a vehicle driving on the destination lane; the overall speed is slower than the original driving data, and the values of the hand steering wheel angle are compact comparing to the original driving data so that the boundaries of the driving styles are narrowed down which indicates

that participants applied relative small steering. The driving styles' boundaries of the longitudinal acceleration, the rate of the hand steering wheel angle and the rate of the longitudinal acceleration are extended but not for the Aggressive boundaries of the longitudinal acceleration; providing the evidence that participants performed relative large instantaneous inputs within this condition. On the other hand, Table 5-10 shows the lower boundaries of the vehicle velocity are increased and its spectrum is shifted to the positive direction; the overall distributions of the hand steering wheel angle and the longitudinal acceleration are slightly expanded; and both the rate of the hand steering wheel angle and the rate of the longitudinal acceleration are condensed. In other words, a relative stable control is manipulated while no vehicle is driven on the destination lane during the period of the right lane change.

Table 5-9 The boundary values and the variance compared to Tabel 5-4 of the right lane change with a vehicle driving on the destination lane.

Driving Style	Boundary / Variance	v (km/hr)	$\delta_{handreal}$ (Degrees)	a_x (g)	$\gamma_{handsteer}$ (Degrees/s)	$\gamma_{longAcc}$ (g/s)
Mild	Lower	86.9	- 4.7	- 0.0815	- 29.6	- 1.6697
	Variance	- 4.70%	+ 0.44%	- 4.49%	- 12.63%	- 12.23%
	Upper	116.0	4.9	0.1337	30.2	1.6718
	Variance	- 4.34%	- 2.42%	+ 6.62%	+ 12.06%	+ 12.47%
Moderate	Lower	78.4	- 7.5	- 0.1442	- 47.1	- 2.6441
	Variance	- 4.68%	+ 1.47%	- 4.27%	- 11.80%	- 11.55%
	Upper	124.4	7.7	0.1964	47.7	2.6462
	Variance	- 4.38%	- 2.69%	+ 5.76%	+ 11.46%	+ 11.71%
Aggressive	Lower	63.0	- 12.5	- 0.2579	- 78.7	- 4.4104
	Variance	- 2.03%	+ 11.78%	+ 6.83%	- 0.40%	- 0.32%
	Upper	139.8	12.8	0.3101	79.3	4.4125
	Variance	- 7.17%	- 12.18%	- 4.35%	+ 0.31%	+ 0.40%

Table 5-10 The boundary values and the variance compared to Tabel 5-4 of the right lane change without a vehicle driving on the destination lane.

Driving Style	Boundary / Variance	v (km/hr)	$\delta_{handreal}$ (Degrees)	a_x (g)	γ_{steer} (Degrees/s)	$\gamma_{longAcc}$ (g/s)
Mild	Lower	96.9	- 4.6	- 0.0790	- 20.6	- 1.3317
	Variance	+ 6.31%	+ 1.28%	- 1.28%	+ 21.84%	+ 10.49%
	Upper	121.7	5.1	0.1232	21.3	1.3281
	Variance	+ 0.39%	+ 0.13%	- 1.75%	- 21.13%	- 10.66%
Moderate	Lower	88.9	- 7.7	- 0.1441	- 34.0	- 2.1876
	Variance	+ 8.14%	- 2.22%	- 4.19%	+ 19.21%	+ 7.71%
	Upper	129.7	8.2	0.1883	34.7	2.1840
	Variance	- 0.36%	+ 2.95%	+ 1.40%	- 18.81%	- 7.81%
Aggressive	Lower	71.1	- 14.7	- 0.2893	- 64.1	- 4.0978
	Variance	+ 15.18%	- 3.45%	- 4.52%	+ 18.29%	+ 6.79%
	Upper	147.5	15.1	0.3335	64.8	4.0942
	Variance	- 2.09%	+ 3.82%	+ 2.87%	- 18.08%	- 6.85%

5.5 Key Findings and Discussions

The driving experiment that was detailed in Chapter 4 successfully collected the driving data from $\mathbf{12}$ different participants. With the purpose of achieving human-like lane change control on the motorway, a systematic procedure of analysing the recorded vehicle dynamic data is therefore presented in this chapter.

Starting with valuing the raw signals and filtering the irrelevant ones through statistic techniques, the rest (i.e. the vehicle velocity v, the hand steering wheel angle $\delta_{handreal}$ and the longitudinal acceleration a_x) can be used as the representative signals which have the ability of transmitting the characteristics of human drivers. In order to evaluate the instantaneous variances, the two

post-processing signals (i.e. the rate of hand steering $\boldsymbol{\gamma_{handsteer}}$ and the rate of longitudinal accelerating $\boldsymbol{\gamma_{longAcc}}$) were also taken into account. These $\mathbf{5}$ signals are treated as the essential parameters of distinguishing different styles of driving in this PhD research.

Since there is no unified criteria of defining the driving styles in literatures and considering the generic principles, this PhD research targets at trisecting the overall driving data and utilises the amplitude of the variance of each sample point to the centroid of the whole data as the index of classification. From the physical point of view, this classification principle indicates that Aggressive driving style contains relatively drastic manipulations while considering the average performance of all the human drivers as the basis, and Mild is on the contrary. Both the lower and the upper boundaries of the vehicle velocity $\boldsymbol{v}$, the hand steering wheel angle $\boldsymbol{\delta_{handreal}}$, the longitudinal acceleration $\boldsymbol{a_x}$, the rate of hand steering $\boldsymbol{\gamma_{handsteer}}$ and the rate of longitudinal accelerating $\boldsymbol{\gamma_{longAcc}}$ for Mild, Moderate and Aggressive driving styles are then specified based on the proposed principle; which can be utilised as the constraints in the later lane change control algorithm.

In addition, an assumption that different environmental conditions might alter the response and the performance of human drivers was investigated in the meantime due to the fact that the recorded lane changes were inevitably performed by the participants under different circumstances during the driving tests. According to the video footages that were captured by the camera in the experiment, three different traffic conditions (i.e. (1) change between Normal Speed Lanes & change from Normal Speed Lane to Overtaking Lane, (2) with or without a front vehicle on the current driving lane and (3) with or without a vehicle on the destination lane) towards the lane change manoeuvre were verified.

Ground on the analysis of these environmental conditions in Section 5.4, the above assumption has been confirmed to be correct. The surrounding traffic indeed had impacts on the participants' performance, however, the influences are not as large as expected which might due to that the vehicle merely requires

small values of actuations to complete a lane change manoeuvre on the motorway. Since the interaction between the driver and the traffic condition is one of the important tasks of achieving human-like driving, the relative researches are worth to further investigate and the previous study in this chapter can be its guidance. The future work of the data collection will be growing the amount of the human driving data and increasing the accuracy of the experimental instruments so as to produce more adaptive analysis results.

6 TRAJECTORY PLANNING USING MODEL PREDICTIVE CONTROL

Model Predictive Control (MPC) is a matured technique in the control system and its characteristic gives the motivation of selecting it as the methodology of the human-like trajectory planning algorithm in this research. This chapter firstly illustrates the preliminary sketch of the trajectory planning algorithm which takes the advantage of MPC control technique, including the selection of the vehicle model and the motorway configurations. Two major simulations are then implemented to accomplish the task of changing lanes on the motorway; beginning with the ordinary lane change planning without considering the factor of the human driver and following up with the simulation while taking the previous analysis of the human driving data in Chapter 5 into account. The last section summarises the pros and cons of the proposed human-like trajectory planning lane change control and concludes the contributions of the work in this chapter.

6.1 MPC-based Trajectory Planning

Since the participants' driving data has been analysed in Chapter 5, the next target is to connect the results with the theory and the knowledge of Model Predictive Control (MPC); not only to introduce the human-like motorway lane change control but also to discuss the differences of the MPC trajectory planning algorithms (i.e. with and without considering the human factor). In order to achieve the above aims, it is essential to design a preliminary sketch of the trajectory planning algorithm. Moreover, it should be noted that the primary objective of this PhD research is to generate a feasible human-like trajectory rather than optimise the tracking control.

Assumptions

Before constructing the algorithms and the simulations, several assumptions have to be made in prior to standardise the problem: (1) the ego vehicle has a perception system which is able to detect and measure both external and internal information. (2) Considering the specifications of the experimental

vehicle (i.e. 2017 Land Rover New Discovery), it is assumed of having a rectangular shape with 2 metres width and 5 metres length. (3) The motorway is completely straight (i.e. the curvature of the motorway is $\mathbf{0}$.). Specifically, the mentioned perception system means an integral system that contains a data fusing algorithm and different types of sensors (e.g. Lidar, Radar, Camera, speed sensor, gyroscope, etc.). So that both the external environment (e.g. the location, the lane boundaries, the centre line of a lane, the distances to surrounding vehicles and obstacles, etc.) and the in-vehicle signals can be measured and input into the planning stage, updating the latest state variables at every time step. These reasonable assumptions not only eliminate the uncertainties that might alter simulation results but also reduce the complexity of the trajectory planning algorithm.

As mentioned previously, the model is one of the essential factors in the MPC algorithm. Therefore, the utilised vehicle model has to be determined before conducting the MPC-based trajectory planning algorithm based on the consideration of the trade-off between the algorithm difficulty and the model accuracy. Although a high fidelity model has a better precision of imitating and reflecting the response behaviour of the vehicle, the additional parameters will inevitably increase the cost of the planning. According to the studies which investigate and analyse the performances between the kinematic and the dynamic bicycle models, the kinematic one has been indicated of requiring less computational power and still providing a similar performance with the dynamic one under the driving circumstances with small lateral acceleration [84][85]. Since the target of this PhD research is the lane change on the motorway which merely requires small lateral accelerations to complete the manoeuvre, the above studies adequately support the motivation of choosing the kinematic bicycle model instead of the dynamic one within the trajectory planning algorithm.

6.1.1 Vehicle Model

A typical sketch of the kinematic bicycle model is presented in Figure 6-1. $\boldsymbol{X}$ and $\boldsymbol{Y}$ are the axes of the global frame. The coordinate of the vehicle centre of

gravity (CoG) is denoted as $(\boldsymbol{x}, \boldsymbol{y})$ and the lengths from the CoG to the front and the rear axles are indicated as $\boldsymbol{l_f}$ and $\boldsymbol{l_r}$ respectively. $\boldsymbol{O}$ is the turning centre, $\boldsymbol{v}$ is the velocity and $\boldsymbol{\theta}$ is the heading of the vehicle. The angle of the vehicle velocity at CoG with respect to the wheelbase axis of the vehicle is $\boldsymbol{\beta}$, which is also known as the slip angle of the car. $\boldsymbol{\delta_f}$ and $\boldsymbol{\delta_r}$ are the steering angles of the front wheel and the rear wheel. As the rear wheels of the ordinary vehicle do not have the functionality of steering, $\boldsymbol{\delta_r}$ is usually assigned to be $\mathbf{0}$ in the kinematic bicycle model. Thus, the motion of the ego vehicle can be described by four nonlinear equations [83], as shown in Equation 6-1 to 6-4.

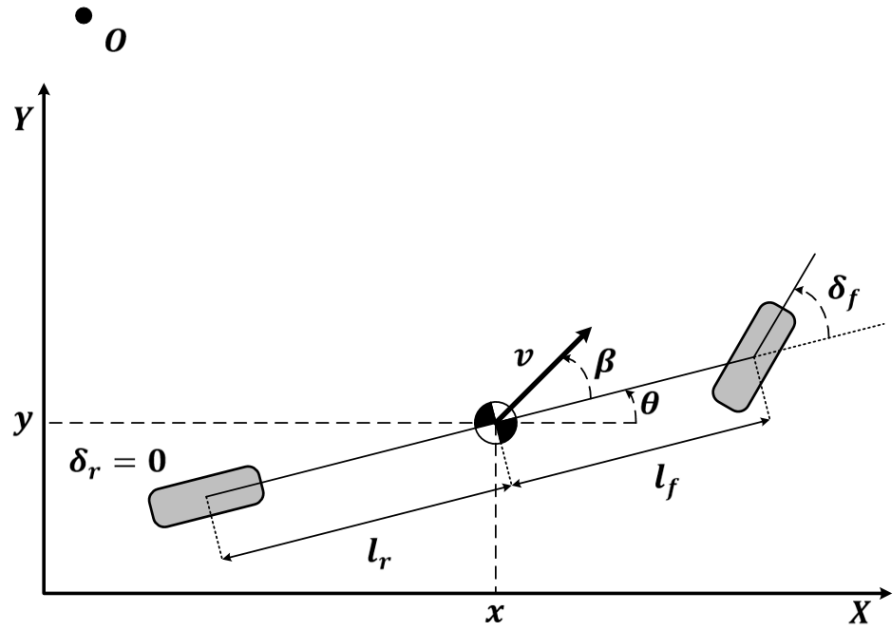

Figure 6-1 The kinematic bicycle model.

$$\dot{\boldsymbol{x}} = \boldsymbol{v}\cos(\boldsymbol{\theta} + \boldsymbol{\beta}) \tag{6-1}$$

$$\dot{\boldsymbol{y}} = \boldsymbol{v}\sin(\boldsymbol{\theta} + \boldsymbol{\beta}) \tag{6-2}$$

$$\dot{\boldsymbol{\theta}} = \frac{\boldsymbol{v}\cos(\boldsymbol{\beta})\tan(\boldsymbol{\delta_f})}{\boldsymbol{l_f} + \boldsymbol{l_r}} = \frac{\boldsymbol{v}}{\boldsymbol{l_r}}\sin(\boldsymbol{\beta}) \tag{6-3}$$

$$\dot{\boldsymbol{v}} = \boldsymbol{a} \tag{6-4}$$

where $\boldsymbol{\beta}$ can be acquired in Equation 6-5.

$$\boldsymbol{\beta = \tan^{-1}\left(\frac{l_r}{l_f + l_r}\tan(\delta_f)\right)} \quad \textbf{(6-5)}$$

6.1.2 Vehicle and Environment Configuration

Considering the above equations of motion of the kinematic model, the two constant parameters $\boldsymbol{l_f}$ and $\boldsymbol{l_r}$ have to be specified. These numbers of the experiment vehicle (i.e. 2017 Land Rover New Discovery) can be acquired from the specifications provided by Jaguar Land Rover company; the wheelbase, $\boldsymbol{l_f}$ and $\boldsymbol{l_r}$ are $\boldsymbol{2925}$ mm, $\boldsymbol{1460}$ mm and $\boldsymbol{1465}$ mm respectively. Furthermore, the steer ratio between the hand steering wheel $\boldsymbol{\delta_{hand}}$ and the front wheel $\boldsymbol{\delta_f}$ is $\boldsymbol{17.6:1}$, which bridges the vehicle model and the recorded steering data of the human participants in the planning algorithm.

Apart from the indispensable parameters of the experiment vehicle, the environmental information has to be defined in the meantime. Since the simulations are focused on the lane change manoeuvre on the motorway, the environment configurations are stated as follows so as to recur the driving scenario of the M1 motorway in the previous experiment as similar as possible:

(1) The platform is a straight and extended motorway which respects left-hand traffic regulations.
(2) Containing **3** lanes and the width of each lane is **3.5** metres.
(3) The ego vehicle starts with driving in the middle of the centre lane.

6.1.3 The framework of the MPC-based trajectory planning algorithm

Based on the analysis outcomes in Section 5.4 that reveal different traffic conditions merely have minor impacts on the participants' control during the lane change manoeuvre on the motorway, having no adjacent vehicle or obstacle is therefore a sensible configuration to standardise and simplify the simulation.

Referring to the block diagram of a model predictive controller in Figure 2-21, it is worthwhile mentioning that both the internal and the system model utilise the

same kinematic bicycle model. Though the general formula of the kinematic model takes the slip effect into account, the slip angle $\boldsymbol{\beta}$ of the vehicle during the lane changing in the following simulations is assumed to be $\mathbf{0}$. It is another reasonable assumption due to the fact that merely a slight steering is required to complete the lane change manoeuvre on the motorway and the focus of this PhD research is the trajectory planning instead of the tracking control of autonomous vehicles.

Hence, the utilised model has six state parameters:

$\boldsymbol{x}$: Global $\boldsymbol{X}$ position of the vehicle centre of gravity (CoG).

$\boldsymbol{y}$: Global $\boldsymbol{Y}$ position of the vehicle centre of gravity (CoG).

$\boldsymbol{\theta}$: Heading angle of the vehicle; where counter-clockwise is positive and $\mathbf{0}$ when facing east.

$\boldsymbol{v}$: Velocity of the vehicle.

$\boldsymbol{a_x}$: Longitudinal acceleration of the vehicle; where positive and negative represent accelerating and decelerating respectively.

$\boldsymbol{\delta_f}$: Front wheel steering angle of the vehicle; where counter-clockwise is positive and $\mathbf{0}$ is aligned with the heading of the car.

and has two manipulated inputs:

$\boldsymbol{\gamma_{longAcc}}$: Rate of the longitudinal acceleration (i.e. longitudinal jerk) of the vehicle.

$\boldsymbol{\gamma_{steer}}$: Rate of the front wheel steering angle of the vehicle.

The reason of merging both $\boldsymbol{a_x}$ and $\boldsymbol{\delta_f}$ into the model states and selecting $\boldsymbol{\gamma_{longAcc}}$ and $\boldsymbol{\gamma_{steer}}$ as the system inputs is to provide the convenience of controlling and tuning the outcomes in the following simulations. After determining the states and the control inputs of the nonlinear model, its equations of motion are then linearised at the nominal operation point through analytical Jacobians and transformed into state space representations:

$$\begin{bmatrix} \dot{x} \\ \dot{y} \\ \dot{\theta} \\ \dot{v} \\ \dot{a}_x \\ \dot{\delta}_f \end{bmatrix} = \underbrace{\begin{bmatrix} 0 & 0 & -v\sin(\theta) & \cos(\theta) & 0 & 0 \\ 0 & 0 & v\cos(\theta) & \sin(\theta) & 0 & 0 \\ 0 & 0 & 0 & \frac{\tan(\delta_f)}{l_f + l_r} & 0 & \frac{v(\tan(\delta)^2 + 1)}{l_f + l_r} \\ 0 & 0 & 0 & 0 & 1 & 0 \\ 0 & 0 & 0 & 0 & 0 & 0 \\ 0 & 0 & 0 & 0 & 0 & 0 \end{bmatrix}}_{A} \begin{bmatrix} x \\ y \\ \theta \\ v \\ a_x \\ \delta_f \end{bmatrix} + \underbrace{\begin{bmatrix} 0 & 0 \\ 0 & 0 \\ 0 & 0 \\ 0 & 0 \\ 1 & 0 \\ 0 & 1 \end{bmatrix}}_{B} \begin{bmatrix} \gamma_{longAcc} \\ \gamma_{steer} \end{bmatrix} \quad \textbf{(6-6)}$$

According to the previous assumption that all the vehicle states can be measured by on-vehicle sensors, the measurement equations can be written as:

$$\begin{bmatrix} \dot{x} \\ \dot{y} \\ \dot{\theta} \\ \dot{v} \\ \dot{a}_x \\ \dot{\delta}_f \end{bmatrix} = \underbrace{\begin{bmatrix} 1 & 0 & 0 & 0 & 0 & 0 \\ 0 & 1 & 0 & 0 & 0 & 0 \\ 0 & 0 & 1 & 0 & 0 & 0 \\ 0 & 0 & 0 & 1 & 0 & 0 \\ 0 & 0 & 0 & 0 & 1 & 0 \\ 0 & 0 & 0 & 0 & 0 & 1 \end{bmatrix}}_{C} \begin{bmatrix} x \\ y \\ \theta \\ v \\ a_x \\ \delta_f \end{bmatrix} + \underbrace{\begin{bmatrix} 0 & 0 \\ 0 & 0 \\ 0 & 0 \\ 0 & 0 \\ 0 & 0 \\ 0 & 0 \end{bmatrix}}_{D} \begin{bmatrix} \gamma_{longAcc} \\ \gamma_{steer} \end{bmatrix} \quad \textbf{(6-7)}$$

The above linearised continues state-space model has to be converted to the discrete form in order to assign to the internal model in the MPC algorithm. Here, the Simpson's rule is applied to obtain the discrete matrices $\boldsymbol{A_d}$, $\boldsymbol{B_d}$, $\boldsymbol{C_d}$ and $\boldsymbol{D_d}$.

The MPC controller starts to calculate the solution of the finite-time optimal control problem through minimising the objective function in Equation 2-10, once the linear-time-invariant (LTI) discrete-time, state-space matrices of the vehicle model are derived. The specified objective function for the following lane change simulations is rewritten as Equation 6-8:

$$\min_{x(k+i),u(k+i)} \sum_{i=1}^{N_p} \left(x(k+i) - x_{ref}(k+i)\right)^T Q(i) \left(x(k+i) - x_{ref}(k+i)\right) + \sum_{i=0}^{N_c-1} \left(u(k+i)\right)^T R(i) \left(u(k+i)\right) \quad \textbf{(6-8)}$$

where N_p is the Prediction Horizon; N_c is the Control Horizon; $x_{ref}(k+i)$ is the reference of the system state; and $Q(i)$ and $R(i)$ are the weighting matrices related to the system state and the manipulated input with time step i ahead from the current time respectively. Both $Q(i)$ and $R(i)$ are time-invariant, and a reference for the manipulated inputs are not required to generate a feasible lane change trajectory in this research.

6.2 Ordinary Trajectory Planning for the Right Lane Change on the Motorway

The first simulation presents the ordinary method of planning a right lane change trajectory on the motorway through MPC technique. The word “ordinary” here represents the algorithm generates a trajectory for an autonomous vehicle without adding the human factor (e.g. the driving style, the ride comfort, the preference, etc.).

Although the overall framework of the algorithm was configured in the previous section, appropriate values still require to be assigned to several variables to obtain the simulation results. As each right lane change on the motorway is a short period driving manoeuvre, the sampling time T_s has to be limited within a small value so that the fidelity of the essential signals can be retained. $T_s = 0.1$ s was first conducted and the outcome specified that it might not be an adequate number to guarantee the detailed information. Furthermore, the log rate of the recorded driving data in the experiment was set to 20 Hz. Hence, T_s was nominated as 0.05 s in the following simulations.

On the other hand, the reference path and the execution point of the lane change manoeuvre for MPC have to be determined in the meantime. The initial conditions of the ego vehicle were set as $x(0) = [0 \quad 0 \quad 0 \quad 30 \quad 0 \quad 0]^T$ and

$\boldsymbol{u(0) = [0 \quad 0]^T}$; which indicates that the vehicle starts from the origin and is driven east at a constant speed of $\boldsymbol{30}$ m/s with no manipulated inputs. By considering the fact that when the idea of making a lane change occurs to a human driver, the destination on the target lane has already been determined in the meantime. As a result, a standard step-line was selected to be the control reference in the algorithm. Ideally, the reference path for a right lane change should be a line with different slopes or any possible curve so as to monitor the dynamic correction of a human driver towards the destination during the lane changing. But this inevitably raises another discussion of how to imitate the human-like calibration process, which is not the primary concern of this PhD research and could be investigated in the future work.

While focusing on the response and the performance of the controller, the reference signal $\boldsymbol{x_{ref}}$ was first assigned as same as the initial conditions (i.e. $\boldsymbol{[0 \quad 0 \quad 0 \quad 30 \quad 0 \quad 0]^T}$) with the purpose of maintaining the forward driving in the centre lane. Once the vehicle reaches $\boldsymbol{30}$ m (i.e. after $\boldsymbol{1}$ s driving), $\boldsymbol{x_{ref}}$ was immediately altered to $\boldsymbol{[0 \quad -3.5 \quad 0 \quad 30 \quad 0 \quad 0]^T}$ so as to trigger a right lane change manoeuvre and designate the target state for the vehicle. The reference path is plotted in Figure 6-2.

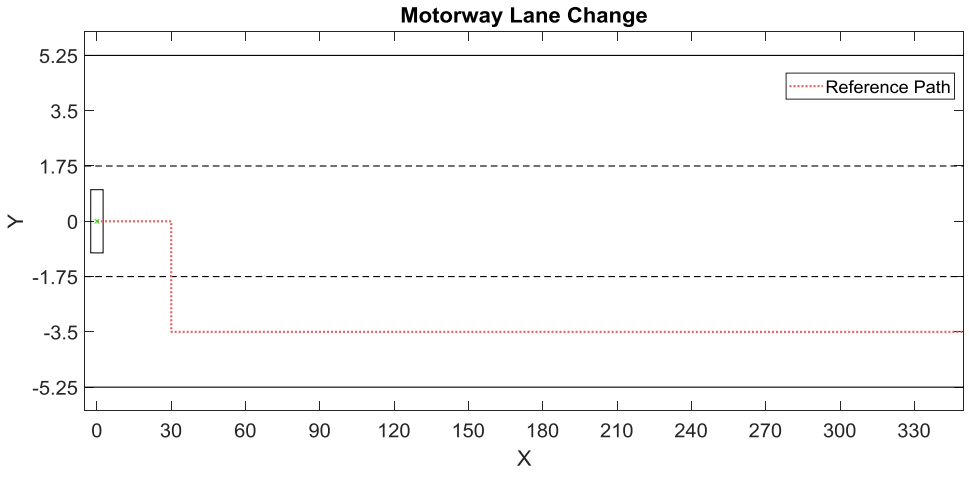

Figure 6-2 The reference path for a right lane change on the motor way.

By modifying the adjustable parameters in the MPC controller, the algorithm is able to theoretically generate infinite numbers of different trajectories to achieve the target reference. Any of them can be seen as the correct answer to solve the lane change problem on the motorway if there is no additional restriction or particular consideration. In other words, these trajectories are purely based on the mathematics and some of them might not be feasible for real humans, which is the primary drawback for the ordinary trajectory planning algorithm. The following paragraphs present one of these trajectories and demonstrate its response while tuning the value of the adjustable parameters. It is worthwhile mentioning that the control horizon $\boldsymbol{N_c}$ was determined as $\mathbf{1}$ since most of the outcomes contained the ripple effect when $\boldsymbol{N_c} \geq \mathbf{2}$, which was also confirmed in the relative research [86].

An instance of the right lane change trajectories which is obtained from the ordinary planning algorithm is shown as the red curve in Figure 6-3. This trajectory is generated through assigning the prediction horizon $\boldsymbol{N_p} = \mathbf{20}$ and the state weighting $\boldsymbol{W_Q} = [\mathbf{0} \quad \mathbf{250} \quad \mathbf{0} \quad \mathbf{2} \quad \mathbf{0} \quad \mathbf{0}]^T$; the only hard constraint can be found in Equation 6-9 which restricts the ego vehicle not to exceed both the right and the left boundaries of the motorway.

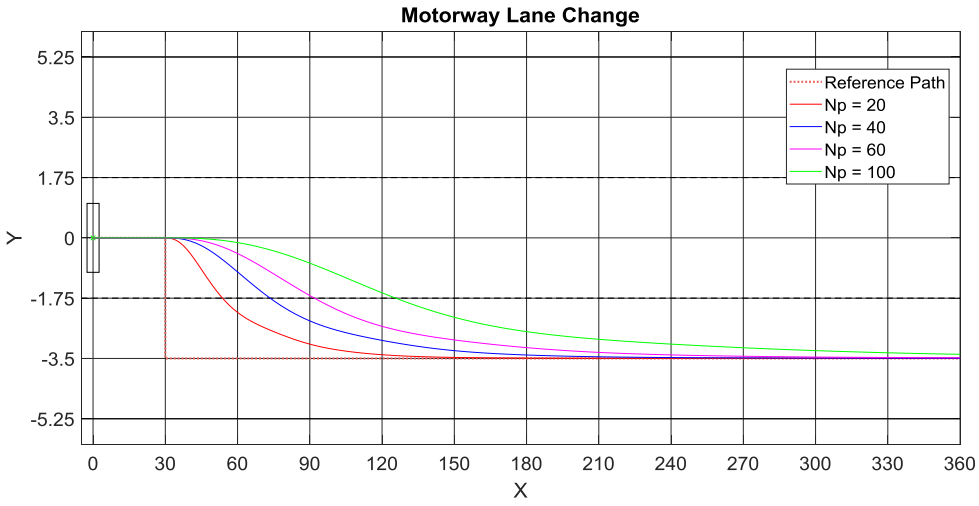

Figure 6-3 The lane change paths with different number of the prediction horizon.

$$-4.25\ m = y_{min} \leq y \leq y_{max} = 4.25\ m \quad \textbf{(6-9)}$$

Each tuning of the adjustable parameters will lead to another possible trajectory for the lane change manoeuvre. For instance, it is almost impossible to acquire the identical trajectory when N_p is varied but the value of W_Q is retained the same. To visualise the relationship between the performance and the prediction horizon, three different trajectories with the same W_Q (i.e. $[0 \quad 250 \quad 0 \quad 2 \quad 0 \quad 0]^T$) were plotted in Figure 6-3 which are $N_p = 40$, $N_p = 60$ and $N_p = 100$. It can be seen that the larger the prediction horizon N_p is, the smaller curvature the trajectory will have. In general, the algorithm with a longer prediction time has the ability to provide a smoother trajectory; however, the duration of completing the lane change manoeuvre is increased in the meantime.

Figure 6-4 and 6-5 depict the variations of both the state parameters and the manipulated inputs which are corresponding to the trajectories in Figure 6-3. It is obvious that the trade-off for delivering a quick response to the target manoeuvre (i.e. short prediction time) is that the vehicle has to perform large amplitude of both the states and the control inputs.

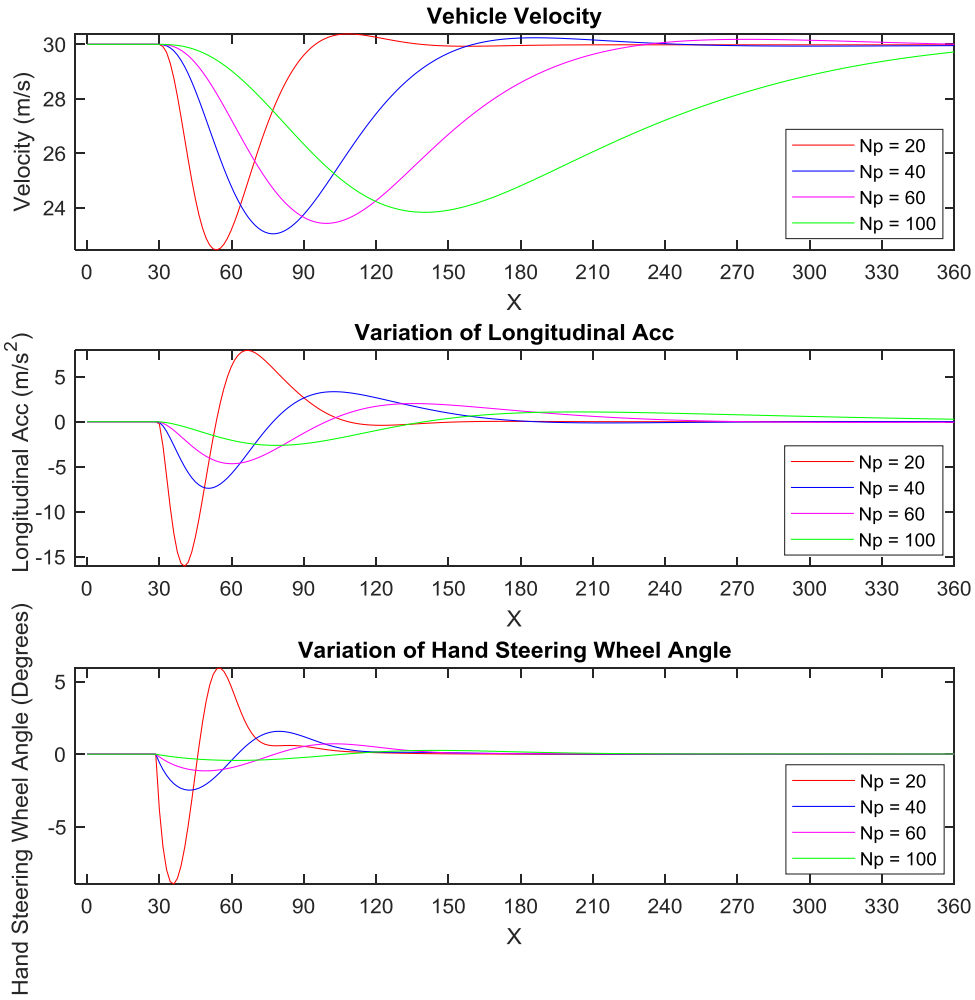

Figure 6-4 The state performance of the trajectories with different number of the prediction horizon.

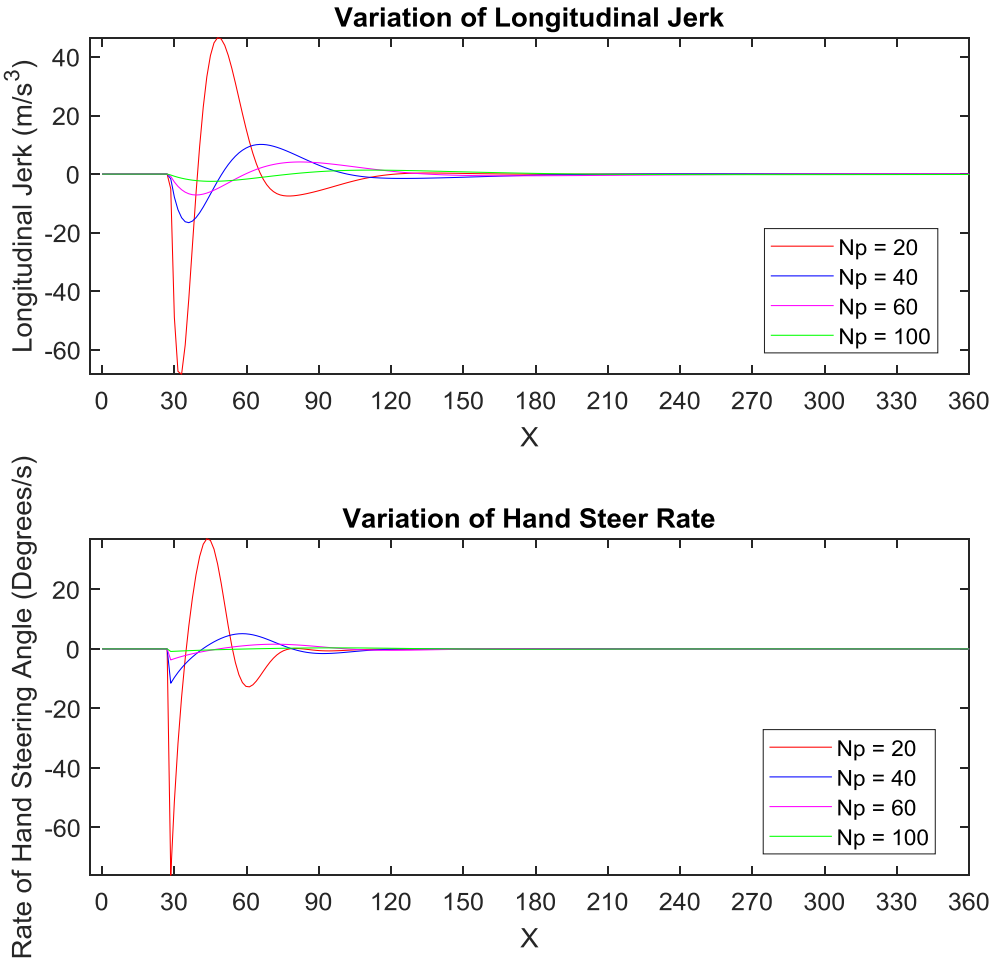

Figure 6-5 The manipulated inputs of the trajectories with different number of the prediction horizon.

Similarly, preserving the same prediction horizon $\boldsymbol{N_p}$ but altering the state weighting $\boldsymbol{W_Q}$ can also affect the outcomes of the algorithm. The trajectories which have the same prediction horizon $\boldsymbol{N_p = 20}$ but different state weighting $\boldsymbol{W_Q}$ (i.e. $[\mathbf{0} \quad \boldsymbol{W_y} \quad \mathbf{0} \quad \mathbf{2} \quad \mathbf{0} \quad \mathbf{0}]^{\boldsymbol{T}}$; $\boldsymbol{W_y = 250}$, $\boldsymbol{W_y = 200}$, $\boldsymbol{W_y = 150}$ and $\boldsymbol{W_y = 100}$) were drawn in Figure 6-6. These trajectory are still constrained by Equation 6-9.

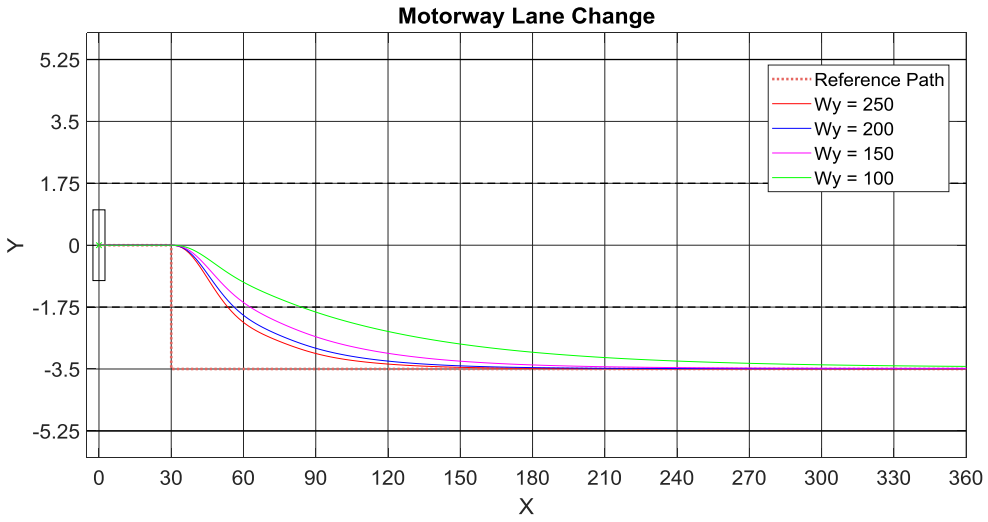

Figure 6-6 The lane change paths with different weighting of the lateral position.

Within the above four trajectories, the one with the largest value of the lateral position weighting $\boldsymbol{W_y}$ performs the harshest curve to approach the reference path and the one with the smallest value is on the contrary. This result aligns with the fact that the weighting describes the importance of a particular variable in MPC. The variations of the vehicle states and the input variables during the lane change manoeuvre can be observed in Figure 6-7 and 6-8, which illustrates the trend that the amplitudes of both the states and the control inputs expand when increasing the weighting of the lateral position.

Again, the ordinary trajectory planning algorithm is able to produce alternative solutions to reach the target reference through altering the combination of the tuneable parameters, even though it is slightly changed. As a result, this algorithm requires further modification to fulfil the primary objective of this PhD research, which is the human-like trajectory planning and will be illustrated in the next section.

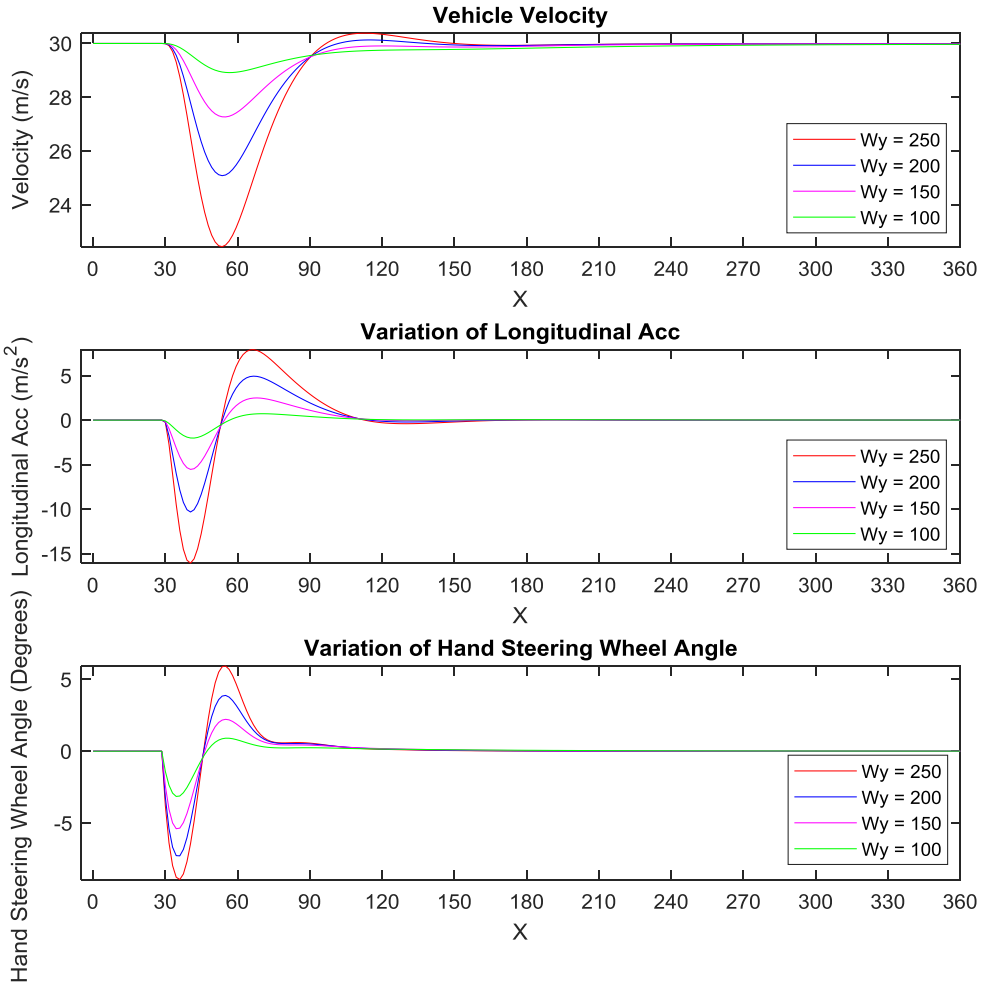

Figure 6-7 The state performance of the trajectories with different weighting of the lateral position.

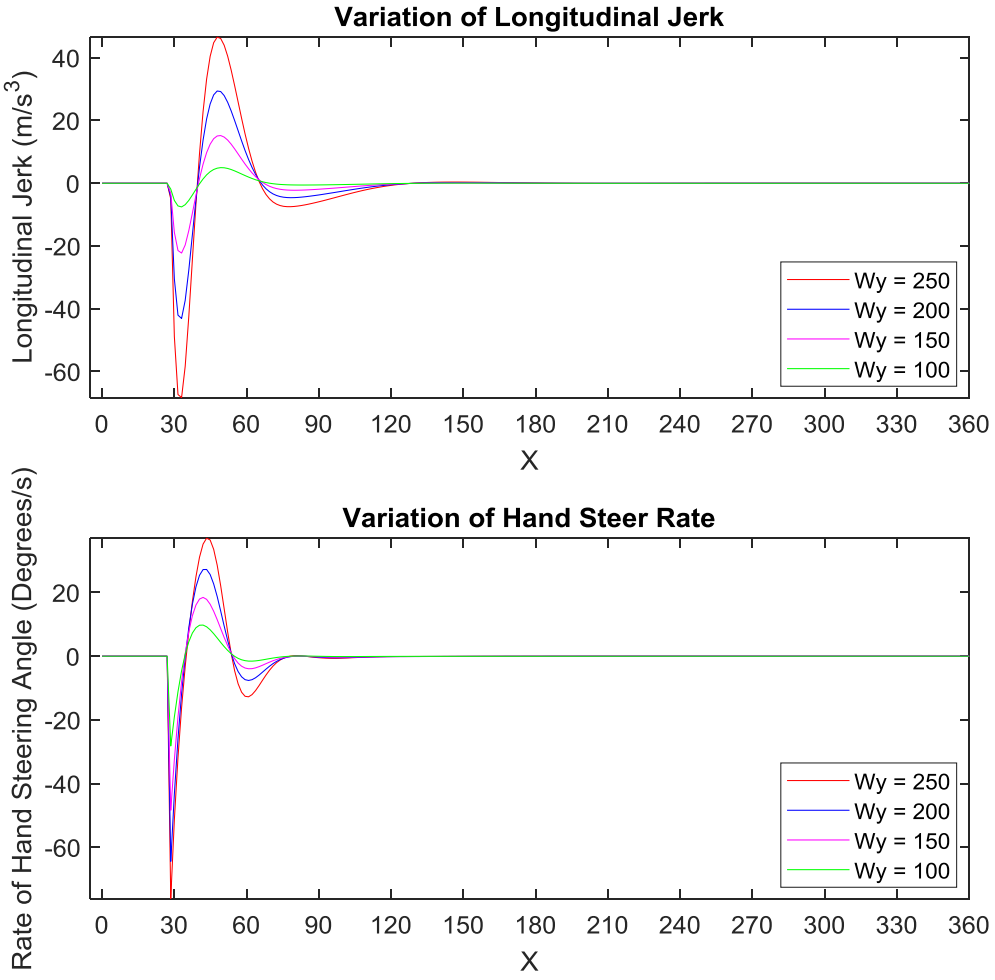

Figure 6-8 The manipulated inputs of the trajectories with different weighting of the lateral position.

6.3 Human-like Trajectory Planning for the Right Lane Change on the Motorway

The trajectories that have been discussed in the previous section can all be accepted as the robotic solutions of completing a right lane change on the motorway. However, some of them become unacceptable options while taking the human factor into consideration. To generate a human-like trajectories which are feasible for real drivers or passengers, the MPC-based trajectory planning algorithm requires further adjustments and has to equip human-related

restrictions. This section introduces how to improve the ordinary trajectory planning algorithm to the human-like one based on the collected driving data from the experiment.

The aforementioned values of the sampling time $\boldsymbol{T_s}$, the control horizon $\boldsymbol{N_c}$, the initial conditions $\boldsymbol{x(0)}$ and $\boldsymbol{u(0)}$ of the vehicle (i.e. $\boldsymbol{T_s = 50}$, $\boldsymbol{N_c = 1}$, $\boldsymbol{x(0) = [0 \quad 0 \quad 0 \quad 30 \quad 0 \quad 0]^T}$ and $\boldsymbol{u(0) = [0 \quad 0]^T}$) and the reference path $\boldsymbol{x_{ref}}$ are adopted as the baseline of the human-like trajectory planning algorithm in this section. In order to provide the algorithm an ability to be operated in real-time, its computational cost has to be taken into account during the modification. The $\boldsymbol{tic\ toc}$ command in MATLAB was therefore applied to the algorithm and confirmed that the longer prediction horizon consumes more power to generate results. On the other hand, Figure 6-3 indicates that the prediction horizon $\boldsymbol{N_p}$ significantly affect the duration of reaching the target reference. According to the collected $\boldsymbol{270}$ right lane changes, the average time for a participant to complete a lane change manoeuvre is $\boldsymbol{7.54}$ s. This observation and the concern of the processing time gave the guidance of choosing an appropriate $\boldsymbol{N_p}$ for the human-like trajectory planning algorithm; $\boldsymbol{N_p = 40}$ were therefore selected.

Apart from $\boldsymbol{N_p}$, another adjustable parameter is the state weighting $\boldsymbol{W_Q}$. This factor describes how important a state variable is while solving the optimising problem to reach the target reference and has a major influence to the amplitudes of the vehicle state. Since the objective of the algorithm is to mimic the behaviour of a human driver and generates a human-like right lane change, the tuning of $\boldsymbol{W_Q}$ has to refer to the driving data as well. Though the original dataset has $\boldsymbol{270}$ right lane change in total, part of them has to be filtered and only the ones that are close to the initial state $\boldsymbol{x(0)}$ are put into consideration. This data refinement guarantees that the human-related information is mined under the similar condition. Figure 6-9 and 6-10 present the data cloud of $\boldsymbol{62}$ right lane changes out of $\boldsymbol{270}$, which have the initial driving velocity between $\boldsymbol{29.5}$ m/s and $\boldsymbol{30.5}$ m/s.

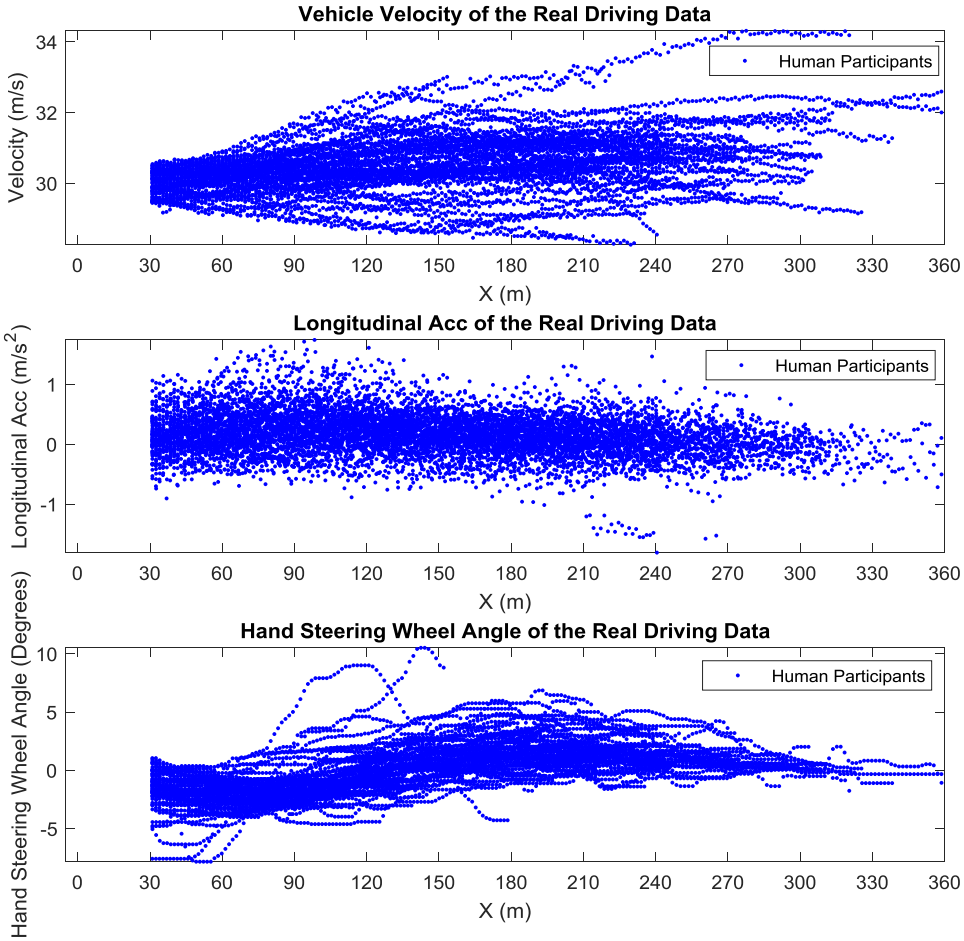

Figure 6-9 The real driving data for the state parameters.

It is clear that most data points that are generated by the human participants appear within a certain amplitude for each parameter. This information instructs the rough range of tuning the state weighting $\boldsymbol{W_Q}$ for the human-like trajectory planning algorithm. Particularly, the weighting of the lateral position $\boldsymbol{W_y}$ was determined in accordance with the hand steering wheel angle $\boldsymbol{\delta_{handreal}}$ and the hand steer rate $\boldsymbol{\gamma_{handsteer}}$; the weighting of the vehicle velocity $\boldsymbol{W_v}$ was based on the longitudinal acceleration $\boldsymbol{a_x}$ and the longitudinal jerk $\boldsymbol{\gamma_{longAcc}}$. The overall weighting of the vehicle state was therefore finalised as $\boldsymbol{W_Q} = [\mathbf{0} \quad \mathbf{150} \quad \mathbf{0} \quad \mathbf{10} \quad \mathbf{0} \quad \mathbf{0}]^{\boldsymbol{T}}$.

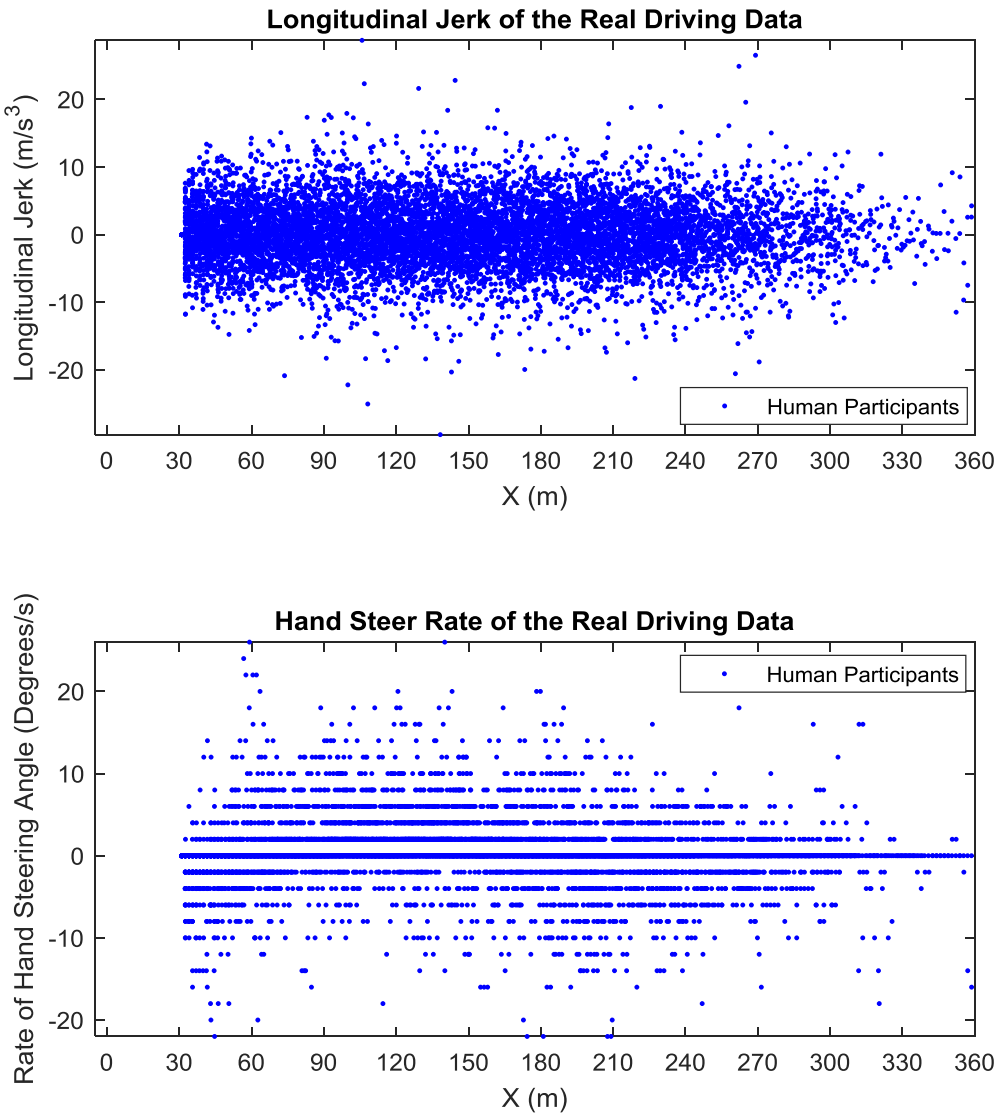

Figure 6-10 The real driving data for the manipulated inputs.

After tuning the adjustable parameters, the algorithm requires an additional restriction to prevent generating a trajectory which is not feasible for humans. Since the analysis results in Chapter 5 concluded the marginal values of the selected signals for different driving styles, these numbers can be implemented as the boundary constraints in the MPC controller. The constraints for Mild driving style are stated in Equation 6-10 to Equation 6-13, and the other two

sets can be written in the similar way. It should be noted that the vehicle velocity v is not constrained in the algorithm.

$$-0.7644\ {}^{m}/_{s^2} = a_{x_{min}} \leq a_x \leq a_{x_{max}} = 1.2289\ {}^{m}/_{s^2} \quad \text{(6-10)}$$

$$-0.0046\ rad = \delta_{f_{min}} \leq \delta_f \leq \delta_{f_{max}} = 0.0050\ rad \quad \text{(6-11)}$$

$$-14.5804\ {}^{m}/_{s^3} = \gamma_{longAcc_{min}} \leq \gamma_{longAcc} \leq \gamma_{longAcc_{max}} = 14.5677\ {}^{m}/_{s^3} \quad \text{(6-12)}$$

$$-0.0261\ {}^{rad}/_{s} = \gamma_{steer_{min}} \leq \gamma_{steer} \leq \gamma_{steer_{max}} = 0.0267\ {}^{rad}/_{s} \quad \text{(6-13)}$$

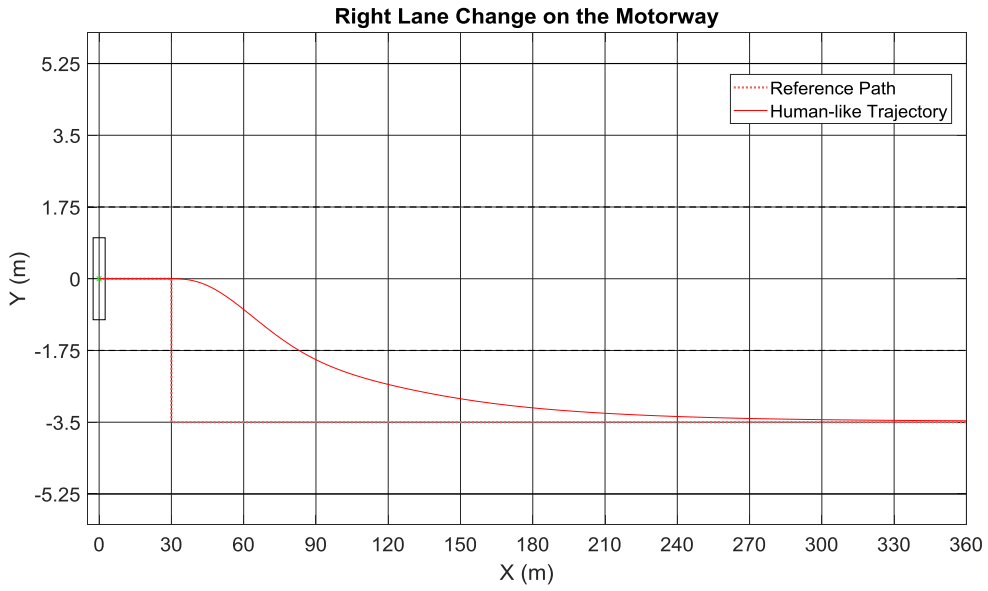

Figure 6-11 The human-like right lane change path.

With the above configurations and modifications, the planning algorithm is now able to produce a human-like trajectory for an autonomous vehicle to perform a right lane change on the motorway. The generated human-like path is schemed in Figure 6-11. Its state variables and the manipulated inputs are plotted in

Figure 6-12 and Figure 6-13 together with the previously selected $\mathbf{62}$ lane change data. The purple dash lines are the constraints for Mild driving style. It can be seen that both the state variables and the manipulated inputs of the human-like trajectory did not violate the configured thresholds. Furthermore, the hand steering wheel angle $\boldsymbol{\delta_{handreal}}$ and the hand steer rate $\boldsymbol{\gamma_{handsteer}}$ of the trajectory match the overall trends that were performed by the human participants. Since these two parameters play important roles in the lateral control, the above comparison results validate the human-like characteristic of the trajectory which is obtained from the aforementioned algorithm. Nevertheless, the figures also point out the main difference is that the human-like parameters seem to be the compressed version in longitudinal direction (i.e. $\boldsymbol{X}$) of the ones from human participants. This observation might due to the slow response time or the long prediction time of human drivers while executing the lane change manoeuvre, which should be investigated in the future work.

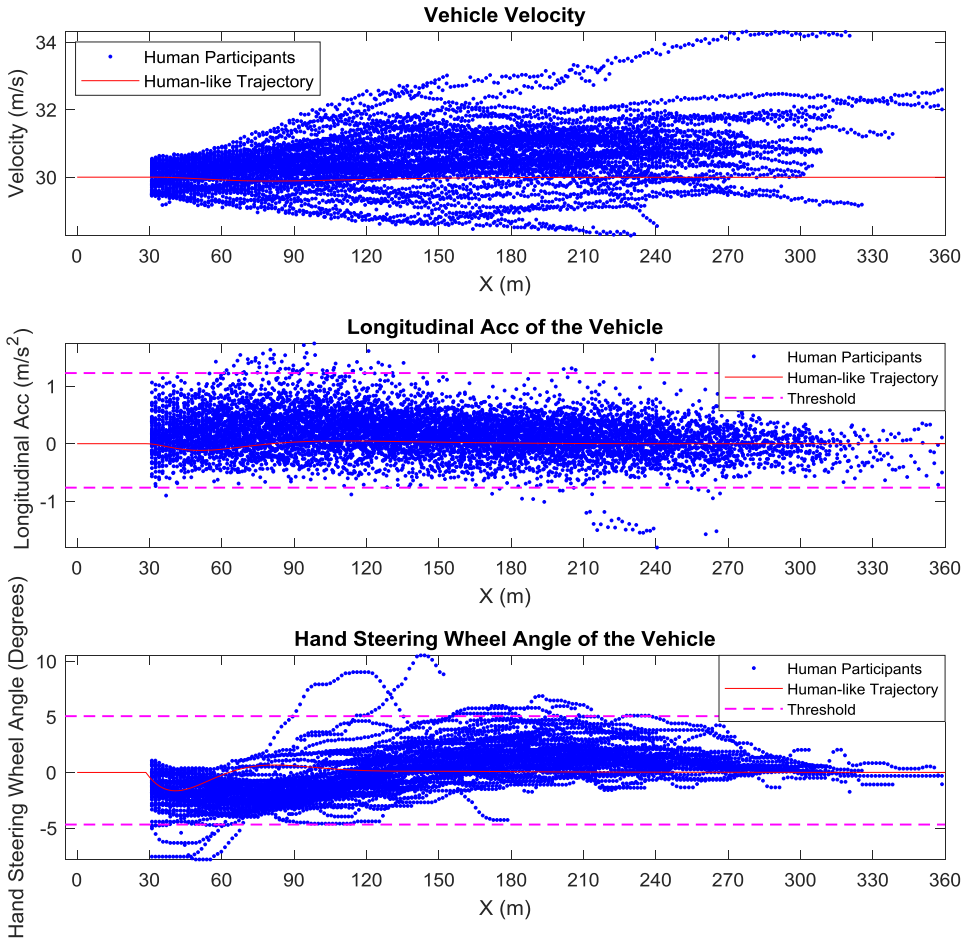

Figure 6-12 The state variables of the human-like trajectory.

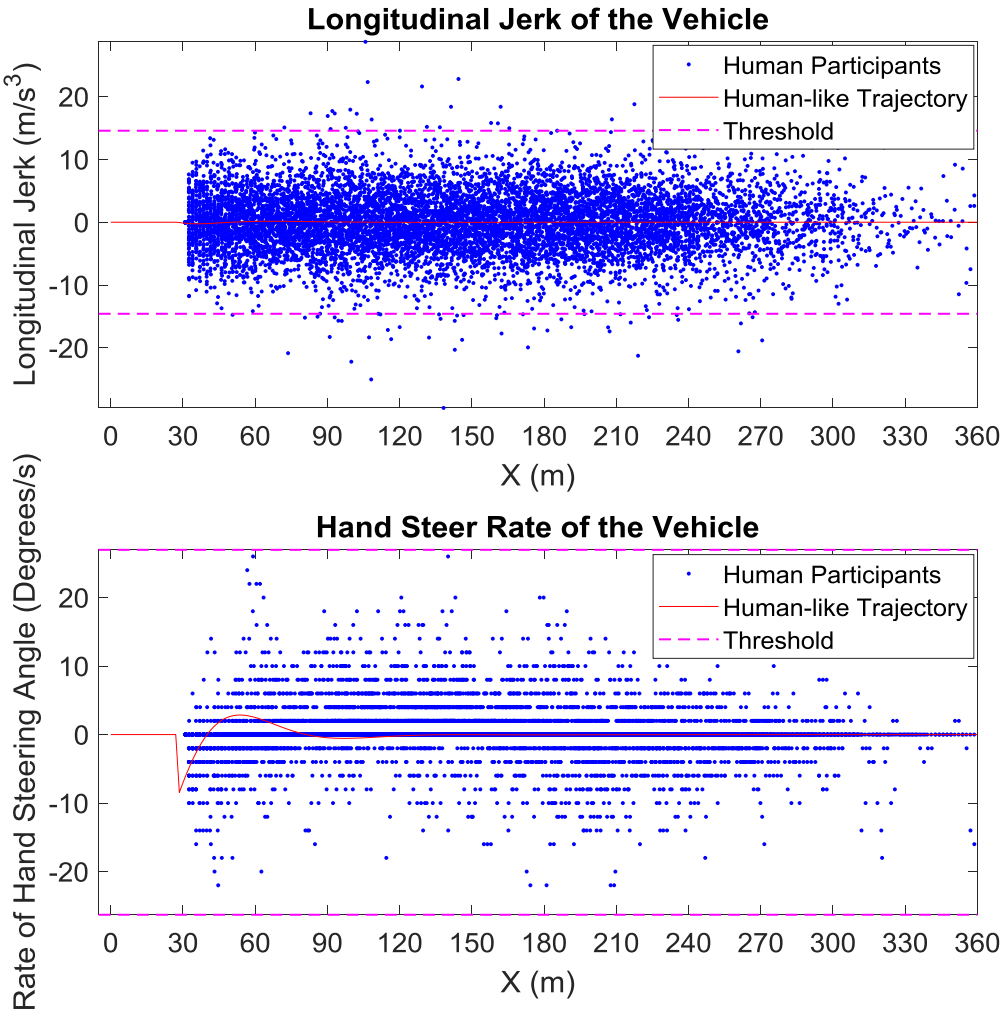

Figure 6-13 The manipulated inputs of the human-like trajectory.

To further verify the performance of the human-like trajectory planning algorithm, two different initial driving velocity $\boldsymbol{v(0)}$ were applied to the algorithm. The velocities were selected based on the lowest and the highest values from the Mild driving data, which are $\boldsymbol{25.3181}$ m/s and $\boldsymbol{33.6710}$ m/s respectively. For each velocity, the algorithm was commanded to deliver two trajectories; one is without taking the constraints of Mild driving style into account and the other is to obey the boundaries. The outcomes are demonstrated in Figure 6-14 to Figure 6-16. It can be observed that all trajectories are able to reach the target reference. Figure 6-15 shows that the two trajectories which were obtained

without configuring the constraints perform large variations in the longitudinal acceleration $\boldsymbol{a_x}$. On the contrary, the other two accelerates the vehicle while respecting the marginal values of Mild driving style. Although the boundaries of other state variables and manipulated inputs did not be violated by all trajectories, they still require to be applied in the algorithm in case an emergency is happened during the lane change period. This comparison highlights the functionality and the necessary of implementing feasible constraints to the human-like trajectory planning algorithm, not only to mimic the human behaviour but also to guarantee the driving safety.

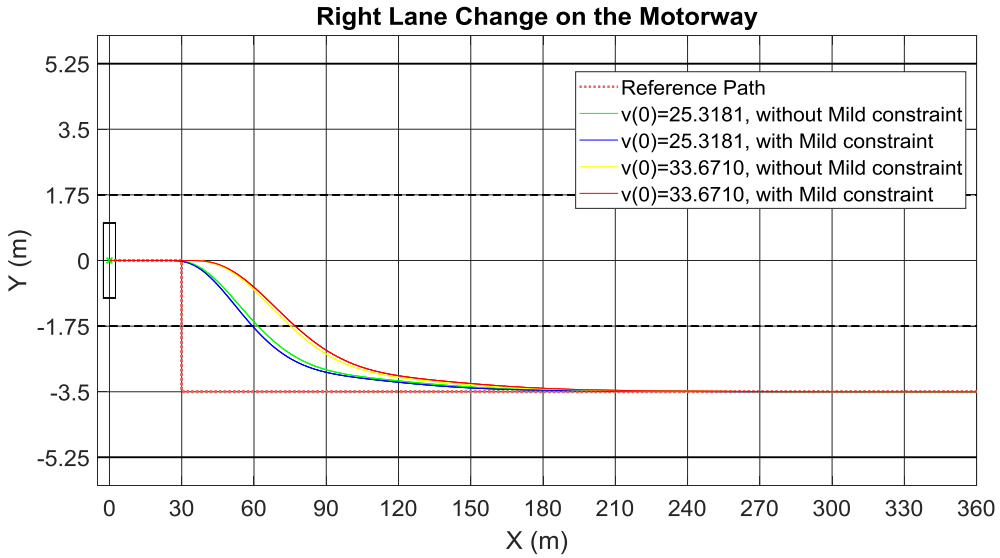

Figure 6-14 The human-like right lane change paths with different initial velocities and the usage of the Mild constraint.

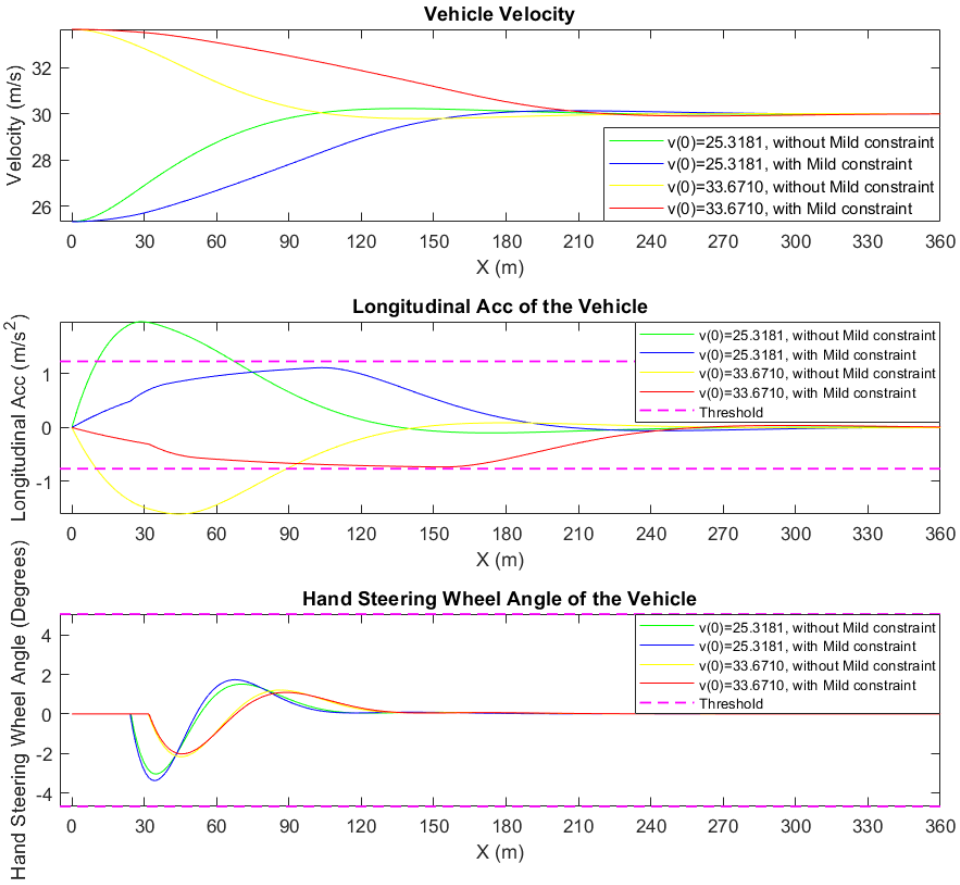

Figure 6-15 The state variables of the human-like trajectories with different initial velocities and the usage of the Mild constraint.

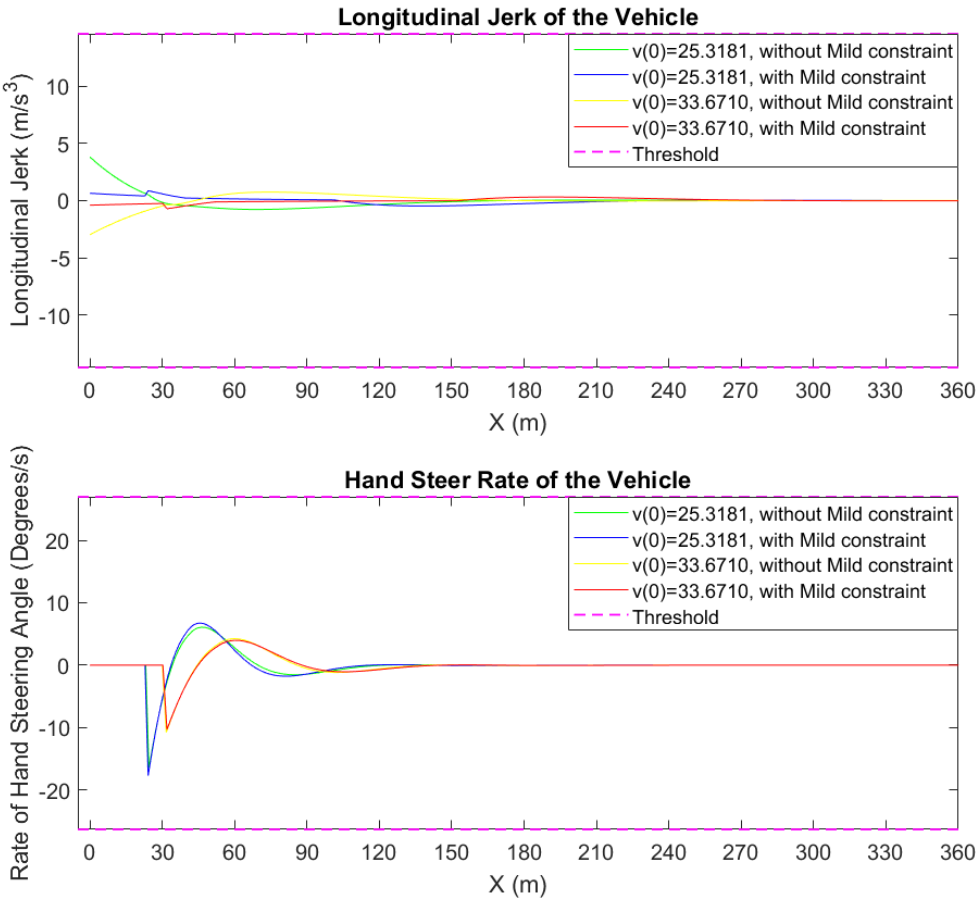

Figure 6-16 The manipulated inputs of the human-like trajectories with different initial velocities and the usage of the Mild constraint.

6.4 Discussions and Summary

Before starting the technical discussions, it should be emphasised that the slip effect was not put into consideration in the simulations. The primary reason is that the vehicle merely requires a small steering angle to accomplish a right lane change manoeuvre on the motorway. Furthermore, this small steering angle demand of the manoeuvre recommends to select the kinematic bicycle model as the vehicle model, which is able to provide a similar performance with less computational power while comparing with the dynamic one.

Based on the conception in the project framework, it can be seen that the proposed human-like trajectory planning algorithm originates from the standard one. Hence, the ordinary MPC-based trajectory planning algorithm was first investigated and simulated. Starting with determining the feasible numbers to the essential parameters of the algorithm and declaring the reference path for the controller to solve the optimising problem. As each right lane change on the motorway is a short period driving manoeuvre, the sampling time $\boldsymbol{T_s}$ has to be limited within a small value so that the fidelity of the essential signals can be retained. Then, two simulations were carried out to evaluate the effects while varying the values of the adjustable parameter (i.e. $\boldsymbol{N_p}$ and $\boldsymbol{W_Q}$). The results concluded that the prediction horizon $\boldsymbol{N_p}$ has a significant impact on the duration of reaching the reference, and the weighting factors $\boldsymbol{W_Q}$ mainly affect the amplitudes of the state variables and the manipulated inputs. Theoretically, the combinations of different values of $\boldsymbol{N_p}$ and $\boldsymbol{W_Q}$ are able to generate infinite trajectories for a vehicle to complete the right lane change on the motorway. However, part of them can be claimed as the robotic trajectory which is not feasible for humans.

To filter those robotic trajectories and deliver the human-like ones, the ordinary planning algorithm requires further adjustments and has to be constrained by human-related restrictions. Yet, the initial condition, the reference path and the configurations were remained the same. The collected human driving data and the analysis results in Chapter 5 were conducted at this stage so as to provide the algorithm the human-like characteristic. The average duration of the collected 270 right lane changes for a participant to complete the manoeuvre is $\boldsymbol{7.54}$ s, suggesting the prediction horizon $\boldsymbol{N_p = 40}$ for the human-like trajectory planning algorithm. While referring to the driving data with similar initial conditions, the overall weighting of the vehicle state was able to finalise as $\boldsymbol{W_Q} = [\boldsymbol{0 \quad 150 \quad 0 \quad 10 \quad 0 \quad 0}]^{\boldsymbol{T}}$. Additionally, the human-related constraints which were obtained from the experiment have to be implemented as the boundaries in the MPC controller. With the above refinements, an enhanced trajectory was then produced. This trajectory has the similar trend to the driving

data that was performed by the human participants, which can be verified as a human-like trajectory. Another two different initial driving velocities were also applied to the proposed human-like trajectory planning algorithm so as to demonstrate its functionality and the stability.

It should be noted that the values of the adjustable variables which were used in the last simulation are not the identical solution to achieve the human-like trajectory. Moreover, either one of the three driving styles' constraints can be applied to the algorithm, depending on the objective of the planning. Unlike most of the traditional methods which simply focus on the efficiency without considering the human factor, this algorithm tries to mimic the performance of human drivers. Although the human-like trajectory might not complete a driving manoeuvre as quick as the robotic one, it has the unique ability to personalise the driving performance. The main contribution of this chapter is presenting a novel approach of constructing a human-like trajectory planning algorithm in accordance with the real human driving data and providing other researchers the draft marginal values of the essential parameters while a human driver is performing a right lane change on the motorway.

To sum up, this chapter combined the methodology of MPC and the human driving data analysis so as to complete the picture of the human-like trajectory planning algorithm. A short discussion about the configurations of the vehicle and the environment was provided at the beginning; the kinematic vehicle model was selected to be applied in the algorithm while considering the trade-off between the computational cost and the performance. Two major simulations were then implemented to accomplish the task of changing lanes on the motorway. The first one demonstrated the lane change planning without considering the human factor and the second one was refined from the ordinary planning algorithm and constrained by the human-related restrictions. Finally, the generated human-like right lane change was compared with the real human driving data that has similar initial conditions, showing the reliable performance of the proposed human-like trajectory planning algorithm.

7 CONCLUSIONS & FUTURE WORKS

This chapter concludes the entire PhD research and its contribution. The proposed human-like trajectory planning algorithm is constructed through a novel approach, which takes the human drivers' driving data into account and provides the MPC the boundary values of three different driving styles. The refined algorithm is now able to obtain the trajectories without violating the applied human-related boundaries. The generated trajectory was validated to be similar to the driving data that is performed by the human participants, which can be verified as human-like trajectories. The potential future works are stated in the meantime, providing clear directions for other researchers who are interested in continuing this research work.

7.1 Conclusions

To fulfil the conception of combining the trajectory planning technique and human characteristics, the database that contains human drivers' driving data has to be constructed in advance. Since the precision of the collected data affects the performance of the planning algorithm, the experiment of capturing lane changes on the motorway was carefully planned and carried out. Although the targeted scenario of this research is the lane change on the motorway, the data within the rural area during the entire driving period was also recorded. This spare driving data might have a chance to be used in future research projects.

Based on the obtained results from both the pre-trial and the main experiment, the signal of the turn indicator cannot be used as the index to verify a lane change manoeuvre. This is due to the fact that the turn indicator is often activated by human drivers with either a positive or a negative time-shifting during a lane change manoeuvre, moreover, some of the drivers even violate the safe regulation and do not switch the indicator on before executing the manoeuvre. On the other hand, the experiment results indicated that most participants performed merely a small variation on the hand steering wheel to change a lane on the motorway. This observation hindered the usage of the

hand steering wheel angle in the lane change identification. Ultimately, the variation of the distance from the vehicle to the left lane boundary was applied to extract each lane change from the original driving data.

To investigate the most representative lane change, only the right single-lane change was considered in this study. Two data statistics techniques were applied to the lane change data so as to analyse the relationships between each available variable and eliminate the irrelevant signals and the duplicate ones with the same human characteristic. After the data refinement, the remaining signals (i.e. the vehicle velocity $\boldsymbol{v}$, the hand steering wheel angle $\boldsymbol{\delta_{handreal}}$, the longitudinal acceleration $\boldsymbol{a_x}$) plus $\mathbf{2}$ post-processing variables (i.e. the rate of hand steering $\boldsymbol{\gamma_{handsteer}}$ and the rate of longitudinal accelerating $\boldsymbol{\gamma_{longAcc}}$) were treated as the essential parameters that describe the characteristics of human drivers. Since the driving style is still a vague concept and does not have a unified definition, this research considered the overall variance as an index and took the advantage of the Gaussian distribution criterion to trisect the overall driving data into ‘Mild’, ‘Moderate’ and ‘Aggressive’ driving styles. The marginal values of the above essential signals which correspond to each proposed driving style were calculated, so as to form the off-line constraint table for the trajectory planning algorithm. On the other hand, the investigation of the traffic influence concluded that the surrounding traffic has minor impacts on the participants’ performance during the right lane change on the motorway. It is worthwhile mentioning that the average time for a human driver to complete a right lane change on the motor way is $\mathbf{7.54}$ s.

In accordance with the previous review among different planning techniques, MPC was selected to be the fundamental framework of the human-like trajectory planning algorithm; which has the capability of anticipating future behaviour of the system and is able to compute the optimal inputs while respecting the configured constraints. The kinematic vehicle model was used to monitor the motion of the vehicle since it provides a good balance between the computational cost and the performance. A number of simulations of the ordinary MPC-based trajectory planning algorithm were first carried out, and the

results indicated that the duration of reaching the reference is mainly affected by the prediction horizon and the amplitudes of the state variables, and the manipulated inputs depend on the corresponding weighting factors. Referring to the recorded human driving data, the adjustable parameters of the ordinary algorithm were tuned to the certain value so that the generated trajectory is operated within the similar amplitudes. This trajectory was verified as the human-like trajectory since its performance matches the overall trend of the data cloud that was performed by the human drivers. Though the trajectory did not violate the marginal value of the off-line boundary table, the constraints of 'Mild' driving style was still applied to the algorithm; not only to ensure the driving safety but also to guarantee the feasibility. The functionality and the stability of the proposed human-like trajectory planning algorithm was then validated through varying the initial driving velocity.

The main contribution of this study is not the detailed configurations of the trajectory planning algorithm but the novel approach of fusing the real human driving data with the traditional planning technique to achieve human-like lane change planning. Both the collected driving database and the driving styles' constraint table can be seen as a unique resource for other researches. Furthermore, the driving styles classification method that was introduced in this PhD research can be applied to either a single driver or multiple drivers. If the driving data is collected from a particular driver, the classification results can help the vehicle autonomy to achieve individualised driving service. On the other hand, if the driving data covers thousands of different drivers, a general indication of the driving styles can be obtained; the more drivers are involved, the more generalised the results will be. Both the academia and the car manufactures can take advantage of it.

7.2 Future Works

As both the academic and the industry foresee the autonomous driving to be one of the ultimate goals in the field of transportation, amount of research and effort have been dedicated to maturing the relevant techniques in recent years. Since the work of this thesis covers a wide range of different knowledge, a lot of

future works can be extended from the study. For instance, the stage of decision making determines the manoeuvre that should be executed, which could refer to the decision that is made by human drivers and generate human-like decision making. It would be interesting to view the comparison and understand the variances between the ordinary decision making and the human-like one. According to the regulation from the UK Department for Transport, a vehicle is prohibited to overtake by moving to a left lane on a motorway. This regulation reveals the potential difference of a drivers' performance between the right lane change and the left one. Hence, a further investigation can be carried out to validate this conjecture. Additionally, the human-like trajectory planning algorithm in this work has been validate with software simulations, which can be further tested in an actual vehicle to verify its performance under real driving circumstances. Moreover, this algorithm can be integrated with a trajectory tracking controller so as to construct a human-like motion control system. Apart from the lane change manoeuvre, this novel human-like functionality could be extended to other driving scenarios. Thus, a higher fidelity dynamic vehicle model that takes the slip effect into account should be used to replace the kinematic vehicle model, which will dramatically improve the performance of the manoeuvres that contain large lateral accelerations. Also, it is clear that the proposed approach in this research obtains human characteristics from the real driving data analysis. In order to grow the size of the human driving database and improve the accuracy, a cooperation with industries is recommended.

REFERENCES

[1] S.Thrun *et al.*, “Stanley: The robot that won the DARPA Grand Challenge,” *Springer Tracts Adv. Robot.*, 2007.

[2] S. M.Veres, L.Molnar, N. K.Lincoln, andC. P.Morice, “Autonomous Vehicle Control Dystems - A Review of Decision Making,” *Proc. Inst. Mech. Eng. Part I J. Syst. Control Eng.*, vol. 225, no. 3, pp. 155–195, 2011.

[3] National Highway Traffic Safety Administration, “National Highway Traffic Safety Administration Preliminary Statement of Policy Concerning Automated Vehicles,” 2013.

[4] U.S. Department of Transportation, “Federal Automated Vehicles Policy,” 2016.

[5] SAE, “Automated Driving - Levels of Driving Automation Are Defined in New Sae International Standard J3016,” 2016.

[6] U.S. Department of Transportation, “Preparing for the Future of Transportation,” 2018.

[7] D.Ferguson, C.Baker, M.Likhachev, andJ.Dolan, “A Reasoning Framework for Autonomous Urban Driving,” in *IEEE Intelligent Vehicles Symposium, Proceedings*, 2008, pp. 775–780.

[8] D.Heinrichs andR.Cyganski, “Automated Driving: How it could enter our cities and how this might affect our mobility decisions,” *disP - Plan. Rev.*, vol. 51, no. 2, pp. 74–79, 2015.

[9] M.Sivak andB.Schoettle, “Motion Sickness in Self-Driving Vehicles,” 2015.

[10] B.Paden, M.Cap, S. Z.Yong, D.Yershov, andE.Frazzoli, “A Survey of Motion Planning and Control Techniques for Self-Driving Urban Vehicles,” *IEEE Trans. Intell. Veh.*, vol. 1, no. 1, pp. 33–55, 2016.

[11] D.González, J.Pérez, V.Milanés, andF.Nashashibi, “A Review of Motion

Planning Techniques for Automated Vehicles," *IEEE Trans. Intell. Transp. Syst.*, vol. 17, no. 4, pp. 1135–1145, 2016.

[12] G.Carbone andF.Gomez-Bravo, Eds., *Motion and Operation Planning of Robotic Systems: Background and Practical Approaches*, vol. 29. 2015.

[13] E.Masehian andD.Sedighizadeh, "Classic and Heuristic Approaches in Robot Motion Planning – A Chronological Review," *World Acad. Sci. Eng. Technol.*, vol. 29, no. 5, pp. 101–106, 2007.

[14] S.Han, B.Choi, andJ.Lee, "A precise curved motion planning for a differential driving mobile robot," *Mechatronics*, vol. 18, no. 9, pp. 486–494, 2008.

[15] C.Urmson, "Autonomous Driving in Urban Environments: Boss and the Urban Challenge," *J. F. Robot.*, vol. 25, no. 8, pp. 426–466, 2008.

[16] C.Katrakazas, M.Quddus, W.-H.Chen, andL.Deka, "Real-time motion planning methods for autonomous on-road driving: State-of-the-art and future research directions," *Transp. Res. Part C Emerg. Technol.*, vol. 60, pp. 416–442, 2015.

[17] D.Gonzalez, J.Perez, V.Milanes, andF.Nashashibi, "A Review of Motion Planning Techniques for Automated Vehicles," *IEEE Trans. Intell. Transp. Syst.*, vol. 17, no. 4, pp. 1135–1145, 2016.

[18] S.Edelkamp andS.Schrödl, "Route Planning and Map Inference with Global Positioning Traces," *Comp. Sci. Perspect. Essays Dedic. to Thomas Ottmann*, pp. 128–151, 2003.

[19] S.Al-Hasan andG.Vachtsevanos, "Intelligent route planning for fast autonomous vehicles operating in a large natural terrain," *Rob. Auton. Syst.*, vol. 40, no. 1, pp. 1–24, 2002.

[20] U.Lee, S.Yoon, H.Shim, P.Vasseur, andC.Demonceaux, "Local path planning in a complex environment for self-driving car," in *4th Annual IEEE International Conference on Cyber Technology in Automation,*

Control and Intelligent Systems, IEEE-CYBER 2014, 2014, pp. 445–450.

[21] D.Dolgov, S.Thrun, M.Montemerlo, andJ.Diebel, “Path Planning for Autonomous Vehicles in Unknown Semi-structured Environments,” *Int. J. Rob. Res.*, vol. 29, no. 5, pp. 485–501, 2010.

[22] Z.Li, M.Chitturi, D.Noyce, B.Ran, M.VChitturi, andD.Noyce, “Development of Next Generation Intersection Control,” 2013.

[23] P.Zhao, J.Chen, T.Mei, andH.Liang, “Dynamic Motion Planning for Autonomous Vehicle in Unknown Environments,” *2011 IEEE Intell. Veh. Symp.*, no. IV, pp. 284–289, 2011.

[24] W.Xu, J.Pan, J.Wei, andJ. M.Dolan, “Motion Planning under Uncertainty for On-Road Autonomous Driving,” in *2014 IEEE International Conference on Robotics and Automation (ICRA),* 2014, pp. 2061–2067.

[25] S.Joachim, G.Tobias, J.Daniel, andD.Riidiger, “Path planning for cognitive vehicles using risk maps,” *IEEE Intell. Veh. Symp. Proc.*, pp. 1119–1124, 2008.

[26] D.Ferguson andM.Likhachev, “Efficiently using cost maps for planning complex maneuvers,” in *Lab Papers (GRASP)*, 2008, p. 20.

[27] M.Bibuli, M.Caccia, andL.Lapierre, “Path-following algorithms and experiments for an autonomous surface vehicle,” *IFAC Proc. Vol.*, vol. 7, no. PART 1, pp. 81–86, 2007.

[28] L.Murphy andP.Newman, “Risky planning: Path planning over costmaps with a probabilistically bounded speed-accuracy tradeoff,” in *Proceedings - IEEE International Conference on Robotics and Automation*, 2011, pp. 3727–3732.

[29] M.Mcnaughton, C.Urmson, J. M.Dolan, andJ.Lee, “Motion Planning for Autonomous Driving with a Conformal Spatiotemporal Lattice,” in *2011 IEEE International Conference on Robotics and Automation*, 2011, vol. 1, pp. 4889–4895.

[30] J.Ziegler andC.Stiller, “Spatiotemporal state lattices for fast trajectory planning in dynamic on-road driving scenarios,” in *2009 IEEE/RSJ International Conference on Intelligent Robots and Systems, IROS 2009*, 2009, pp. 1879–1884.

[31] J. M.Wille, F.Saust, andM.Maurer, “Stadtpilot: Driving autonomously on Braunschweig’s inner ring road,” in *2010 IEEE Intelligent Vehicles Symposium*, 2010, pp. 506–511.

[32] M.Bibuli, M.Caccia, andL.Lapierre, “The MIT–Cornell collision and why it happened,” *J. F. Robot.*, no. 25, pp. 775–807, 2008.

[33] Y.Kuwata, J.Teo, G.Fiore, S.Karaman, E.Frazzoli, andJ. P.How, “Real-time motion planning with applications to autonomous urban driving,” *IEEE Trans. Control Syst. Technol.*, vol. 17, no. 5, pp. 1105–1118, 2009.

[34] D.Madas *et al.*, “On path planning methods for automotive collision avoidance,” *2013 IEEE Intell. Veh. Symp.*, no. Iv, pp. 931–937, 2013.

[35] J.Jansson andJ.Johansson, “Decision Making for Collision Avoidance Systems,” *Soc. Automot. Eng.*, pp. 1–8, 2002.

[36] S. M.Veres, L.Molnar, N. K.Lincoln, andC. P.Morice, “Autonomous vehicle control systems -- a review of decision making,” in *Proceedings of the Institution of Mechanical Engineers, Part I: Journal of Systems and Control Engineering*, 2011, vol. 225, no. 2, pp. 155–195.

[37] M.Nilsson, “Decision Making for Automated Vehicles in Merging Situations - using Partially Observable Markov Decision Processes,” 2014.

[38] J.Reeds andL.Shepp, “Optimal paths for a car that goes both forwards and backwards,” *Pacific J. Math.*, vol. 145, no. 2, pp. 367–393, 1990.

[39] J.Horst andB.Anthony, “Trajectory generation for an on-road autonomous vehicle,” *Proc. SPIE*, vol. 6230, pp. 62302J-62302J–12, 2006.

[40] J.Funke *et al.*, “Up to the limits: Autonomous Audi TTS,” *IEEE Intell. Veh.*

Symp. Proc., pp. 541–547, 2012.

[41] M.Brezak andI.Petrovic, “Real-time approximation of clothoids with bounded error for path planning applications,” *IEEE Trans. Robot.*, vol. 30, no. 2, pp. 507–515, 2014.

[42] V.Delsart, T.Fraichard, andL.Martinez, “Real-time trajectory generation for car-like vehicles navigating dynamic environments,” in *Proceedings - IEEE International Conference on Robotics and Automation*, 2009, pp. 3401–3406.

[43] Y.Cong, O.Sawodny, H.Chen, J.Zimmermann, andA.Lutz, “Motion planning for an autonomous vehicle driving on motorways by using flatness properties,” in *Proceedings of the IEEE International Conference on Control Applications*, 2010, pp. 908–913.

[44] W.Xu, J.Wei, J. M.Dolan, H.Zhao, andH.Zha, “A Real-Time Motion Planner with Trajectory Optimization for Autonomous Vehicles,” in *IEEE International Conference on Robotics and Automation*, 2012, pp. 2061–2067.

[45] I.Bae, J.Moon, H.Park, J. H.Kim, andS.Kim, “Path generation and tracking based on a Bezier curve for a steering rate controller of autonomous vehicles,” in *IEEE Conference on Intelligent Transportation Systems, Proceedings, ITSC*, 2013, no. Itsc, pp. 436–441.

[46] D.Gonzalez, J.Perez, R.Lattarulo, V.Milanes, andF.Nashashibi, “Continuous curvature planning with obstacle avoidance capabilities in urban scenarios,” in *2014 17th IEEE International Conference on Intelligent Transportation Systems, ITSC 2014*, 2014, pp. 1430–1435.

[47] M.Wang, T.Ganjineh, andR.Rojas, “Action annotated trajectory generation for autonomous maneuvers on structured road networks,” in *ICARA 2011 - Proceedings of the 5th International Conference on Automation, Robotics and Applications*, 2011, pp. 67–72.

[48] T.Gu andJ.Dolan, “Toward human-like motion planning in urban

environments," *Intell. Veh. Symp. Proceedings, …*, pp. 2–7, 2014.

[49] M.Likhachev *et al.*, "Trajectory planning for Bertha - A local, continuous method," *Int. J. Rob. Res.*, vol. 35, no. April, pp. 450–457, 2014.

[50] T.Lee andJ.Son, "Relationships between Driving Style and Fuel Consumption in Highway Driving," 2011.

[51] B.V.Padma Rajan, A.McGordon, andP. A.Jennings, "An investigation on the effect of driver style and driving events on energy demand of a PHEV," 2012.

[52] O.Taubman-Ben-Ari, M.Mikulincer, andO.Gillath, "The multidimensional driving style inventory - Scale construct and validation," *Accid. Anal. Prev.*, vol. 36, no. 3, pp. 323–332, 2004.

[53] F. U.Syed, D.Filev, andH.Ying, "Fuzzy rule-based driver advisory system for fuel economy improvement in a hybrid electric vehicle," in *Annual Conference of the North American Fuzzy Information Processing Society - NAFIPS*, 2007, pp. 178–183.

[54] R.Stoichkov, "Android Smartphone Application for Driving Style Recognition," Technische Universitat Munchen, 2013.

[55] E.Ericsson, "Independent driving pattern factors and their influence on fuel-use and exhaust emission factors," *Transp. Res. Part D Transp. Environ.*, vol. 6, no. 5, pp. 325–345, 2001.

[56] M.Heucke, C.Marina Martinez, F.-Y.Wang, B.Gao, andD.Cao, "Driving Style Recognition for Intelligent Vehicle Control and Advanced Driver Assistance: A Survey," *Trans. Intell. Transp. Syst. (Under Rev.*, 2016.

[57] J.Neubauer andE.Wood, "Accounting for the Variation of Driver Aggression in the Simulation of Conventional and Advanced Vehicles," 2013.

[58] D. A.Johnson andM. M.Trivedi, "Driving style recognition using a smartphone as a sensor platform," in *IEEE Conference on Intelligent*

Transportation Systems, Proceedings, ITSC, 2011, pp. 1609–1615.

[59] N.Karginova, S.Byttner, andM.Svensson, “Data-driven methods for classification of driving styles in buses,” 2012.

[60] D.Dorr, D.Grabengiesser, andF.Gauterin, “Online driving style recognition using fuzzy logic,” in *Intelligent Transportation Systems (ITSC), 2014 IEEE 17th International Conference on*, 2014, pp. 1021–1026.

[61] L.Xu, J.Hu, H.Jiang, andW.Meng, “Establishing Style-Oriented Driver Models by Imitating Human Driving Behaviors,” *IEEE Trans. Intell. Transp. Syst.*, vol. 16, no. 5, pp. 2522–2530, 2015.

[62] M.VanLy, S.Martin, andM. M.Trivedi, “Driver classification and driving style recognition using inertial sensors,” in *IEEE Intelligent Vehicles Symposium, Proceedings*, 2013, no. Iv, pp. 1040–1045.

[63] T.Shamir, “How should an autonomous vehicle overtake a slower moving vehicle: Design and analysis of an optimal trajectory,” *Autom. Control. IEEE Trans.*, vol. 49, no. 4, pp. 2002–2005, 2004.

[64] F.You, R.Zhang, G.Lie, H.Wang, H.Wen, andJ.Xu, “Trajectory planning and tracking control for autonomous lane change maneuver based on the cooperative vehicle infrastructure system,” *Expert Syst. Appl.*, vol. 42, no. 14, pp. 5932–5946, 2015.

[65] W.Chee andM.Tomizuka, “Lane change maneuver of automobiles for the intelligent vehicle and highway system (IVHS),” *Am. Control Conf. 1994*, no. June, pp. 3586–3587, 1994.

[66] W.Chee andM.Tomizuka, “Vehicle Lane Change Maneuver in Automated Highway Systems,” 1994.

[67] Z.Shiller andS.Sundar, “Emergency Lane-Change Maneuvers of Autonomous Vehicles,” *ASME J. Dyn. Syst. Meas. Control*, vol. 120, no. 1, pp. 37–44, 1998.

[68] C.Hatipoglu, Ü.̈Özguner, andK. A.Redmill, “Automated lane change

controller design," *IEEE Trans. Intell. Transp. Syst.*, vol. 4, no. 1, pp. 13–22, 2003.

[69] J. E.Naranjo, C.Gonzalez, R.Garcia, andT.DePedro, "Lane-change fuzzy control in autonomous vehicles for the overtaking maneuver," *IEEE Trans. Intell. Transp. Syst.*, vol. 9, no. 3, pp. 438–450, 2008.

[70] Y.Wen *et al.*, "Lane Change Trajectory Prediction by using Recorded Human Driving Data To cite this version : Lane Change Trajectory Prediction by using Recorded Human Driving Data," in *IEEE Intelligent Vehicles Symposium (IV)*, 2013, no. IV.

[71] E. F.Camacho andC. B.Alba, *Model Preictive Control*. Springer Science & Business Media, 2013.

[72] L.Wang, *Model predictive control system design and implementation using MATLAB®*. Springer, 2009.

[73] F.Borrelli, P.Falcone, T.Keviczky, J.Asgari, andD.Hrovat, "MPC-based approach to active steering for autonomous vehicle systems," *Int. J. Veh. Auton. Syst.*, vol. 3, no. 2/3/4, p. 265, 2005.

[74] D. J.Cole, A. J.Pick, andA. M. C.Odhams, "Predictive and linear quadratic methods for potential application to modelling driver steering control," *Veh. Syst. Dyn.*, vol. 44, no. 3, pp. 259–284, 2006.

[75] O.Garcia, J. V.Ferreira, andA. M.Neto, "Design and Simulation for Path Tracking Control of a Commercial Vehicle Using MPC," *2014 Jt. Conf. Robot. SBR-LARS Robot. Symp. Rob.*, no. figure 2, pp. 61–66, 2014.

[76] J.Funke, M.Brown, S. M.Erlien, andJ. C.Gerdes, "Collision Avoidance and Stabilization for Autonomous Vehicles in Emergency Scenarios," *IEEE Trans. Control Syst. Technol.*, vol. 25, no. 4, pp. 1204–1216, 2017.

[77] C.Shen, Y.Shi, andB.Buckham, "Integrated path planning and tracking control of an AUV: A unified receding horizon optimization approach," *IEEE/ASME Trans. Mechatronics*, vol. 22, no. 3, pp. 1163–1173, 2017.

[78] M.Elbanhawi, M.Simic, andR.Jazar, “In the Passenger Seat: Investigating Ride Comfort Measures in Autonomous Cars,” *IEEE Intell. Transp. Syst. Mag.*, vol. 7, no. 3, pp. 4–17, 2015.

[79] C.Diels, “Will autonomous vehicles make us sick?,” *Contemp. Ergon. Hum. Factors*, no. October, pp. 301–307, 2014.

[80] C.Diels andJ. E.Bos, “Self-driving carsickness,” *Appl. Ergon.*, vol. 53, pp. 374–382, 2015.

[81] S.Wright, “Correlation and Causation.pdf,” *Journal of Agricutural Research*, vol. XX, no. 7. pp. 557–585, 1931.

[82] “Correlation and dependence.” [Online]. Available: https://en.wikipedia.org/wiki/Correlation_and_dependence.

[83] M.Abe andW.Manning, “Vehicle Dynamics and Control,” in *Vehicle Handling Dynamics*, 2009.

[84] J.Kong, M.Pfeiffer, G.Schildbach, andF.Borrelli, “Kinematic and dynamic vehicle models for autonomous driving control design,” *IEEE Intell. Veh. Symp. Proc.*, vol. 2015-Augus, pp. 1094–1099, 2015.

[85] P.Polack, F.Altche, B.DAndrea-Novel, andA.DeLa Fortelle, “The kinematic bicycle model: A consistent model for planning feasible trajectories for autonomous vehicles?,” *IEEE Intell. Veh. Symp. Proc.*, no. Iv, pp. 812–818, 2017.

[86] S.Zhao, A.Maxim, S.Liu, R. D.DeKeyser, andC.Ionescu, “Effect of control horizon in model predictive control for steam/water loop in large-scale ships,” *Processes*, vol. 6, no. 12, pp. 1–14, 2018.

APPENDICES

Appendix A Potential Solutions of Sensors Installation for Autonomous Vehicle

Theoretically, a person who would like to perform a well-organised action or decision must consider almost every impact factor towards the result in advance. For instance, if a human driver prefer to achieve a smooth and safe lane change manoeuvre while driving on motorways, almost every environmental features at the present moment (e.g. the distance to front vehicle, the relative speeds between ego and surrounding vehicles, the available space for vehicle to merge, etc.) should be taken into account; all the information is observed through the human's perception system. Similarly, the autonomy of an autonomous vehicle is requested to analyse all the surrounding information before executing any specific action during self-driving; the combination of different types of sensors can be therefore treated as the perception system of autonomous vehicle.

It is worthwhile mentioning that the FOV of an ideal autonomous vehicle's perception system should reach 360-degree coverage in order to obtain all necessary information for motion planning and guarantee the driving safety. Moreover, the usage of different types of sensors has the capability to provide better perception performance due to individual strengths and weaknesses of sensors. Based on the previous sensory instruments investigation report and the related articles that have been reviewed in Chapter 2.4, this sub-chapter introduces three self-designed perception systems for the future autonomous vehicle research platform.

A.1 Basic Version

App.Figure A-1 The Basic Version of sensors installation.

The Basic Version design utilises only one video Camera, one long range Radar, and four short range Radars to form the perception system. Although this design is the simplest solution, it still fulfils the major requirement of reaching 360-degree sensing coverage. App.Figure A-1 and App.Figure A-2 illustrate the precise location of each type of sensor: the forward-detecting video Camera is installed between the rear view mirror and the front windshield so as to capture essential images in front of the vehicle; one long range Radar is mounted into the front bumper to detect front obstacles and compensate the observation from the video Camera; four short range Radars are assigned to the corners of the vehicle to fill the blank perception area.

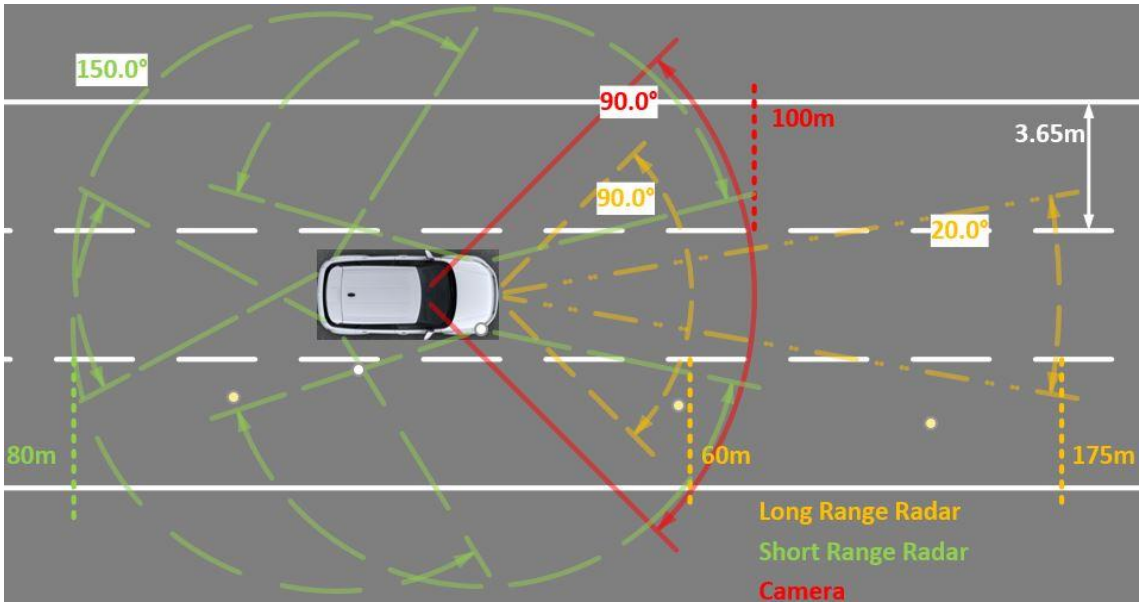

App.Figure A-2 The perception system coverage of the Basic Version.

With the Basic Version, the autonomous vehicle is able to recognise front environment including lane marking, traffic signs, front vehicles and even pedestrians. Furthermore, surrounding obstacles can be detected within 80 metres which will assist the motion planning for self-driving and enable the autonomy to achieve ACC and prevent collisions in motorway scenarios. The below tables summarise the Basic Version perception system as well as its general cost.

The utilised sensors of the Basic Version are summarised as:	
• 1 Camera	GBP 850
• 1 Long Range Radars	GBP 3,840
• 4 Short Range Radars	GBP 13,400
	Total: GBP 18,090

The primary features which can be achieved by the Basic Version are summarised as:
• Adaptive Cruise Control and detect a leading vehicle in motorway scenarios
• Lane markings, signs, and traffic lights perception
• Front obstacles recognition and classification (including pedestrians, vehicles and barriers)
• Surrounding obstacles detection within 80m (including their relative positions and velocities)
• Free-space analysis

A.2 Medium Version

App.Figure A-3 The Medium Version of sensors installation.

The Medium Version design has a similar sensor distribution comparing to the Basic Version, but with a rotation Lidar added. This version contains one video Camera, one long range Radar, four short range Radars and one 360-degree rotation Lidar. The video Camera and the long range Radar remain in the same locations as the Basic Version. The added rotation Lidar is mounted on the vehicle roof with the purpose of scanning surrounding environment through laser beams. Since the Lidar can achieve 360-degree observation, the operational FOV of four short range Radars can be reduced to increase their sensing accuracy. The precise locations of above mentioned sensors are shown in App.Figure A-3 and App.Figure A-4.

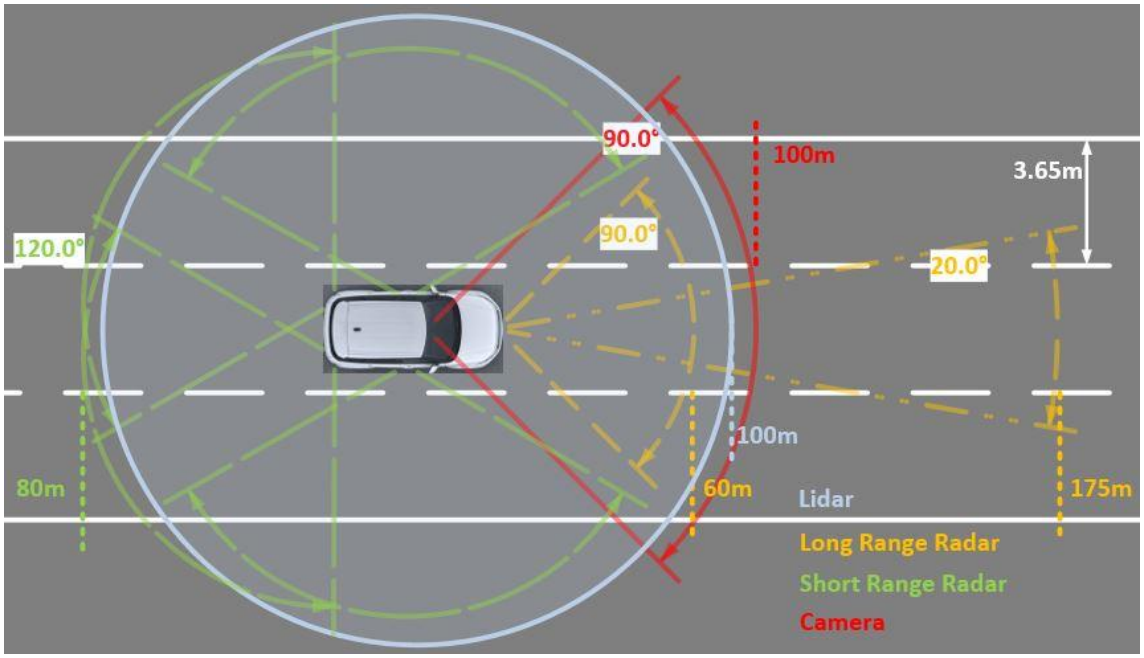

App.Figure A-4 The perception system coverage of the Medium Version.

This Medium Version equips all the Basic Version's features and enlarges the detecting range of surrounding obstacle to 100 metres. By utilising a 360-degree Lidar, a detailed-dynamic 3D map of the environment can be constructed. Moreover, any obstacles within 80 metres will be detected by at least two different types of sensors, which ensures the functionality of the perception system and guarantee the driving safety when an unpredictable error is happened to one or two sensors. The below tables summarise the Medium Version perception system, its general cost and the functionalities of using the Medium Version design.

The utilised sensors of the Medium Version are summarised as:	
• 1 Camera	GBP 850
• 1 Long Range Radars	GBP 3,840
• 4 Short Range Radars	GBP 13,400
• 1 Lidar	GBP 5,910
	Total: GBP 24,000

The primary features which can be achieved by the Medium Version are summarised as:
• Adaptive Cruise Control and detect a leading vehicle in motorway scenarios
• Lane markings, signs, and traffic lights perception
• Front obstacles recognition and classification (including pedestrians, vehicles and barriers)
• Surrounding obstacles detection within 100m (including their relative positions and velocities)
• Any obstacle within 80m will be detected by at least two different types of sensors.
• Free-space analysis
• Generate a detailed-dynamic 3D map of the environment

A.3 Advanced Version

App.Figure A-5 The Advanced Version of sensors installation.

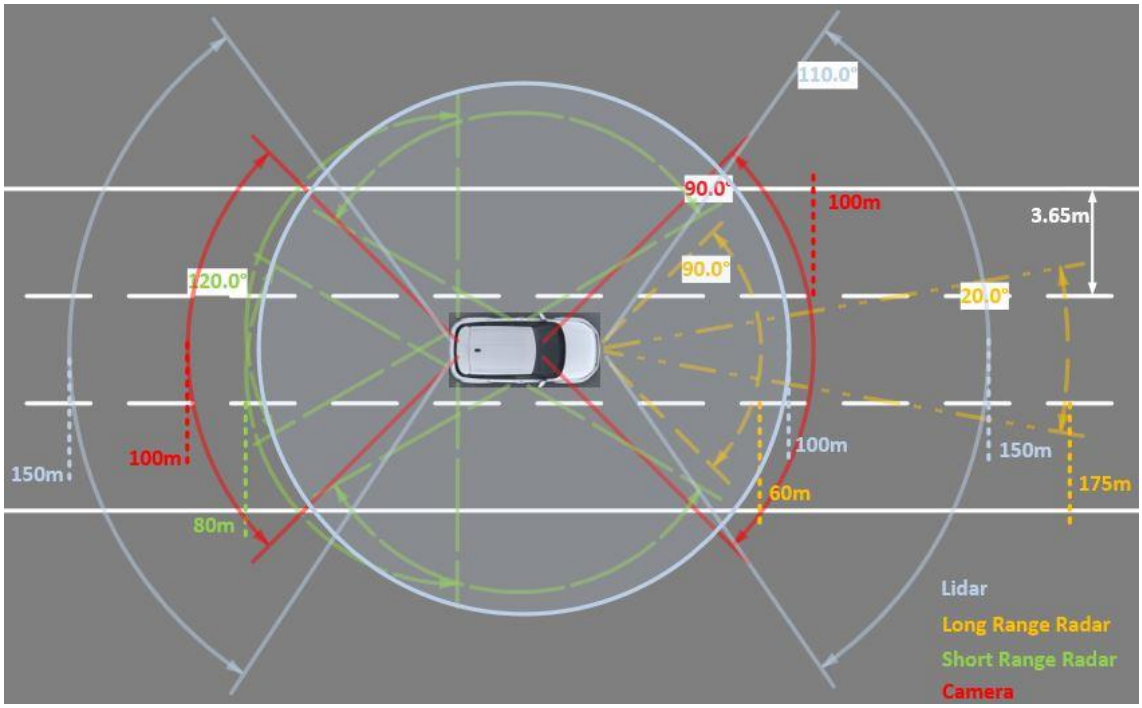

App.Figure A-6 The perception system coverage of the Advanced Version.

The last design is the Advanced Version; it tries to increase the accuracy of the front and back detection and enlarges the operation distance up to 150 metres. As depicts in App.Figure A-5 and App.Figure A-6, one backward-looking video

camera and two field Lidars that have longer effective distance are added. The added Camera and one of the field Lidars are assign to the rear windshield to record the environmental information behind the vehicle. The other field Lidar is arranged near the long range Radar which is located under the front bumper to extend the front perception distance. It should be noted that any obstacle within 80 metres will be detected by at least two different types of sensors. The below tables summarise the Advanced Version perception system, its general cost and the functionalities that can be provided by the Advanced Version design.

The utilised sensors of the Advanced Version are summarised as:	
• 2 Camera	GBP 1,700
• 1 Long Range Radars	GBP 3,840
• 4 Short Range Radars	GBP 13,400
• 1 Rotation Lidar	GBP 5,910
• 2 Field Lidars	GBP 25,600
	Total: GBP 50,450

The primary features which can be achieved by the Basic Version are summarised as:
• Adaptive Cruise Control and detect a leading vehicle in motorway scenarios
• Lane markings, signs, and traffic lights perception
• Front & behind obstacles recognition and classification (including pedestrians, vehicles and barriers)
• Surrounding obstacles detection within 100m (including their relative positions and velocities)
• Any obstacle within 80m will be detected by at least two different types of sensors.
• Enlarge the forward and backward sensing distance to 150m
• Free-space analysis
• Generate a detailed-dynamic 3D map of the environment

Appendix B Human Driving Data Analysis

B.1 Histograms with a distribution fit of the remaining signals

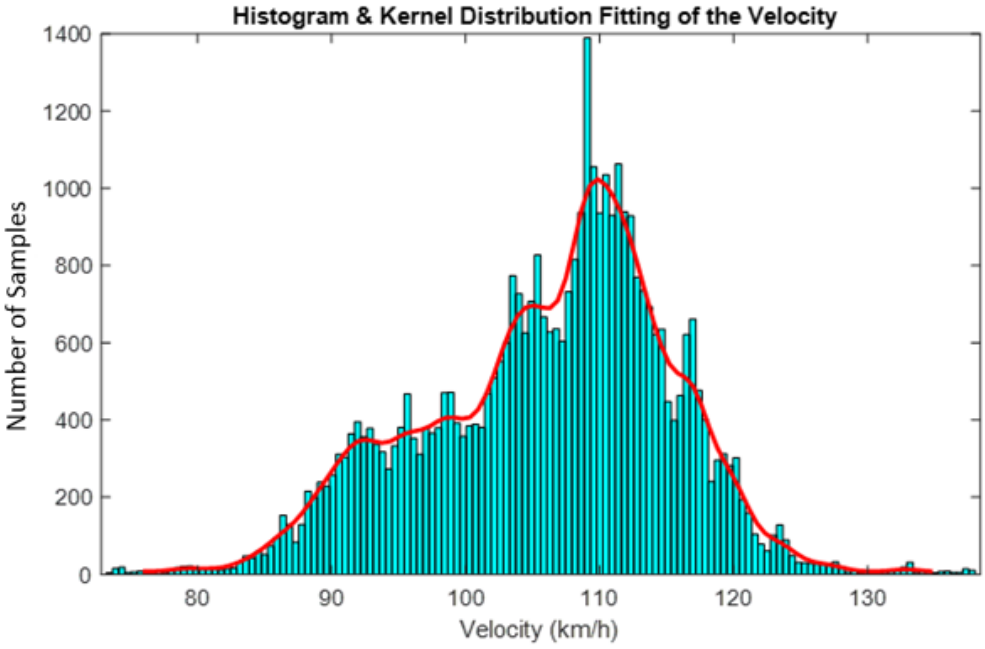

App.Figure B-1 Histogram of the Velocity for the right lane changes on motorway.

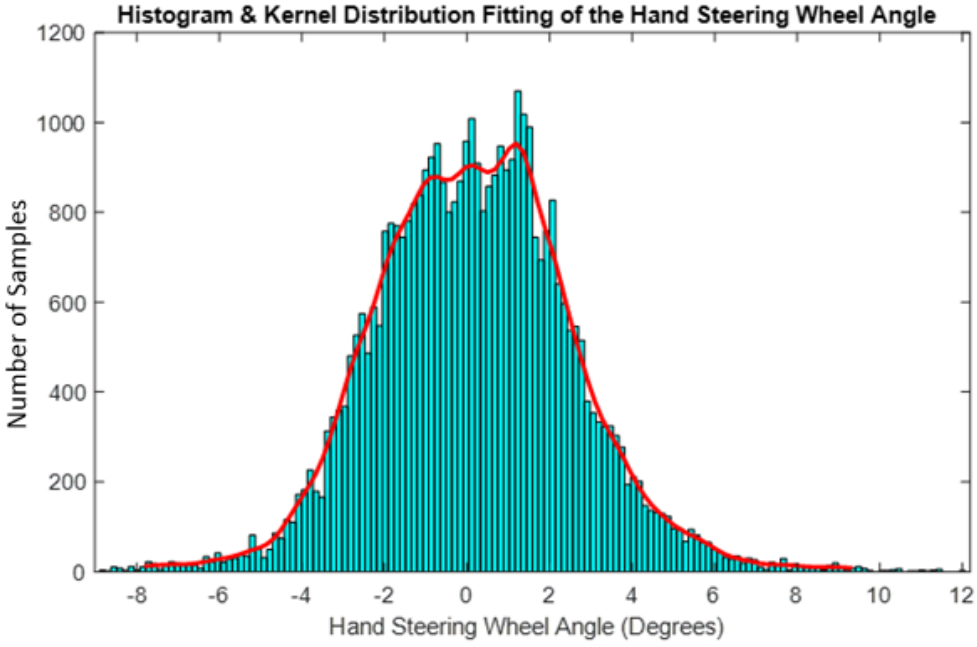

App.Figure B-2 Histogram of the Hand Steering Wheel Angle for the right lane changes on motorway.

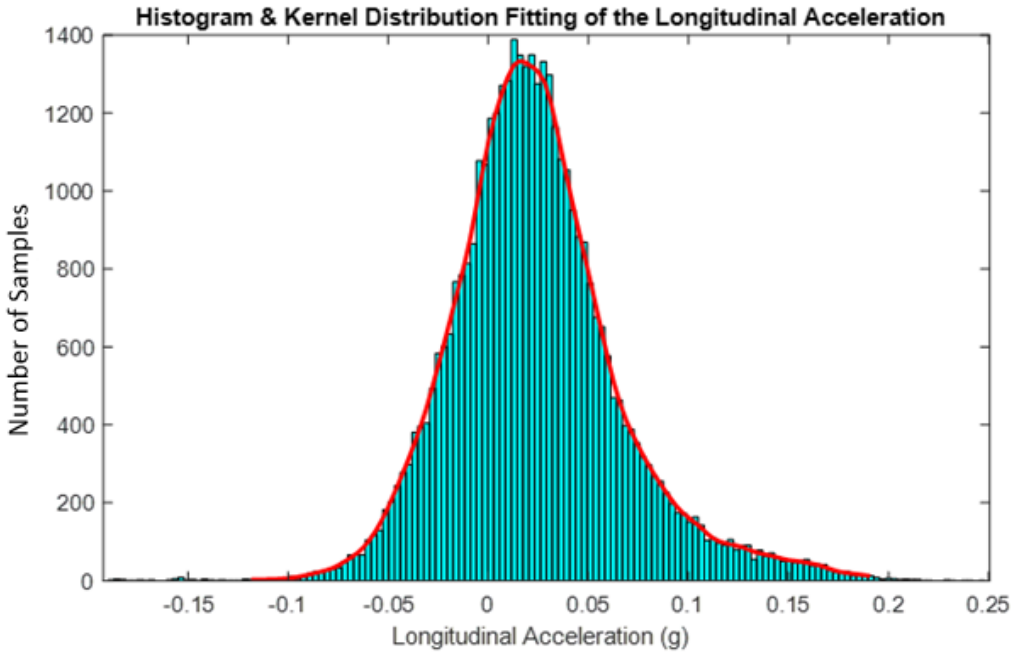

App.Figure B-3 Histogram of the Longitudinal Acceleration for the right lane changes on motorway.

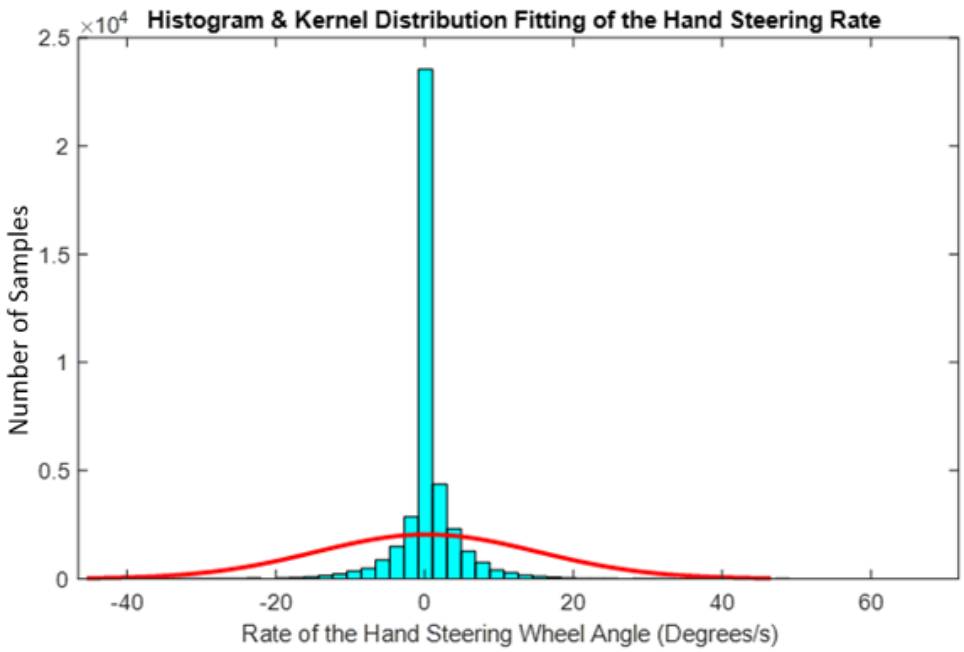

App.Figure B-4 Histogram of the Rate of the Hand Steering Wheel Angle for the right lane changes on motorway.

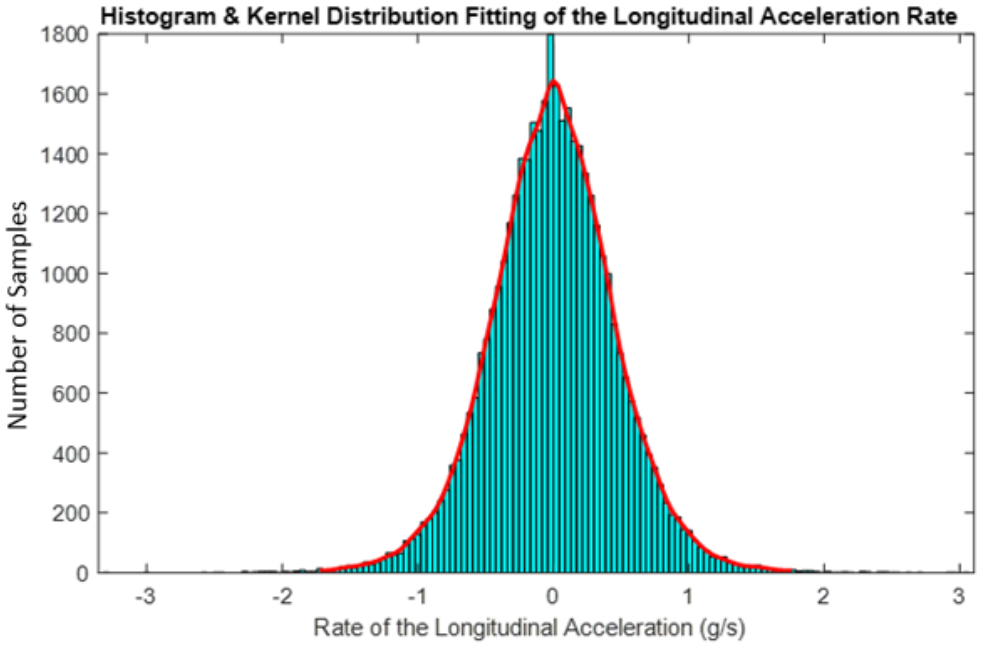

App.Figure B-5 Histogram of the Rate of the Longitudinal Acceleration for the right lane changes on motorway.

Appendix C ITSC Conference Paper

Multi-Point Turn Decision Making Framework for Human-Like Automated Driving

Chun-Wei Chang[1], Chen Lv[1], Huaji Wang[1], Hong Wang[2], Dongpu Cao[1], Efstathios Velenis[1], Fei-Yue Wang[3]
[1]Advanced Vehicle Engineering Centre, Cranfield University, Bedford, United Kingdom
[2]Department of Mechanical and Mechatronics Engineering, University of Waterloo, Waterloo, Canada
[3]Qingdao Academy of Intelligent Industries, Qingdao, China
[1]{c.chang, c.lyu, huaji.wang, d.cao, e.velenis}@cranfield.ac.uk; [2]wanghongbit@gmail.com; [3]feiyue.wang@ic.ac.cn

***Abstract*—This paper proposes a new methodology of achieving human-like automated driving, and presents a decision making framework and the minimum thresholds of the occupied widths of multi-point turn for autonomous vehicles. The concept of human-like automated driving and the multi-point turn decision making framework for autonomous vehicles are proposed at first. Then, the geometric characteristics that are provided by the reference paths of turn around manoeuvres are analysed. The minimum operation widths from U Turn to Five-Point Turn are investigated respectively, and the methodology and results are then generalized to solve the multi-point turn (i.e. N-Point Turn) scenario. Finally, by using the derived results and characteristics analysed above, the functions that are able to evaluate the most feasible turn around manoeuvre within the current situation are provided.**

Keywords—human-like automated driving; turn around manoeuvre; multi-point turn; decision making.

I. INTRODUCTION

The on-vehicle automation system is primarily developed to replace the human driver in driving tasks in order to enhance the driving performance and traffic efficiency [1]-[7] and avoid the possible fatalities [8]-[12] (e.g. correcting manipulation mistakes, reducing the traffic crashes related to human behaviours and decisions, etc.). However, most published researches neglect that the human imperfection and preference not always leads to negative consequences. An explicit example is the motion sickness, which has been confirmed that it is one of the primary after-effects while riding an autonomous vehicle [13]-[16]. In order to mitigate the undesired influence and increase the public acceptance, a functionality which is able to imitate the behaviours of human drivers on the premise of safety is required. This paper aims to deliver the preliminary effort of achieving the human-like turn around automated driving.

Being one of the common vehicle driving scenarios in both rural and urban area, the turning manoeuvre has been researched for over twenty years [17], [18]. Turn around is a specific version of turning manoeuvres, and can be seen as a general terminology that describes the vehicle behaviours while reorienting to the opposite heading direction. This manoeuvre is often executed under emergent or unexpected situations; for instance, driving into a dead end street, avoiding front obstacles and traffic [19], interrupting by a higher-priority driving mission, redirecting to the new destination, etc. As the pioneer in developing autonomous vehicles, Google realises that turn around is one of the trickiest driving tasks even for a professional driver to master. Therefore, Google Cars are assigned to execute hundreds of multi-point turns per week with the purpose of improving the performance while operating these difficult driving manoeuvres [20].

Since the heading direction of a vehicle can be adjusted through steering the front wheels during forward or backward movements, turn around manoeuvres can be divided into two categories: One enables the vehicle to achieve target (i.e. turn 180 degrees) without any transition between forward driving and reversing, including detours and U Turn; the other is comprised of multiple forward and backward reorientations, which is so called N-Point Turn. Apart from the former has the possibility to provide efficient performance but requires a broad area, the latter can be manipulated within the permitted width less than two standard traffic lanes.

This paper presents a multi-point turn decision making framework and derives the related minimum thresholds of the occupied widths; the reference paths are referred to the Reeds-Shepp path [21] so as to approach human-like behaviours that drivers prefer to make a brief stop while operating the hand steering wheel from one direction to the other. The remaining sections of the paper are organised as follows. Section II introduces the human-like automated driving framework and the multi-point turn decision making flowchart for autonomous vehicles. Section III remarks the geometric characteristics that are followed by the reference paths of multi-point turn and derives the minimum operation widths from U Turn to Five-Point Turn respectively, which can be generalized to N-Point Turn. By taking advantage of the outcomes which are acquired from the prior derivations, two equations that calculate the minimum number of multi-point turn based on the environmental information are provided in Section IV. Finally, the contributions of this paper are concluded in Section V.

II. PROPOSED FRAMEWORKS

Fig. 1 presents the framework for achieving human-like automated driving. The concept of human-like automated driving can be primarily divided into three parts, which are

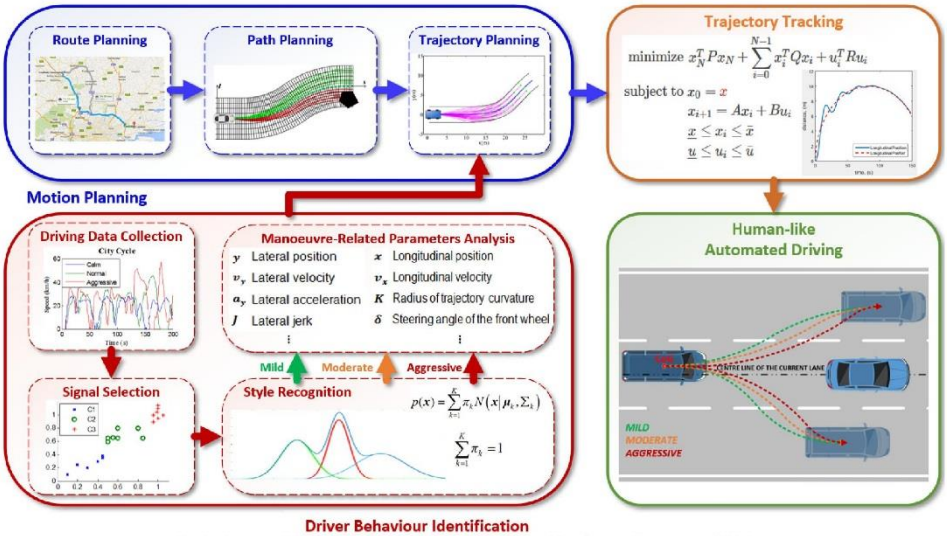

Fig. 1. The general framework for an autonomous vehicle to achieve human-like automated driving.

the motion planning, the driver behaviour identification and the tracking control. In the motion planning section, the target is to utilise existed planning techniques to generate the vehicle-dynamics-based trajectory of the determined driving task [5], [9], [22]-[25]. On the other hand, the purpose of the driver behaviour identification part is to classify the real driving data from human drivers into selected number of different driving styles (e.g. Aggressive, Moderate, and Mild) through machine learning techniques [26]. Once the values of style-related parameters are generated, the results will be combined with the vehicle-dynamics-based trajectory in the motion planning section to modify relevant variables and enable the trajectory planner to provide human-like trajectories. Finally, the control algorithm tracks the trajectories of different driving styles in the tracking control part and enables the autonomous vehicle to perform human-like automated driving.

The perception system of an autonomous vehicle is composed of several types of sensors (e.g. Radar, Camera, Lidar, GPS, etc.). It provides the autonomy with surrounded environment information so as to execute decision making and planning process and guarantee the driving safety. In this paper, we assume that the ego vehicle equips a decent perception system which has the ability to observe and measure all the required environmental information. It should be noticed that the following figures and examples are based on left-hand traffic regulations (e.g. UK, JP, etc.).

Fig. 2 shows a basic traffic scenario while the vehicle is performing driving tasks, where P is the middle point of the vehicle rear axis; a is the lateral distance from point P to the right permitted border and d is the full permitted width which limits the active area of the vehicle. As mentioned previously, the request of executing 180 degrees turn cannot be expected in most instances and will have a higher priority. Hence, it is crucial to evaluate the feasibility of achieving the turn around target under the current environmental conditions and select the most convenient solution.

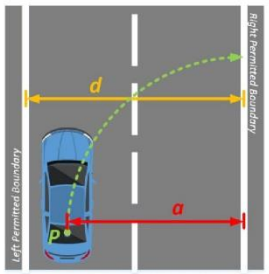

Fig. 2. A typical scenario while activating the turn around manoeuvre.

There is no doubt that a turn around manoeuvre can be treated as a high-risk activity since its operational area will overflow the current driving lane. As each transition between a forward and a reverse cornering costs a period of time, the 180 degrees turning with the less number of points is preferred to shorten the risk period. In order to realise the above functionalities, a general decision making framework is proposed in Fig. 3. D_1, D_3 and D_N represent the minimum utilised width of U Turn, Three-Point Turn and N-Point Turn respectively, where N is requested to be an odd number according to the property of multi-point turn.

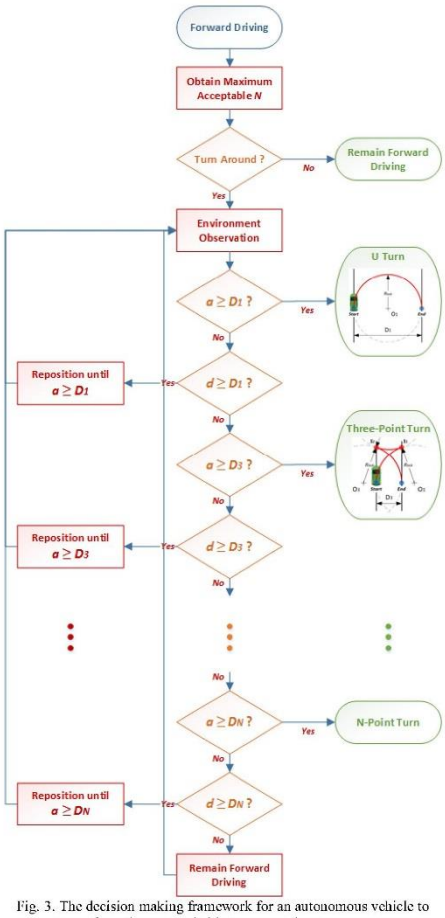

Fig. 3. The decision making framework for an autonomous vehicle to perform the most suitable turn around manoeuvre.

Starting with normal forward driving, the vehicle autonomy is assumed to be able to determine the necessity of turn around and the maximum acceptable value of N referring to the traffic conditions, the vehicle dimensions and the passenger's command. Once the request has been approved, both the full width d and the lateral distance a between P and the right boundary will be measured by the vehicle perception sensors. If a is equal to or greater than D_1, a U Turn will be selected and executed from the current position; if a is less than D_1 but d is equal or greater than D_1, the vehicle will remain forward driving and reposition its location until the new a is equal to D_1 in order to operate a U Turn from the new location. The same strategy is evaluated in selecting Three-Point Turn up to maximum acceptable N-Point Turn. Considering the preference of passengers and the constraints of vehicle dimensions, the vehicle is asked to remain forward driving if d cannot support the maximum acceptable N-Point Turn. This forward driving stage will be maintained until the new d is equal or greater than one of $D_1, D_3, \ldots, D_N$.

III. Analysis of the Turn Around Manoeuvres

This section illustrates and derives the narrowest requested road width D_1, D_3, D_5 and D_N, and the optimal reference paths that are based on geometric circles for a vehicle to achieve turn around tasks. To simplify the problem, the ego vehicle is considered as a point model (i.e. the point P in Fig. 2); and its heading direction is required to converse (i.e. turn 180 degrees) to complete the manoeuvre. A turn around manoeuvre comprises one or more forward and backword movements (Exception: U Turn is formed with only one forward movement); and will occupy the adjacent area which might be the oncoming traffic lane. Considering the safety and the efficiency, we assume that the hand steering wheel is steered to either the left or the right full lock position with cornering radius R_{lock} during each forward or backward driving; where R_{lock} can be calculate from the turning circle provided by car manufacturer. Moreover, the left and the right road boundaries are assumed to be two parallel lines and the turn around mission has to be operated within the area.

A. Geometric Properties and Constraints

The hand steering wheel (e.g. Ackermann Steering Angle in the Bicycle Model) controls the vehicle cornering radius and the driving path. As the hand steering wheel continues inputting the full lock steering signal while turning, the driving path becomes an arc or a circumference of the circle which has radius R_{lock}. Therefore, three geometry-related properties and constraints are depicted below.

1) Remark 1: The reference path of N-Point Turn is formulated by N arcs from N different circles, where N is an odd number.

2) Remark 2: Two circles that govern the sequential path pieces for a vehicle to converse the cornering direction are "tangented" at the transition point, at which the vehicle is requested to stop and manipulate the hand steering wheel to the opposite full lock position. Hence, the centres of the two circles are symmetric with each other to the transition point.

3) Remark 3: Each forward or reverse cornering has the ability to adjust the heading direction of the vehicle. With the purpose of finding the narrowest operation width, the process of executing a N-Point Turn has to get the utmost out of the available space. In other words, the start, the end and the transition points of the reference path have to be placed on either the left or the right road borders.

B. U Turn (N=1)

To converse the heading direction of a vehicle, U Turn is the simplest and most efficient solution a driver can operate, as shown in Fig. 4a. The reference path of U Turn can be treated as the arc of a semicircle with radius r if the steering angle is fixed. With manipulating the hand steering wheel at the full

lock position ($r = R_{lock}$) while cornering, the minimum threshold of the road width D_1 for a vehicle to perform a U Turn can be acquired as in (1).

$$D_1 = 2r = 2R_{lock} \quad (1)$$

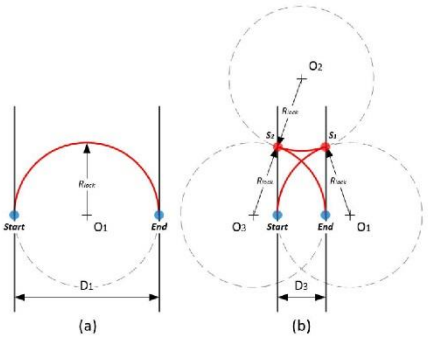

Fig. 4. The reference path (red curves) and the narrowest requested road width of (a) U Turn and (b) Three-Point Turn.

C. *Three-Point Turn (N=3)*

Although U Turn is preferable to other turn around manoeuvres, it might not be suitable under normal driving scenarios. The primary reason is that the driving path of U Turn will cross more than two standard traffic lanes, but the permitted width for a vehicle to converse the driving direction is often less than D_1. In order to achieve the turn around task within the above situation, the vehicle has to be stopped before breaking through the right road boundary and made a reverse with opposite steering but not to exceed the left road boundary; once the lateral distance to the right road boundary could afford the remaining turning, the vehicle makes the second stop and performs another forward cornering to finish the turn around manoeuvre, which is known as Three-Point Turn.

In general, Three-Point Turn comprises two forward and one reverse cornering. According to the geometric properties and the full lock position steering assumption, the reference path of Three-Point Turn can be decomposed into the arcs from three different circles with same radius R_{lock}. Fig. 4b depicts the scenario of utilising the narrowest road width to operate a Three-Point Turn, where O_1, O_2, and O_3 are the centres of circles that guide the vehicle to drive from the start point to the right road boundary, reverse to the left road boundary, and finalise the remaining cornering respectively; S_1 and S_2 are the vehicle stop points (i.e. transition points) at the right and the left road boundaries; D_3 is the minimum requested road width to implement a Three-Point Turn. Note that the points O_1, *End*, *Start* and O_3 are on the same line which is vertical to the road direction.

To find D_3, the line $\underline{O_1Start}$ and the line $\underline{O_3End}$ are first discussed; both their lengths are equal to R_{lock}. Accordingly, the lengths of the line $\underline{O_1End}$ and the line $\underline{O_3Start}$ are equal, and can be acquired as $(R_{lock} - D_3)$. Considering the properties of congruent triangles, the lateral distances from O_2 to the left and the right road boundary can be determined, which also illuminate the relation between D_3 and R_{lock}, as shown in (2).

$$D_3 = 2R_{lock} - 2D_3 = 2R_{lock} / 3 \quad (2)$$

D. *Five-Point Turn (N=5)*

Five-Point Turn is another possible strategy to complete the turn around mission. It will consume more time, but can be applied to the situation which the permitted width is narrower than the minimum threshold D_3 of Three-Point Turn. The reorientation sequence for Five-Point Turn requires an additional forward and an additional backward cornering to compensate for the diminished width, since the maximum achievable turning angle of each path piece (e.g. from *Start* to S_1, from S_1 to S_2, etc.) is reduced.

In other words, the arcs from five different circles formulate the reference path of Five-Point Turn, including three forward and two reverse turnings. Taking the geometric properties and the aforementioned assumptions into account, a specific distribution of the five circles with same radius R_{lock} is able to minimise the occupied width, which is illustrated in Fig. 5. O_1, O_2, O_3, O_4 and O_5 are the centres of the above circles that guide the vehicle to complete the turn around manoeuvre. S_1 and S_3 are the transition points when the vehicle reaches the right border during the Five-Point Turn; S_2 and S_4 are the ones at the left border. D_5 is the lateral distance that represents the lower limit of the available width to perform a Five-Point Turn. Similar to Fig. 4b, the points O_1, *End*, *Start* and O_5 can be connected to form the line that is vertical to the left and the right operation borders.

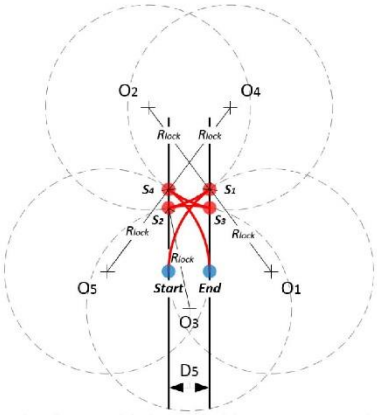

Fig. 5 The reference path (red curves) and the narrowest requested road width of Five-Point Turn.

The length D_5 can be obtained through deriving the side lengths of the congruent triangles. Start with calculating the lengths of the line $\underline{O_1End}$ and the line $\underline{O_5Start}$, which are both equal to $(R_{lock} - D_5)$ and confirm the lateral distances from O_2

to the right boundary and from O_4 to the left boundary. By subtracting D_5 from the results, both the lateral distance between O_2 and the left boundary and the lateral distance between O_4 and the right boundary can be acquired as (R_{lock} – $2D_5$). Owing to the equivalent distances of the line $\underline{O_2S_2}$, the line $\underline{O_3S_2}$, the line $\underline{O_4S_3}$ and the line $\underline{O_3S_3}$ which are equal to the full lock cornering radius R_{lock}, these line are able to form another two pair of congruent triangles with the left and the right boundaries. Hence, the lateral distances from O_3 to the left and the right operational boundary can be determined in the meantime. Accordingly, the summation of these two distances (i.e. the lateral distances from O3 to the left and the right operational boundary) generates the outcome of the length D_5, and the relation is stated in (3).

$$D_5 = 2R_{lock} - 4D_5 = 2R_{lock} / 5 \tag{3}$$

E. N-Point Turn

The operational tactic of N-Point Turn is similar to Three-Point Turn and Five Point Turn: the vehicle starts with the forward cornering from a certain position, and recursively adjusts its heading direction through numerous forward and reverse reorientations within the permitted space (i.e. between the left and the right boundary) until the remaining turning can be achieved by the final forward cornering without breaking the right boundary.

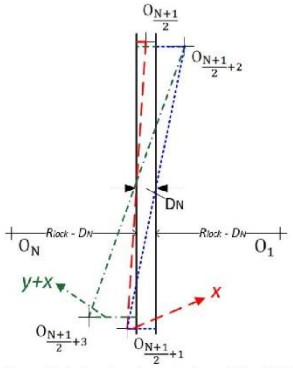

Fig. 6 The chart of deriving the min. operation width of N-Point Turn.

According to the distribution patterns from U Turn to Five-Point Turn, several regulations were observed and can be utilised to solve the narrowest operation width D_N for N-Point Turn. First, the reference path of N-Point Turn is composed of N arc pieces which are belong to N different circles with same radius R_{lock}. Moreover, the centres of the initial circle and the final circle (i.e. O_1 and O_N) can be connected by extending the line $\underline{StartEnd}$, which is vertical to the road direction. Then, the functionality of No.[(N + 1)/2] circle is to bridge the vehicle heading direction from less than 90 degree to over 90 degree (the heading direction at the start point and the end point are defined as degree 0 and degree 180 respectively); and the centre of this circle is located at a point on the central line of the road. On the other hand, the coordinates of two sequential centres (e.g. $O_{[(N+1)/2]}$ and $O_{[(N+1)/2+1]}$) are symmetric to their transition point with distance R_{lock}, which the point is on either the left or the right border.

Fig. 6 shows the draft distribution of sequential centres near the operation area, where O_1 to O_N are the centres of circles that provide N arc pieces to form the reference path of N-Point Turn. We first assume the lateral distance from $O_{[(N-1)/2+1]}$ to the left border is x, and the lateral distance between $O_{[(N+1)/2-1]}$ and $O_{[(N+1)/2+3]}$ is y. In order to calculate x and y, the properties of congruent triangles have to be applied. By focusing on the red congruent triangles, the distance between $O_{[(N+1)/2]}$ and the left border has the same length with x and is shown in (4). The blue congruent triangles illustrate that the width from $O_{[(N+1)/2-1]}$ to the right border is equal to the width from $O_{[(N-1)/2+2]}$ to the right border, which is (x – D_N). Furthermore, the green congruent triangles determine that the lateral distance from $O_{[(N+1)/2+2]}$ to the left border has the same length (x + $2D_N$) with the width between $O_{[(N+1)/2+3]}$ and the left border, which can be expressed as y + x. Consequently, the relation between y and D_N can be stated in (5).

$$x = D_N / 2 \tag{4}$$

$$y = 2D_N \tag{5}$$

The above procedures are derived recursively so as to compute the lateral distances between every two adjacent centres from $O_{[(N+1)/2-1]}$ to O_N, which are all equal to y. Hence, the lateral distance from O_N to the left border (i.e. R_{lock} – D_N) can be expressed by x and y, and the equation is stated in (6). Combing these three equations (i.e. (4), (5) and (6)), the narrowest occupied width D_N of N-Point Turn can be expressed by the cornering radius R_{lock}, as in (7).

$$R_{lock} - D_N = [\frac{N - (\frac{N+1}{2} + 1)}{2}] * y + x \tag{6}$$

$$D_N = 2R_{lock} / N \tag{7}$$

The validity of D_N can be confirmed by comparing the outcomes of aforementioned D_1, D_3 and D_5 in (1), (2) and (3). Note that Fig. 6 only presents the situation that $O_{[(N+1)/2]}$ is above the line $\underline{O_1O_N}$; the opposite situation (i.e. $O_{[(N+1)/2]}$ is below the line $\underline{O_1O_N}$) can be derived with the similar techniques and will deliver the same result as in (7).

IV. Discussions

Based on the relationship between the minimum occupied width of N-Point Turn that has been derived in the previous section and the vehicle full lock steering radius, we intends to form the functions which have the ability to continuously evaluate the most feasible turn around manoeuvre under current traffic conditions. Since the number of partitions during reorienting has to be odd numbers to complete a 180 degree turning, $\boldsymbol{O}$ is first defined as the set of the positive odd numbers, as shown in (8).

$$\boldsymbol{O} = \{\, m \mid m = 2n + 1 \,,\, n \in \boldsymbol{N} \} \tag{8}$$

Considering the proposed turn around decision making framework in Fig. 3, the environment observation process will be activated once the turn around manoeuvre is approved. Therefore, the lateral distance from the current position to the right available boundary (i.e. a) and the full permitted width (i.e. d) can be measured and provided as known variables to the targeted functions. Through inputting these two variables and the vehicle minimum cornering radius R_{lock} which can be acquired from the vehicle dynamic data to (9) and (10), the function f_1 is able to compute the minimum number of partitions of N-Point Turn that can achieve the turn around mission; the latter function f_2 will provide the result while considering the full permitted width.

$$f_1(R_{lock}, a) = min\{k \in \boldsymbol{O} \mid k \geq (2R_{lock}/a)\} \quad (9)$$

$$f_2(R_{lock}, d) = min\{k \in \boldsymbol{O} \mid k \geq (2R_{lock}/d)\} \quad (10)$$

According to the derivation outcomes in Section Three, (1), (2), (3), and (7) indicate that the minimum required widths of different turn around manoeuvres only depend on its partition number and the minimum cornering radius of the vehicle. The reason is that the ego vehicle is assumed and treated as a point-mass model in this paper, but it occupies a certain volume and cannot be neglected in reality. Hence, the work of re-analysing the vehicle from a point-mass model to a more complex model (e.g. bicycle model, four wheel model, etc.) and extending the outcomes of this paper to meet the realistic requirements will be focused in the next stage.

V. Conclusions And Future Work

This paper proposes a new framework of achieving human-like automated driving, which combines the real human driving data and the vehicle-dynamics-based motion planning. A general turn around decision making is then suggested, which can be referred while an autonomous vehicle intends to perform a turn around manoeuvre. The geometric characteristics that are followed by the reference paths of turn around manoeuvres are also analysed. Following with investigating the minimum operation widths from U Turn to Five-Point Turn respectively, the methodology and results are generalized to the N-Point Turn. Lastly, the derivative results and characteristics analysed above are treated as the input variables so as to formulate the functions that are able to evaluate the most feasible turn around manoeuvre within the current situation. Currently, the team is conducting multi-point turn road testing by different human drivers, characterising driving styles, and developing algorithms for multi-point turn decision making, path planning and tracking control for human-like automated vehicles.

References

[1] N. A. Stanton and M. S. Young, "Vehicle automation and driving performance," Ergonomics, vol. 41, no. 7, pp. 1014–1028, 1998.

[2] F. Y. Wang, X. Wang, L. Li, et al, "Steps toward parallel intelligence," IEEE/CAA Journal of Automatica Sinica, vol. 3, pp. 345–348, 2016.

[3] C. M. Martinez, X. Hu, D. Cao, E. Velenis, B. Gao, and M. Wellers, "Energy management in plug-in hybrid electric vehicles: recent progress and a connected vehicles perspective," IEEE Transactions on Vehicular Technology, vol. 66, pp. 4534–4549, 2017.

[4] F. Y. Wang, J. Zhang, Q. Wei, X. Zheng, and L. Li, "PDP: parallel dynamic programming," IEEE/CAA Journal of Automatica Sinica, vol. 4, pp. 1–5, 2017.

[5] X. Li, Z. Sun, D. Cao, Z. et al, "Real-time trajectory planning for autonomous urban driving: Framework, Algorithms, and Verifications," IEEE/ASME Transactions on Mechatronics, vol. 21, pp. 740–753, 2016.

[6] H. Guo, J. Liu, D. Cao, H. Chen, R. Yu, and C. Lv, "Dual-envelop-oriented moving horizon path tracking control for fully automated vehicles," Mechatronics, 2017.

[7] F. Y. Wang. "Control 5.0: from Newton to Merton in popper's cyber-social-physical spaces." IEEE/CAA Journal of Automatica Sinica, vol. 3, pp. 233–234, 2016.

[8] E. Rosén, J. E. Källhammer, D. Eriksson, M. Nentwich, R. Fredriksson, and K. Smith, "Pedestrian injury mitigation by autonomous braking," Accid. Anal. Prev., vol. 42, no. 6, pp. 1949–1957, 2010.

[9] X. Li, Z. Sun, D. Cao, D. Liu, and H. He, "Development of a new integrated local trajectory planning and tracking control framework for autonomous ground vehicles," Mechanical Systems and Signal Processing, vol. 87, pp. 118–137, 2017.

[10] C. Lv, H. Wang, and D. Cao, "High-Precision Hydraulic Pressure Control Based on Linear Pressure-Drop Modulation in Valve Critical Equilibrium State," IEEE Transactions on Industrial Electronics, 2017.

[11] L. Li, Y. Lv, and F. Y. Wang, "Traffic signal timing via deep reinforcement learning," IEEE/CAA Journal of Automatica Sinica, vol. 3, pp. 247–254, 2016.

[12] L. Li, W. L. Huang, Y. Liu, N. N. Zheng, and F. Y. Wang, "Intelligence Testing for Autonomous Vehicles: A New Approach," IEEE Transactions on Intelligent Vehicles, vol. 1, pp. 158–166, 2016.

[13] C. Diels, "Will autonomous vehicles make us sick?," Contemp. Ergon. Hum. Factors, pp. 301–307, October 2014.

[14] M. Elbanhawi, M. Simic, and R. Jazar, "In the passenger seat: investigating ride comfort measures in autonomous cars," IEEE Intell. Transp. Syst. Mag., vol. 7, no. 3, pp. 4–17, 2015.

[15] M. Sivak, B. Schoettle, "Motion sickness in self-driving vehicles," 2015.

[16] C. Diels and J. E. Bos, "Self-driving carsickness," Appl. Ergon., vol. 53, pp. 374–382, 2015.

[17] W. Nelson, "Continuous-curvature paths for autonomous vehicles," Int. Conf. Robot. Autom., pp. 1260–1264, 1989.

[18] Y. Kuwata, J. Teo, G. Fiore, et al, "Real-time motion planning with applications to autonomous urban driving," IEEE Trans. Control Syst. Technol., vol. 17, no. 5, pp. 1105–1118, 2009.

[19] Y. Chen and S. Yasunobu, "Soft target based obstacle avoidance for car-like mobile robot in dynamic environment," IEEE Int. Conf. Fuzzy Syst., 2007.

[20] Google, "Mastering the Three-Point Turn," Google Self-Driving Car Project Monthly Report, October 2016.

[21] J. Reeds and L. Shepp, "Optimal paths for a car that goes both forwards and backwards," Pacific J. Math., vol. 145, no. 2, pp. 367–393, 1990.

[22] X. Hu, L. Chen, B. Tang, D. Cao, H. He, "Dynamic path planning for autonomous driving on various roads with avoidance of static and moving obstacles," Mechanical Systems and Signal Processing, in press.

[23] H. Guo, J. Liu, R. Yu, D. Cao, H. Chen, "Dual-envelop-oriented moving horizon trajectory tracking control for fully automated vehicles," Mechatronics, in press.

[24] F. Wang, H. Chen, K. Guo, D. Cao, "A novel integrated approach for path following and directional stability control of road vehicles after a tire blow-out," Mechanical Systems and Signal Processing, vol. 93, pp. 431–444, 2017.

[25] G. Jia, L. Li, D. Cao, "Model-based estimation for vehicle dynamics states at the limit handling," ASME Journal of Dynamic Systems, Measurement and Control, 137 (10), 104501, 2015.

[26] C. M. Martinez, M. Heucke, F. Wang, B. Gao, D. Cao, "Driving style recognition for intelligent vehicle control and advanced driver assistance: a survey," IEEE Transactions on Intelligent Transportation Systems, in press.